FLOW-SOUND-STRUCTURE INTERACTION IN SPRING-LOADED VALVES

FLOW-SOUND-STRUCTURE INTERACTION IN SPRING-LOADED VALVES

By SALIM EL BOUZIDI, B. SC. E, M. A. SC.

A Thesis Submitted to the School of Graduate Studies in Partial Fulfilment of the Requirements for the Degree of Doctor of Philosophy

McMaster University

DOCTOR OF PHILOSOPHY (2018)

MCMASTER UNIVERSITY

MECHANICAL ENGINEERING

HAMILTON, ONTARIO

TITLE: Flow-Sound-Structure Interaction in Spring-Loaded Valves

AUTHOR: Salim El Bouzidi, B.Sc.E (University of New Brunswick), M.A.Sc. (University of Guelph)

SUPERVISOR: Dr. Marwan Hassan

School of Engineering, University of Guelph

SUPERVISOR: Dr. Samir Ziada,

Department of Mechanical Engineering, McMaster University

NUMBER OF PAGES: xvii, 160

Abstract

This thesis provides a comprehensive investigation of flow-sound-structure coupling in spring-loaded valves subjected to air flow. While they are commonly used in a multitude of applications, these types of valves have been found to experience severe vibrations when interaction is present among the structure, the hydrodynamic field, and the acoustic field for a range of operational valve structural characteristics, flow parameters, and connected piping length.

The first part of this investigation was aimed at characterizing experimentally the valve's dynamic behaviour and the parameters affecting the onset of self-excited instability. The occurrence of instability was mainly driven by the presence of acoustic feedback: the connected length of piping had to be sufficiently long, with a longer pipe correlating to more severe vibrations. In addition, it was found that the valve's oscillation frequency depends on the modal characteristics of the combined valve-piping system, rather than the structural natural frequency alone. Furthermore, an increase in the valve's spring stiffness caused the vibrations to become more severe. Meanwhile, other parameters such as initial spring preload force and valve plate area only had moderate effects on the stability behaviour of the valve.

The second part of the investigation sought to develop a theoretical model that could simulate the valve's response when subjected to air flow while considering the effects of acoustic feedback and impact on the seat and limiter. Thus, a structural model of the valve was developed based on a single-degree-of-freedom model of the system with impact computed based on a pseudo-force method. The hydrodynamic field relied on a one-dimensional unsteady Bernoulli description of the flow. Finally, the acoustic interaction was accounted for using the one-dimensional wave equation resolved using

a finite difference scheme. The model has demonstrated great agreement with the experimental results. It has shown an ability to predict the modal characteristics of the system as well as correctly predict the effect of increased stiffness or increased piping length on vibration amplitude.

The final part of the investigation consisted in designing countermeasures to mitigate the effects of this self-excited instability mechanism. A concentric Helmholtz-type cavity resonator, an orifice plate, and an anechoic termination are placed at the downstream side of a model valve which were seen to be unstable in the experimental and modelling phases of the investigation. All tested devices were able to eliminate the self-excited instability mechanism. The applicability and robustness of each of these methods were discussed.

Acknowledgements

First and foremost, I would like to thank my co-supervisors, Dr. Marwan Hassan and Dr. Samir Ziada, for their guidance and support throughout the course of my Ph.D. Although my degree may be coming to an end, I still look forward to their advice and mentorship as I begin my career. I am also grateful for the support of the members of my supervisory committee, Dr. Ravi Selvaganapathy and Dr. Michael Tait.

I would like to thank fellow members of the Flow-Induced Vibration and Aeroacoustics Laboratory. They made this experience enjoyable and provided valuable feedback on my research throughout these years.

I am immensely grateful to my grandmother, Zohra Mechhadi, who despite not having been fortunate to have learned how to read or write, always emphasized the value of education and learning. I am thankful for the unwavering support of my uncle, Abderrazzak Mouafik, without whom I would not be standing here today.

I am also forever thankful to Brianna Harris, who has been an excellent proofreader of my work, and an even better partner to share this journey with me. Thank you for the emotional support you provided during stressful times.

I would like to dedicate the work in this thesis to the memory of my mother, Fatima Zahra Haddadi (1963-2009), as a recognition for her dedication and countless sacrifices.

Contents

List of Figures

Declaration of Academic Achievement

I, Salim El Bouzidi, declare this thesis to be my own work. I am the sole author of this document. No part of this work has been submitted for a higher degree at another institution.

To the best of my knowledge, the content of this document does not infringe on anyone's copyright.

My co-supervisors, Dr. Marwan Hassan and Dr. Samir Ziada, and the members of my supervisory committee, Dr. Ravi Selvaganapathy and Dr. Michael Tait, have provided guidance and support at all stages of this project. I completed all of the research work.

Chapter 1

Background

1.1 Introduction

Valves possess basic yet fundamental functions in industrial processes. They can be used to regulate the flow (control valves), to ensure directionality of the flow (non-return or check valves), or for pressure relief (safety and relief valves). While their purpose may seem primitive, their ability to operate within nominal conditions is critical, as failures have often had serious consequences. One of the most high profile cases involving valve malfunction was the Three Mile Island Accident, where a pressure relief valve was stuck open and caused serious loss of cooling water (Rogovin, 1979) that significantly contributed to the most serious nuclear accident in the history of power generation in the United States. Another valve failure case that has permeated popular culture occurred much more recently, and involved a failure of a flow control valve in Cooling Loop A onboard the International Space Station (NASA, 2013). This required a hazardous 5-hour, 30-minute spacewalk in order to replace the 260-pound pump controller module that is attached to an external truss. While the cause of valve

malfunction in the two cases mentioned so far isn't necessarily due to flow-induced vibration, as the root causes of failure have never been revealed, the above instances serve well to show that the prevalent response in the industry is to replace valves upon failure, rather than investigate the underlying reason for malfunction. This is despite the fact that a well designed valve can go a long way in reducing operation and maintenance expenses by avoiding the usually costly shutdowns, or in the serious case of the Three Mile Island incident, leakage of radioactive material into the environment.

1.2 Flow-Induced Vibration (FIV) in Valves

Flow-Induced Vibration in valves is usually of major concern, and not only can it cause premature wear and failure requiring replacement, but it can also result in uncomfortable and in some instances unsafe noise levels. Furthermore, even during normal operation the performance of the valve can be hindered due to vibration. In 2003, the Vogtle Electric Generating Plant experienced a discharge control valve failure, which was attributed to degradation induced by flow-induced fatigue failure of a pin that secures the plug assemby (US-NRC, 2006). This failure mode had been known to the valve manufacturer (Fisher Controls) since 1988, and yet almost two decades later it had remained unresolved, even in an industry where life threatening incidents due to valve failure had previously occurred, such as the aforementioned Three Mile Island Accident. In 2005, Unit 2 at San Onofre Nuclear Generating Station (SONGS) experienced an abnormal reduction through a butterfly valve used for emergency shutdown cooling of the reactor core. A shutdown inspection of the valve indicated that it could not fully open due to a loss of pins connecting the valve disc to the valve stem (US-NRC, 2006). This failure was attributed to flow-induced vibration. While the Nuclear Regulatory Committee (NRC) mandated corrective action items, such as

the replacement of the taper pins and staking of the pins to the valve disc, no attempt was made to uncover the true reason for this failure. Since the excitation source was not suppressed, and the magnitude of the fluid forces was not known, it is not clear how effective the remedies proposed by the NRC would have been at preventing reoccurrence.

Valves used in hydraulic circuits tend to experience a high frequency "chirp" (Margolis and Hennings, 1997), and while several mechanisms have been proposed, the problem is not yet fully understood. Finally, high Mach number natural gas pipelines under maintenance require purging prior to performing repairs. As a result, a section of the pipeline is isolated, and its pressure is relieved into the atmosphere through a valve, resulting in a "loud roaring sound" throughout the gas blowdown operation that can last up to three hours (TransCanada Corp., 2005).

Based on the above mentioned cases, it might seem as though the reason that valve degradation due to flow-induced vibration is allowed to reoccur without a thorough understanding of the root cause is apathy of the operator or the manufacturer. This is perhaps one reason why that happens to be the case, as valves are usually inexpensive components, and their replacement cost can be factored into the operating cost of the plant. Another reason would be due to the technically challenging nature of flow-induced vibration problems in valves. Given the scope of this thesis, this is of course the most compelling reason. Due to the variety in design, scale, and purpose, a "one-size fits all" solution against undesirable vibrations appears to be an elusive goal. An extensive amount of literature has shown that valve vibration occurs for a plethora of reasons, and is manifested in various forms. Vibration induced fatigue failure can occur simply because of the complex flow profile around valve plugs or plates which might consist of 90 degree elbows (Killmann, 1972). Alternatively, a spring-loaded valve might experience oscillations which are dynamically coupled with

the flow characteristics, that also oscillate due to the motion of the valve (Habing and Peters, 2006). Additionally, certain types of ball valves, due to their nonlinear spring supports, can exhibit a type of frequency response referred to as the "backbone curve" along with nonlinear stability properties, even under simple forced excitation cases (Nayfeh and Bouguerra, 1990). In some cases, coupling can occur with both the flow field as well as the acoustic field of the system, whereby the actual frequency of oscillation of the valve differs from its own natural frequency (Ziada et al., 1986). The above mentioned hydraulic circuits can experience stability problems that could depend on the load carried (Margolis and Hennings, 1997).

All the cases mentioned above required a separate and unique problem statement tailored to the application's operating conditions. This is perhaps one of the most challenging aspects of this problem, as there is yet to be any systematic design approach that could result in reliable prevention of unwanted vibrations. It hence makes sense that the Boiler and Pressure Vessel Code merely provides some short and general guidelines to avoid this nuisance, but mandates that in the case of nuclear power generation new valve designs need to be tested in the actual conditions of operation. Despite this, some compressor manufacturers have proposed some design procedures against vibration (Woollatt, 1972), as they may provide some useful preliminary information.

1.3 Self-Excited Oscillations of Spring-Loaded Valves

The proposed work aims to investigate self-excited oscillations in spring-loaded valves, which are used in a variety of applications. While the aim is to develop general

models that are applicable to a wide range of geometries and operating conditions, multi-ring disk valves will be taken as a reference, as they operate in severe conditions and are prone to failure as a result of flow-induced vibrations (Ziada et al., 1986; Oengören, 1987; Shine, 1987). Such a valve is shown in Figure 1.1. These valves are

(a) (b)

Figure 1.1: Sample multi-ring disk valve.

typically used at the inlet and the outlet of reciprocating compressors, in "push to open" configurations, where they are able to open with relatively short transients for a given pressure drop. The rings provide a large flow area in and out of the compressor cylinder to minimize pressure losses. To better visualize the flow, a cross-sectional drawing of a typical multi-ring disk valve is provided in Figure 1.2. The valve shown is 110 mm in diameter, and consists of concentric annular channels machined into two thick plates. The top one is referred to as the valve stopper while the second one is the valve seat. In the gap within the two thick plates one can find two thin metal plates. One serves as the valve plate, and is supported by compression springs that are attached to the valve stopper, while the other is the damper plate and simply serves as a soft impact surface for the valve plate. If the pressure difference across the valve is high enough to overcome the spring preload force, the valve plate is raised, and the

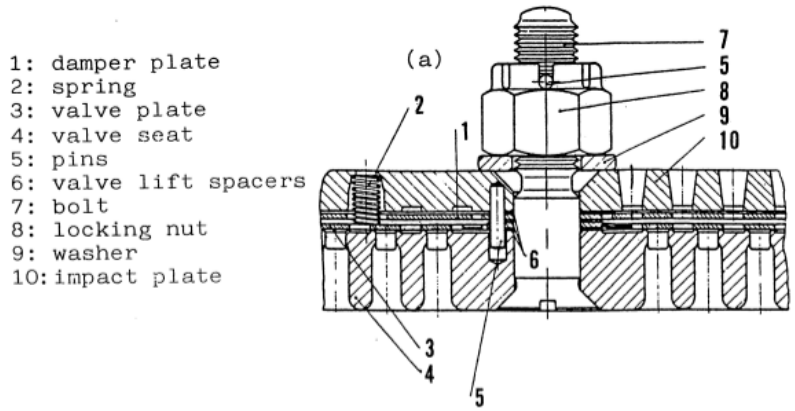

Figure 1.2: Cross-section of a typical multi-ring disc valve. (Oengören, 1987)

flow enters the annular channels of the multi-ring disk valve from the bottom and exits through the top.

In order to simplify the complex flow patterns, a single annular channel of the valve is considered, which is outlined by a dashed line in Fig. 1.3. In addition, another assumption is to consider that an axisymmetric channel will be hydraulically representative of the annular channels in the compressor valve, at least in the context of flow-sound-structure interaction. The resulting channel can be seen on the right-hand side of Fig. 1.3. These simplifications will allow the findings of this study to be applicable to a generalized spring-loaded valve design, rather than the specific case

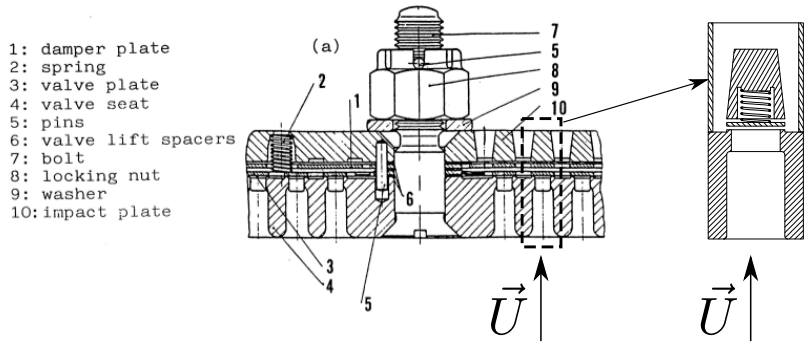

Figure 1.3: Generalized one-dimensional valve channel considered. Modified from Oengören (1987)

of a disk-type compressor valve. Finally, the valve plate motion is considered purely translational, as previous literature has shown that no tilting or rocking motion occurs during instability. This last point will be elaborated upon in Chapter 2.

1.4 Objectives

The objectives of this investigation were to:

- Experimentally characterize the valve instability occurring as a result of the interaction between the valve structure, the flow field, and the acoustic field. This will serve as a validation basis for a numerical model and help identify conditions under which the valve undergoes unstable oscillations.
- Develop a numerical model, which can be used as a tool for valve design to determine whether a given configuration will result in unstable behaviour. Furthermore, this model can be used to assess the life and wear of valves due to impact.
- Develop practical countermeasures which can be implemented to suppress destructive oscillations in valves.

1.5 Thesis Outline

This thesis consists of three journal articles that address three different aspects of an investigation into the flow-sound-structure interaction mechanism in spring-loaded valves. A preface to the articles, consisting of an introduction and a detailed literature review, is also provided. An epilogue, summarizing the work completed, major findings, and resulting contributions, follows the series of journal articles. Chapter 2 contains a

comprehensive literature survey regarding characterization, modelling, and mitigation efforts in the spring-loaded valve instability literature, to put the work presented in this thesis in context. Chapter 3 provides the first journal article, titled "Experimental Characterisation of the Self-Excited Vibrations of Spring-Loaded Valves", which covers the experimental work conducted in order to determine the physical characteristics of the instability, and the system parameters affecting it most. Chapter 4 provides the second journal article, titled "Self-Excited Vibrations of Spring-Loaded Valves Operating at Small Pressure Drops", which encompasses the methodology for developing the coupled nonlinear reduced order model of the valve, and model predictions compared with experimental data. Chapter 5 contains the third journal article, titled "Acoustic Methods to Suppress Self-Excited Oscillations in Spring-Loaded Valves", which covers the design and assessment of practical countermeasures to mitigate the vibrations of spring-loaded valves in the industry. Conclusions and recommendations for future work are given in Chapter 6. Finally, Appendix A contains supplementary material regarding calibration of the sensors and measurement equipment.

1.6 A Note to the Reader

Due to the editorial requirements of this thesis, stemming from the act of including three journal articles, there is some overlap between some of the chapters. Namely, the introduction sections in Chapters 3–5 contain similarities, although in each case the material is targeted towards specific aspects of the investigation covered in the publication. In addition, the experimental facility is identical for all three sections, but is described in greater detail in Chapter 3 due to its experimental scope. Since the literature survey is fragmented across the three journal publications, a consolidated comprehensive literature review is provided in Chapter 2, which describes the state of

the literature while highlighting the gap in the literature, which prompted the work presented in this thesis. Furthermore, the conclusion, provided in Chapter 6, reiterates the key conclusions stated in Chapters 3–5 while highlighting their placement within the context of this investigation, as well as the original contributions that lie therein.

Chapter 2

Literature Review

2.1 Excitation Mechanisms

Valves can be subjected to a variety of excitation mechanisms, which can all be categorized according to the classification of Naudascher (1963). These are:

- Forced oscillations: these are caused by external loadings that are weakly correlated if not completely independent of the structural behaviour. The valve response can hence be easily computed so long as the forcing function is known.

- Self-controlled oscillations: in certain cases there can be periodic flow phenomena such as vortex-shedding that apply a periodic load on the structure. Outside a certain fluid force frequency and amplitude range, the structure reacts according to the case of forced oscillations. Within this range, the fluid force is dependent on the structural motion, and a feedback mechanism comes into play. Most of the evidence regarding whether one should be concerned with the occurrence of these types vibrations is empirical, and consequently is typically available for

specific cases.

- Self-excited oscillations: In this case, the external loading on the structure is dependent on its motion and the system oscillations grow unstable after the system is initially disturbed. These oscillations exhibit self-amplification and nonlinear limit cycle behaviour.

In addition to the general classification of Naudascher (1963), some insight specific to the case of hydraulic control devices can be gained from the work of Kolkman (1976). His work indicated that the hydraulic forces acting on a valve can be in phase with the valve displacement and velocity, providing added stiffness and damping to the system, respectively. Furthermore, it is seen that for a low valve velocity, the valve not only experiences a damping effect but the fluid velocity is also proportional to the valve lift. At high valve velocities on the other hand, the system experiences added stiffness, mainly due to the fluid inertia which tends to dominate and cause the flow characteristics to remain steady through the valve. He also provides some guidelines regarding geometrical considerations that need to be made to minimize sensitivity to flow-induced vibration. Essentially, the geometry should be selected such that unstable separation of the flow is avoided as much as possible. This requirement is obviously difficult to achieve in valve designs.

2.2 Early Investigations

The earliest investigations of spring-loaded valve stability issues were conducted by Kasai (1968). The author's approach mainly involved a theoretical treatment of stability issues in poppet valves with elastic supports, which are frequently used in hydraulic circuits. Hydraulic circuits are known to have a variety of concerns with

regards to valve dynamics, which can be manifested in a delayed dynamic response of the valve and through "chirp" sounds. The theoretical framework that was first presented by Kasai (1968) and later on further extended by Hayashi (1995) resulted in a nonlinear coupling between the inertia of the hydraulic fluid in the inlet piping system and the poppet valve. By using a linearized ordinary differential equation to characterize the poppet valve displacement, the net energy over a period of vibration of the poppet valve can be computed:

$$\Delta E = -\pi\delta\omega x_0^2 + \pi A_{ep} p_0 x_0 \sin\phi \tag{2.1}$$

where δ is the viscous damping, x_0 is the valve displacement amplitude, p_0 is the chamber pressure amplitude, and A_{ep} is the effective flow area of the poppet valve. While the first term is always negative, the sign of the second term depends on the phase angle ϕ between the pressure in the hydraulic chamber and the valve displacement. Hence if $\sin\phi$ is positive, and the second term is large enough such that the energy is added over a cycle rather than dissipated, then the system is unstable, and the vibration of the poppet valve is of course amplified.

There are various physical causes to the phase angle ϕ. One reason is the compressibility of oil in the valve chamber, however small. Transmission delay to a long pipeline can also be a contributing factor. Other delays due to actuators, pumps, and other control valves can also be the source for this phase angle ϕ, and cause instability.

Hence, two types of instabilities were observed. By investigating the valve lift as a function of supply pressure, it can be seen that as the downstream length is increased, the instability region grows. This stability characteristic is referred to as local stability, and is manifested through self-excited vibration if the system is in that region for a sufficiently long pipe. These regions are shown in Figure 2.1, where the three curves A,

B, C denote increasing downstream lengths, respectively. On the other hand, global

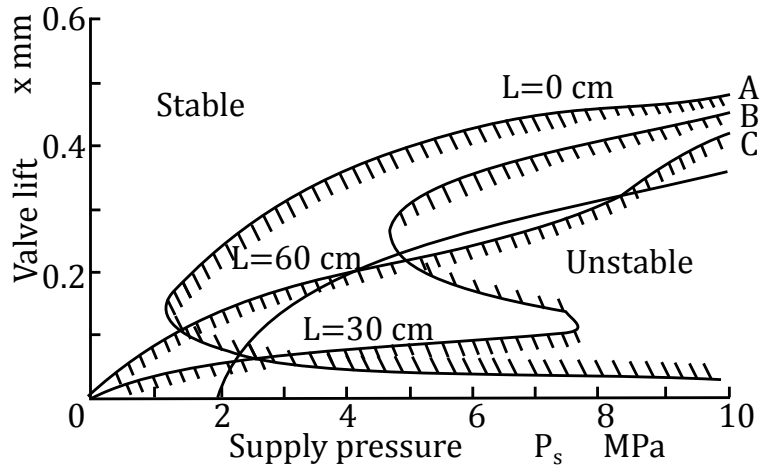

Figure 2.1: Self-excited poppet valve local instability regions. (Hayashi, 1995)

“hard" excitations were found to depend on the velocity perturbation in the hydraulic chamber. When it exceeds a certain threshold or critical value, limit cycle oscillations can be observed. This self-excited oscillation is manifested through amplitude growth to a stable limit cycle. This is certainly a stability feature of a nonlinear system.

While the above approach provided an interesting theoretical framework for looking at nonlinear stability behaviour in hydraulic control devices manifested through the occurrence of chaos and bifurcation, there are certain shortcomings to be noted. First, there is very little experimental data available to provide confidence in the prediction capabilities of these models. Furthermore, the upstream and downstream effects are only considered to be inertial. These two concerns make these types of models of little use beyond providing a qualitative understanding of nonlinear stability in control valves undergoing self-excited oscillations.

2.3 Steady-Fluid Loading Studies

One of the other early studies attempted to investigate the detailed flow properties around the valve disc for the purpose of computing the unsteady forces on a compressor valve plate was conducted by Killmann (1972). He considered the flow at five chosen locations around various valve configurations. These configurations differ in the aspect ratio between the valve plate diameter D and the inlet hole diameter d. For illustration purposes, two cases are shown in Figure 2.2.

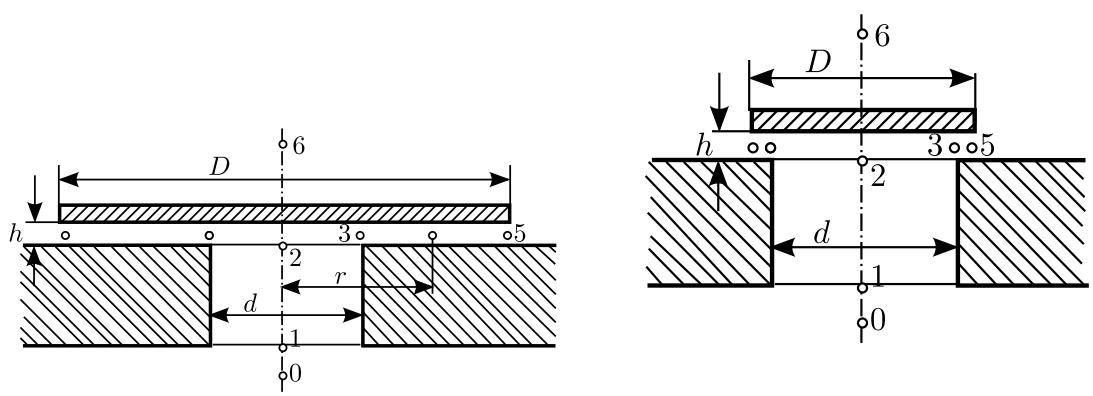

(a) Large D/d ratio. (b) Small D/d ratio.

Figure 2.2: Valve-seat assemblies with different D/d ratios. (Killmann, 1972)

The pressure field on the valve plate was computed by considering the flow to be incompressible, steady, and free of losses. Ignoring the effects of gravity, the static pressure at each of the locations 1–5 can be computed based on the total pressure p_0 and the dynamic head.

Using the above considerations, Killmann (1972) developed net pressure and dynamic head profiles on the valve plate, which are shown in Figure 2.3. Figure 2.3a corresponds to the configuration shown in Figure 2.2a, while Figure 2.3b corresponds to the configuration in Figure 2.2b. The hatched areas show the net pressure differential

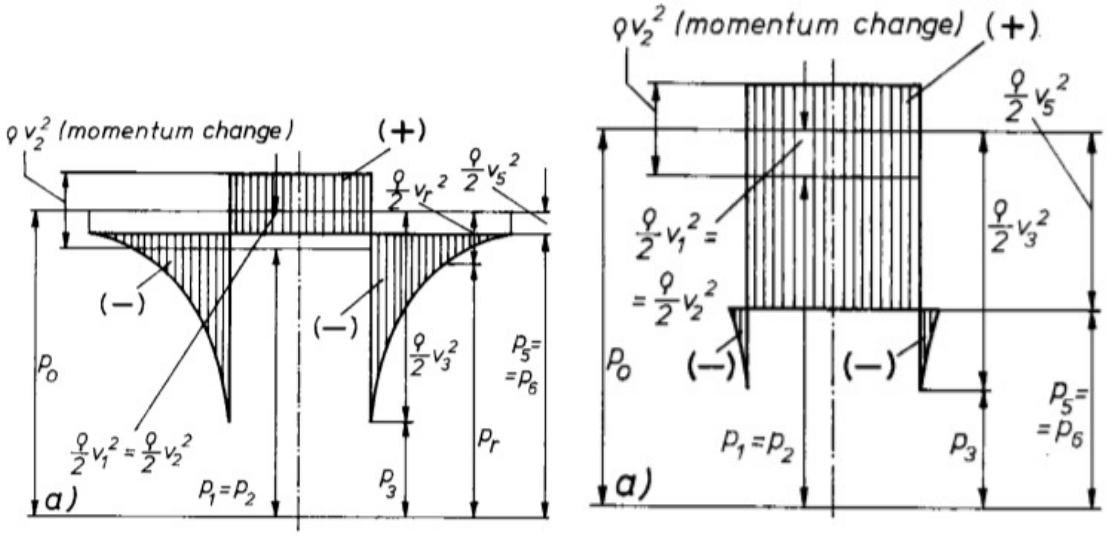

(a) Large D/d ratio. (b) Small D/d ratio.

Figure 2.3: Pressure differential profile along the valve disc. (Killmann, 1972)

along the valve disc. It is seen that in both cases, the area of the valve plate directly above the bore of the inlet pipe is always subjected to uniform positive pressure differential, which would result in a force that is pushing the disc away from the seat. This can be attributed to the fact that within that region the flow is stagnating and required to complete a 90 degree change in direction. Meanwhile, the area beyond the bore is affected by the radial diffuser effects as the flow is directed around the valve disc. Based on the drastic difference in pressure profiles between the small and large D/d cases considered, one expects that this should have some significant effect on the net force on the valve. Killmann (1972) also provides a static stability criterion based on the net force acting on the valve.

It can hence be concluded that the work of Killmann (1972) gives great insight based on established techniques regarding the steady fluid forces acting on a valve. However, unsteady effects are not considered. Other effects, such as flow inertia, coupling with structural effects, or acoustic interaction are also neglected. Furthermore, no

experimental validation has been provided to this model. That said, the work of Tsui et al. (1972) confirms the trends for pressure distribution over the valve observed by Killmann (1972).

2.4 Fluid-Structure Interaction in Valves

The studies mentioned so far only looked at certain aspects of valve vibrations, such as nonlinear stability and steady fluid force distribution on valve plates, and have been fairly limited in scope or practicality. To that effect, Kolkman (1976) was the first to provide a comprehensive overview of modelling considerations for valves, seals, and gates, in addition to a classification to the excitation mechanisms. Furthermore, the author also provides stability predictions based on valve configurations and flow conditions. The approach of Kolkman (1976) relies upon assuming that the flow discharge Q, the gate's flow area A_g, and the head difference ΔH across the system vary with small amplitudes. That is:

$$Q = Q_0 + Q' \tag{2.2}$$

$$A_g = A_{g0} + A_g' \tag{2.3}$$

$$\Delta H = \Delta H_0 + \Delta H' \tag{2.4}$$

where the quantities with the 0 subscript represent the mean components of the indicated variable while the primed quantities represent the unsteady fluctuating component. Hence, the force acting upon the valve can be obtained based on the dynamic head, and one may write an equation of motion:

$$-m\ddot{y} - c\dot{y} - ky = \rho g A_c \Delta H' \tag{2.5}$$

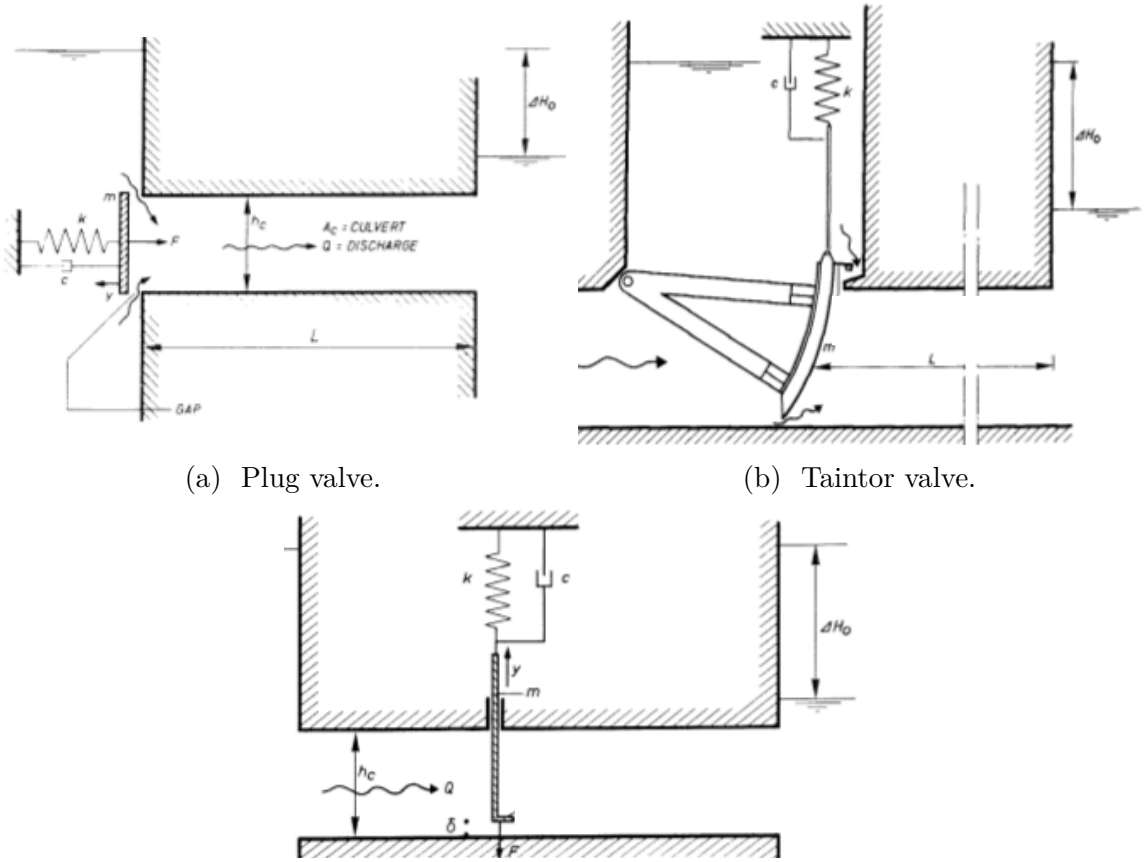

(a) Plug valve.

(b) Taintor valve.

(c) Hydraulic gate.

Figure 2.4: Various valve geometries considered by Kolkman (1976).

where y is the valve displacement. The fluctuating component of the head across the valve may be calculated based on the classical equation for discharge capacity with valve piston effects. This model may be applied to a variety of valves, gates, and seals, such as the ones shown in Figure 2.4. Following this approach results in a single linear differential equation which is simply an equation of motion with added mass, damping, and stiffness that are supposed to account for fluid effects. This means that one can develop a simple linear stability criterion to predict valve stability based on system parameters. However, one must keep in mind the following:

- While simple in implementation, it is not possible to use this model for valves

where a small amplitude assumption for the valve displacement and flow parameters does not hold. This is the case for multi-ring disc valves, where it has been reported that a valve may experience oscillations with amplitudes equal to the maximum lift (*i.e.* the valve moves from seat to limiter over a cycle of oscillation). For these same valves, dynamic pressures can reach amplitudes equal to 35% of the static pressure. It becomes clear that the small amplitude assumption may not hold in this particular case.

- Whereas the straight-forward linear stability criterion that one is able to develop using this approach may be seen as an asset, it is clear that self-excited vibrations in valves exhibit nonlinear stability behaviour that will not be captured by this criterion. Such behaviour is manifested through limit cycle oscillations as well as stability properties that are dependent on the initial conditions of the valve and external force amplitudes rather than the system geometry and parameters by themselves.

In order to overcome the small amplitude limitations of the previous model, Weaver and Ziada (1980) postulated that it was possible to consider the flow as incompressible, inviscid, and one-dimensional in order to use the unsteady Bernoulli equation to represent the flow characteristics before and past the valve. The unsteady Bernoulli equation is stated as:

$$\frac{P_i}{\gamma} + \frac{V_i^2}{2g} = \frac{P_j}{\gamma} + \frac{V_j^2}{2g} + h_{ij} + I_{ij}\frac{dQ_{ij}}{dt} \tag{2.6}$$

where P is the pressure, γ is the specific weight of the fluid, V is mean flow velocity, h represents turbulent losses, and Q is the discharge. i and j are two locations in the system. I_{ij} is the inertance of the fluid in the system between i and j. The flow across the valve is simplified by considering an orifice plate as a suitable model for the flow

across the valve, as shown in Figure 2.5. This model is described in further detail in

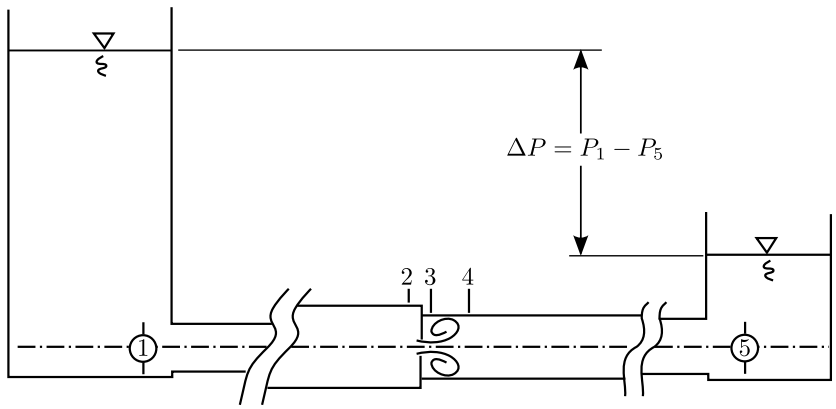

Figure 2.5: Unsteady Bernoulli model of the hydrodynamic system. (Weaver and Ziada, 1980)

Chapter 4, as the approach followed to describe the hydrodynamic effects around the spring-loaded valve for the proposed work is similar. Weaver and Ziada (1980) also found that self-excitation in most valves is not damping controlled. That is, negative damping alone does not account for certain observed behaviour. For instance, negative damping cannot explain a decrease in oscillation frequency for an increase in valve spring stiffness which is a counter-intuitive concept in itself. Hydrodynamic loads in phase with the valve displacement are hence required.

This model has been shown to work remarkably well by simplifying complex flow patterns around various valve geometries, as confirmed by experimental validation of the model for swing check valves (Weaver and Ziada, 1980). Its implementation to predict limit cycle oscillations for plug valves was also successful, as evidenced by D'Netto and Weaver (1987). This model, however, neglects acoustic effects, which have been shown to be significant in the literature for spring-loaded compressor valves.

2.5 Acoustic Interaction & Spring-Loaded Valves

A first characterization of the acoustic effects for a typical multi-ring disc valve was provided by Ziada et al. (1986). The valve was placed in steady flow, with various upstream pipe lengths. What was found that is radically different from other investigations up until that point was that the valve oscillation frequency depended on the acoustic properties of the system. This can be seen in Figure 2.6. The markers

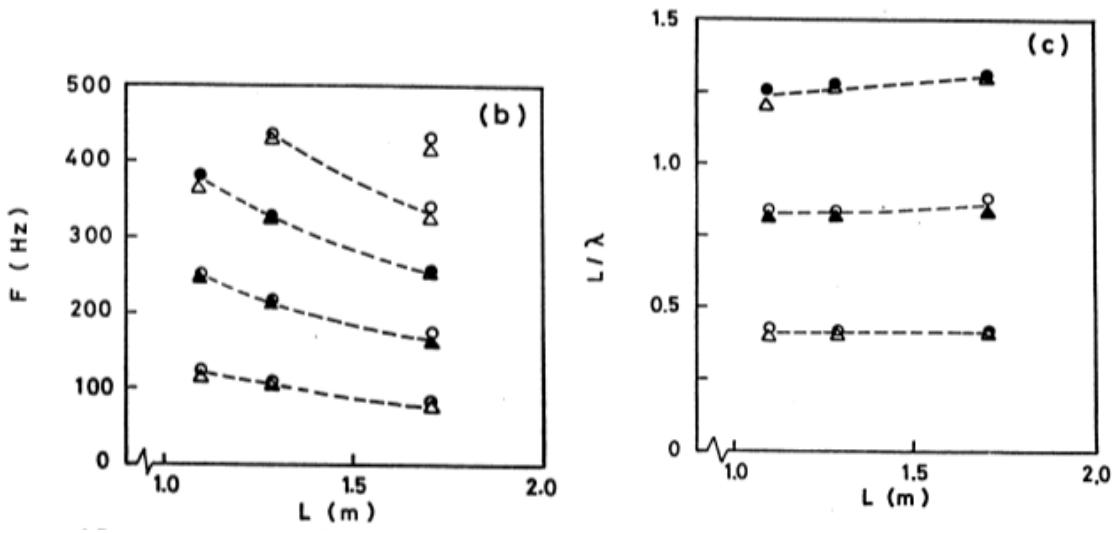

(a) (b)

Figure 2.6: Spring-loaded multi-ring disk valve oscillation frequencies and wavelengths for various spring stiffness values. (Ziada et al., 1986)

indicate the use of different stiffness values on the valve spring. It can be seen that increasing the upstream pipe length gradually decreased the frequency of oscillation. Meanwhile, the valve stiffness only had a role in determining which mode was dominant. Furthermore, while one would expect that for the first mode $L/\lambda_1 = 0.5$, as would be the case for an open pipe, Figure 2.6b clearly shows that the actual wavelength is smaller. Furthermore, it was revealed that the self-excitation mechanism always occurred while the valve was parallel to its seat. The authors also found that with

asymmetrical spring stiffness, to introduce tilting of the valve plate, it was possible to suppress the valve's vibrations to acceptable levels. Further experimental investigations

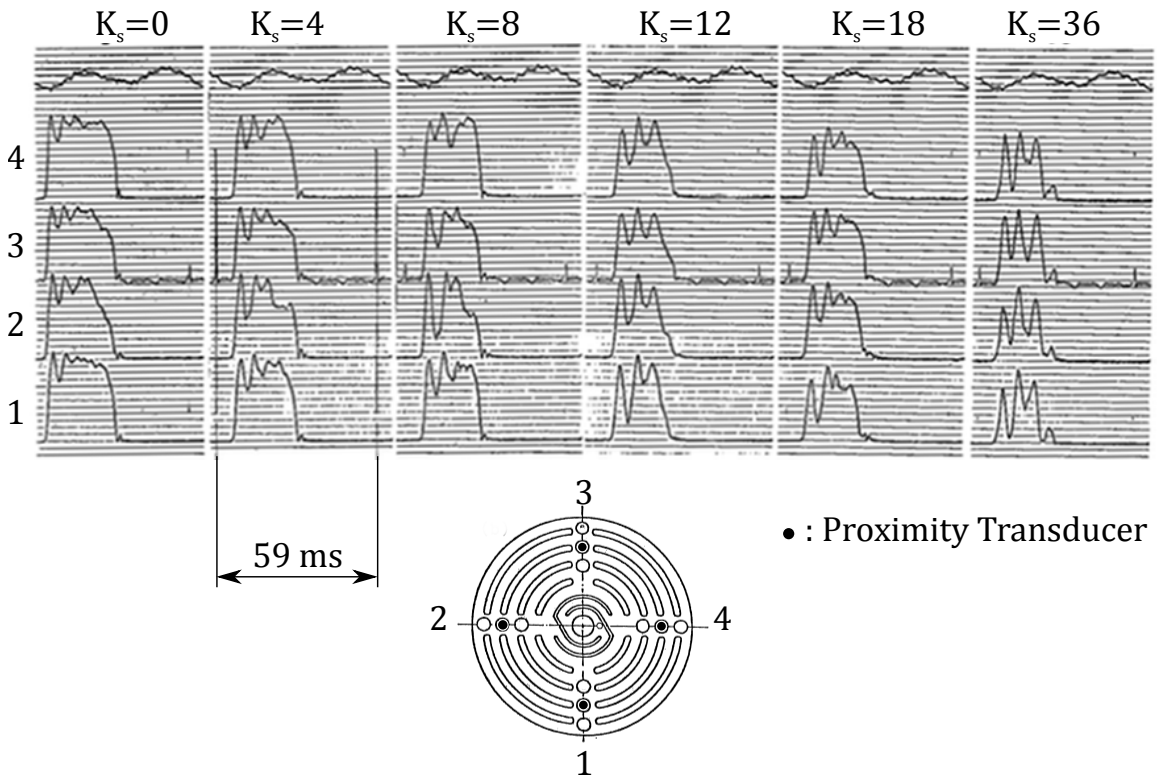

Figure 2.7: Valve plate displacement at four different locations for pulsating flow over a cycle of valve opening. $K_s = 0$–36 N/mm. (Oengören, 1987)

were conducted on the same valve by Oengören (1987). The device was subjected to pulsating flow, as is the case in reciprocating compressors. Time signals of different proximity sensors measuring the valve plate displacement at different locations are provided in Figure 2.7. Once again, one can notice that all transducer measurements are nearly identical and in phase, suggesting that the valve plate is oscillating while remaining parallel to its seat, *i.e.* no rocking motion is involved. Another important discovery was that the valve would experience self-excited oscillations regardless of whether the flow was steady or pulsating. As a matter of fact, the valve's pulsating flow response is merely its dynamic response under steady flow super-imposed upon

its nominal opening profile.

Furthermore, one can notice that an increase in the stiffness of the system increases the valve's dynamic response. This is counterintuitive as it is common knowledge that flexible structures (low stiffness) are more likely to vibrate at higher amplitudes.

While their findings shed some light on the flow-sound-structure coupling in multi-ring disc valves, these studies (Ziada et al., 1986; Oengören, 1987; Shine, 1987) were conducted for the purpose of selecting a proper stiffness for a particular valve design. Consequently, it is not possible to generalize the results to all spring-loaded valves, although one may still gain some insight regarding system parameters with most influence on the valve's dynamic behaviour.

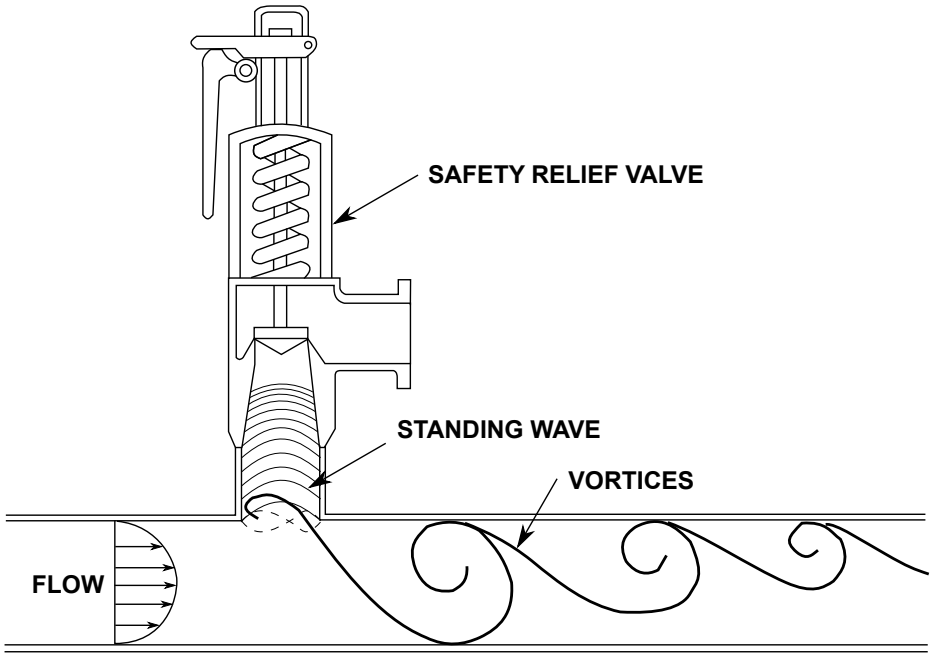

Figure 2.8: Vortex-generation induced instability mechanism for a safety-relief valve. Reproduced from Baldwin and Simmons (1986).

Further insight stemming from practical issues in spring-loaded valves is provided by Baldwin and Simmons (1986). After conducting over 40 field tests of safety-relief valves in power plants, they postulated that the instability is due to a flow-sound structure

interaction mechanism. Furthermore, they propose vortex generation as a precursor to the instability. The overall scenario is illustrated in Fig. 2.8. It can be seen that a common configuration for a pressure relief valve consists in mounting the valve on a perpendicular side branch to the pipeline, often with some inlet length. However, flows over side branches and cavities are known to generate vortices, which upon impingement on the trailing cavity edge will produce upstream pressure pulsations. The feedback mechanism between the pressure pulsations and vortex-shedding mechanism will in turn amplify the magnitude of the pressure oscillations. The vortex-shedding frequency is dictated by the upstream flow velocity U and the side branch gap-length L, as described by the following relationship:

$$St = \frac{fL}{U} \tag{2.7}$$

where St is the Strouhal number, a non-dimensional quantity commonly used to relate length and time scales in periodic flow structures. If the aforementioned vortex-shedding frequency coincides with an acoustic resonance frequency of the side branch, the acoustic pulsations may be large enough at the safety-relief valve plate that chatter or leakage could occur. In addition to proposing an instability mechanism in safety-relief valves, Baldwin and Simmons (1986) also provided a stability map for valves operating at given Mach and Strouhal numbers. Beyond indicating a broad range of problematic Strouhal numbers ($St < 0.6$), their map shows that compressibility effects (*i.e.* the effect of Mach number) are only weakly correlated to the onset of instability. Unfortunately, while their tool provides the designer with a criterion to determine whether certain operational conditions are likely to become problematic, the Strouhal number range identified is far too broad. In addition, their stability map does not provide a relative measure of vibration severity under given conditions.

Ishii et al. (1993) also investigated the acoustic coupling for a reed valve in a refrigerant compressor. They attempted to clarify the effect of the cylinder and piston. Their experimental setup is shown in Figure 2.9. The illustration shows a magnetic exciter, which is only used for validation of the theoretical resonance frequencies by exciting the cylinder at its Helmholtz frequency. It is then replaced with a reed valve for the remainder of the experiment. It can be seen that while the location of the

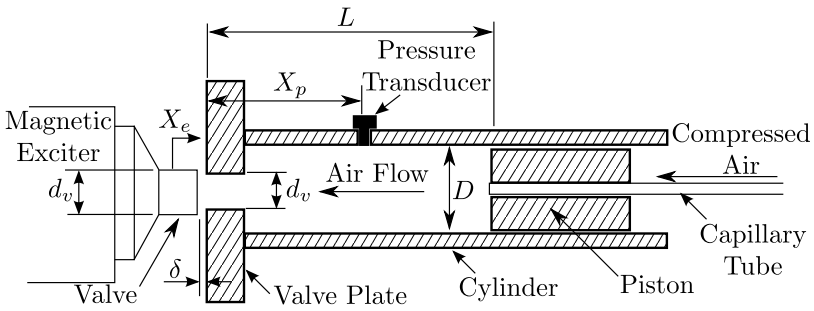

Figure 2.9: Valve-cylinder experimental setup. (Reproduced from Ishii et al. (1993))

piston was adjustable, it was maintained at a static location for the duration of the experiment. A constant pressure differential was maintained through a compressed air supply tube. The valve displacement amplitude and phase were investigated for various piston locations. While they concluded that vibration frequency of the reed valve is influenced by the Helmholtz resonance frequency, their experimental findings did little to reinforce this hypothesis. There is certainly an upward trend as the flow-path length is decreased, which is consistent with the hyperbolic nature of the Helmholtz resonance frequency, which is inversely proportional to the cylinder volume. Nonetheless, the correlation is rather weak based on their results, and it is not clear if the authors are suggesting that the oscillation frequency is that of a combined valve-cylinder acoustic system, or if it is simply the acoustic frequency.

In order to account for the fluid compressibility effect within a piping system of a hydraulic control valve, Misra et al. (2002) developed a dynamic model of a feedwater

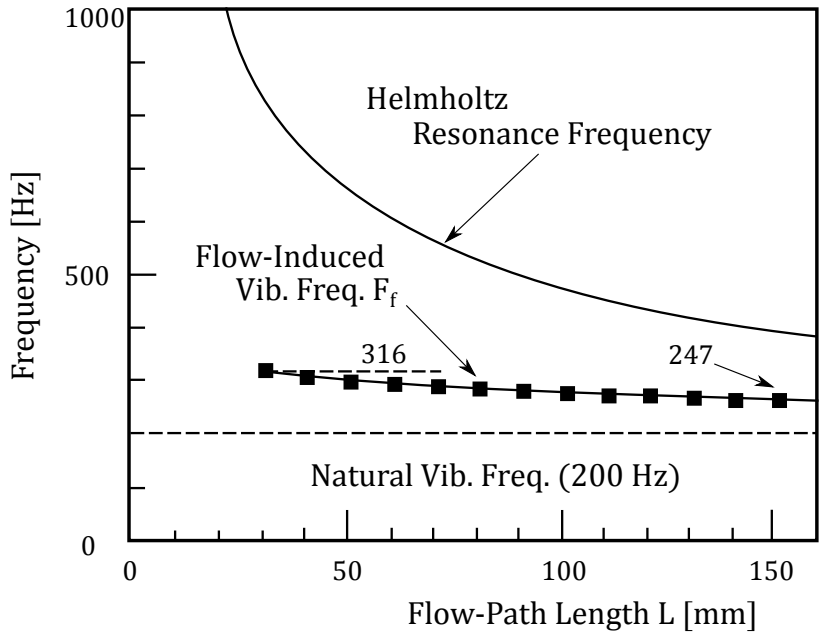

Figure 2.10: Frequency phase plot for various cylinder volumes.(Ishii et al., 1993)

system based on the approach of Hayashi et al. (1997). The valve structure was modelled as a single degree of freedom system subjected to a hydraulic force and an actuator pressure. The hydraulic force depends on the upstream and downstream pressures and the momentum of the jet surrounding the poppet valve. The mass flow rate of the jet was determined based on flow coefficients provided by the manufacturer. The upstream pressure was computed based on Bernoulli's equation. The fluctuating pressures in the system were computed using the Euler equation. While the parametric study was extensive as it covered various operating conditions, no experimental validation was provided to the self-excited oscillation prediction capability of this model. In addition, the hydrodynamic model is linear and would be inadequate for large amplitude oscillation, as is the case for multi-ring disc valves. The acoustic wave reflection was also not considered, as the authors only took into account the wave emitted at the valve as it affects the rest of the system.

In the latest work that pertains to compressor valves, building on the assumption

of quasi-steady flow, Habing and Peters (2006) analyzed a gas compressor valve and considered the fluid force exerted on the flow to be in phase with the valve lift. However, they allowed for a phase between the fluid inertia and the pressure drop. That is:

$$\Delta p = \frac{1}{2}\rho_{up}\left(\frac{Q_v}{\alpha L_g h}\right)^2 + \rho_{up}\frac{L_p}{A_p}\frac{d}{dt}Q_v \tag{2.8}$$

where L_p is the valve port length, L_g is the total edge length of the valve plate, ρ_{up} is the upstream density. This model was then used to numerically solve for the valve displacement.

In their model, the unsteady values required to compute the fluid forces (Δp and Q_v) were determined experimentally by means of the two-microphone method. Furthermore, they only provided validation for the quasi-steady component of the model, stating that accounting for inertia effects, *i.e.* through the so called extended valve theory model, "does not describe the fluid-structure interaction processes significantly better".

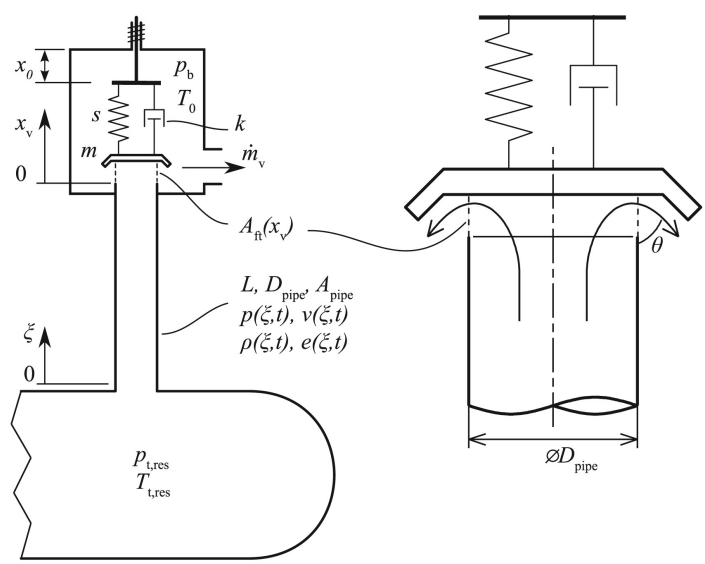

Figure 2.11: Pressure relief valve configuration modelled by Erdődi and Hős (2017).

In more recent work, studies have focused on pressure relief valves in pipelines.

Moussou et al. (2010) conducted an experimental study on a pressure relief valve in a water pipeline that lead to the development of a theoretical model of the valve based on empirical static coefficients. The model developed is primarily used to determine whether instability would occur rather than predict the oscillatory time response of the valve. The model does however take into account acoustic effects through experimental measurement of acoustic reflection spectra. Allison and Brun (2016) considered flow-sound-structure interaction in a pilot-operated pressure relief valve, which is a common spring-loaded valve design. Their experimental tests demonstrated the existence of acoustic coupling and the onset of self-excited oscillations. Meanwhile, the reduced-order model they developed accounts for acoustic effects by solving 1-D compressible momentum and continuity equations. On the other hand, it is not clear what approach they are using to model impact on the seat and stopper. Nevertheless, this approach demonstrates the potential for simplified analytical models in spring-loaded valve design. Finally, Erdődi and Hős (2017) developed a gas-dynamics model for a pressure-relief valve in the configuration shown in Fig. 2.11. Their model appears to capture the essence of the instability mechanism. However, their validation originates from Computational Fluid Dynamics (CFD) simulations of their valve rather than experimental data. Furthermore, their elastic impact model does not allow for prediction of the contact forces acting on the valve, which can be instrumental for fatigue-life predictions of plant components.

So far, valve vibration has been presented as a nuisance to industrial processes. This is not always the case. There are certain cases where this is the desired outcome, such as in musical reed instruments. Most wind instruments rely upon a system composed of an acoustic exciter and an acoustic resonator in order to produce music (Hirschberg et al., 1990). In reed instruments, the reed is a flexible strip that acts as an acoustic excitation source by oscillating similarly to a valve due to a pressure differential between

the player's mouth and the atmosphere. The actual nature of the excitation source is still a matter of debate. It is postulated that the reed acts as an inlet impedance to the resonator. Another possible explanation is the existence of a fluid resonant mechanism where the oscillating reed causes oscillating jets to form around it, thus providing the required sound source.

The insight on wind instruments stems from early work by Wilson and Beavers (1974) on clarinets. They developed a simplified mouthpiece-resonator test rig and demonstrated that for a lightly damped reed, the clarinet operates at the duct mode that is the closest to the reed's natural frequency at low blowing pressures. In addition, heavy reed damping can be used to ensure that the tones are generated at the lowest mode of the clarinet. Later work by Atig et al. (2004) numerically investigated the amplitude limiting factors causing saturation by studying the effect of linear and non-linear losses at the open end of the clarinet tube. Their model shows that the playing range of a clarinet may be predicted satisfactorily through linear losses. Given the application, these studies have primarily focused on predicting the sound generating features of the instrument, resulting in numerical models that oversimplify the fluid dynamics and dynamic behaviour of the reed.

Another area where flow-sound-structure interaction is a desired outcome is human speech. Several studies have aimed to characterize the self-excited instability of vocal folds. In one such study (Deverge et al., 2003), the authors built and tested mechanically-oscillating models of vocal folds to determine the effect of fold geometry on upstream and downstream unsteady pressure. These experimental results are used as a validation basis for several reduced-order models of the fluid behaviour. However, they do not consider acoustic feedback, nor do they consider structural coupling, as the oscillation of the vocal folds is forced.

2.6 Vibration Mitigation Techniques in Valves

The variation in design, operational requirements, and geometry creates a serious challenge for developing vibration suppression techniques for valves that could be generalized. Consequently, for the few studies available that provide a discussion of solutions to self-excited oscillations in valves, the suggested remedies are unfortunately application specific. The current section seeks to provide an overview of existing attempts to suppress oscillations in spring-loaded valves, and extract insight which maybe useful in a general spring-loaded valve case.

As previously mentioned, Baldwin and Simmons (1986) identified a fluid-resonant mechanism trigged by vortex excitation as a possible cause for safety-relief valve failure in power plants. They reasonably deduced that an effective approach to suppress this valve oscillation was through a reduction of the flow separation and sharp-edge impingement over the side-branch cavity where the safety-relief valve is mounted. Hence, they used common pipe fittings to propose altered designs of the side branch cavity that reduced the potential for vortex generation as well as the pressure feedback mechanism, mainly through rounding of the edges and Strouhal number mismatch. The two designs suggested can be seen in Fig. 2.12. These two designs differ mainly in the types of fittings used which may be more practical for different ranges of L/d nozzle ratios. In order to attenuate the oscillations of a safety-relief valve, with the prerequisite knowledge of the critical frequencies (and conversely critical Strouhal numbers), the designer must size the nozzles such that there is a mismatch between the cavity mode and the vortex generation frequency.

The solutions proposed by Baldwin and Simmons (1986) provide optimistic prospects for valve cases (such as safety-relief valves) where instability issues are present but operational constraints do not allow for modification of the valve's parameters. They

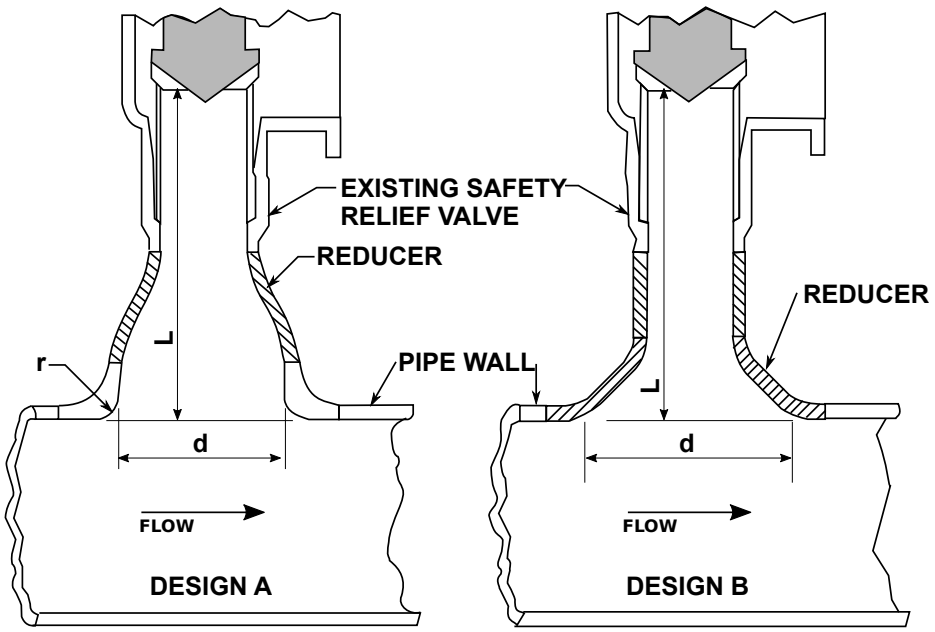

Figure 2.12: Solutions for safety-relief valves proposed by Baldwin and Simmons (1986).

demonstrate that through a reduction of the triggering vortex-generation mechanism it is possible to effectively address dynamic instability issues in valves. However, the nature of their solution limits it to applications with vortex generation due to a side branch cavity.

In the case of the reciprocating compressor valve investigated by Ziada et al. (1986), the authors sought to utilize their observation that vibration was most severe when the valve plate was parallel to its seat. Given that the valve plate in the compressor valve they considered is supported by multiple springs placed at various azimuthal and radial positions, it was possible to force tilting by using springs of different stiffness at diametrically opposite ends of the valve plate. This forced tilting was seen to greatly eliminate the valve oscillations. Further investigation on the same valve design by Shine (1987) indicated that using softer springs in conjunction with increasing the valve spring preload force could reduce the oscillations while still opening at desired

cylinder pressures.

The countermeasures offered by Ziada et al. (1986) and Shine (1987) provide some methods of alleviating dynamic instability in valves that take advantage of specific features of multi-ring disk-type compressor valves. While the forced tilting was shown to suppress the vibration, it would result in the valve plate edge slamming on the seat and stopper during opening and closing. This concentrated loading impact case would likely cause premature failure or wear for the valve. Furthermore, it may not be possible to find a suitable spring preload and stiffness that would eliminate oscillations and still allow the valve to operate as designed. This is especially the case for safety-relief valves, which are designed by forcing a static instability threshold at the opening pressure of the valve. This static instability threshold allows the valve to toggle from completely shut to completely open, rather than linearly open, and depends on the stiffness value of the valve spring.

To conclude, while some studies have attempted to provide solutions to the problem of self-excited vibrations in spring-loaded valves, the suggested remedies have been limited in scope to a specific application. There have not been any suggested solutions that may address instability issues for a general case of a spring-loaded valve experiencing oscillations due to flow-sound-structure interaction. Therefore, it is hypothesized that a practical approach to attenuating the valve vibrations would rely on eliminating the acoustic feedback mechanism, which should provide a robust methodology that is independent of specific intricacies of a particular valve design or application.

2.7 Summary

The existing literature has emphasized that a one-dimensional model of the valve with a simplified geometry subjected to steady flow is able to capture the essence

of the flow-sound-structure interaction mechanism. As a result, the experimental and modelling work herein will consider the valve to be subjected to steady flow and experiencing translational motion in the axial direction of the flow only.

To conclude, while there have been some significant strides in understanding the precursors and spring-loaded valve dynamics, it is clear that there remains a need to understand the underlying mechanisms that are responsible for self-excited oscillations in spring-loaded valves. Furthermore, the role of pipe acoustics needs to be understood, since there is ample empirical evidence of their effect, but the nature of the interaction mechanism has yet to be fully characterized. In addition, a comprehensive model that accounts for non-linear discharge characteristics, valve contact dynamics, and acoustic interaction is needed. Also, there is a lack of practical methods for mitigating these types of oscillations. For this purpose, an appropriate experimental facility is designed, a modelling approach is suggested, and countermeasures are designed and tested in the following chapters.

Chapter 3

Experimental Characterization of the Self-Excited Vibrations of Spring-Loaded Valves

Complete Citation:

El Bouzidi, S., Hassan, M., & Ziada, S. (2018). Experimental characterisation of the self-excited vibrations of spring-loaded valves. *Journal of Fluids and Structures*, 76, 558-572.

Relative Contributions:

S. El Bouzidi: Performed experimental work. Conducted analysis and interpretation of results. Prepared manuscript for publication.

M. Hassan: Co-supervisor of S. El Bouzidi. Provided guidance on experimental work and feedback on manuscript.

S. Ziada: Co-supervisor of S. El Bouzidi. Provided guidance on experimental work and feedback on manuscript.

Abstract

Valves are omnipresent in industrial processes. As a result, they must perform reliably according to their specifications. Spring-loaded valves are particularly susceptible to vibrations, as they are inherently flexible, often operate at small openings, and therefore they are more likely to interact with the surrounding flow. The current study experimentally investigates the self-excitation mechanism of a model spring-loaded valve with an emphasis on the interaction between the system flow and sound fields, and the valve structure. Tests are performed for various values of valve stiffness and maximum allowable valve lift. In each case, the pressure drop across the valve is increased gradually until the valve becomes fully open. The valve was found to oscillate at the fully coupled resonance frequency resulting from the interaction of the valve vibration with the acoustic field of the piping system. The oscillation amplitude was found to be positively correlated to both the pipe length and spring stiffness value. Furthermore, initial spring compression was found to have only moderate effects on the range of static pressures that would cause instability.

Keywords

valves, dynamics, vibration, acoustics, flow-induced vibration

3.1 Introduction

Valves are critical components to industrial processes. Whereas they are often designed to be replaceable and inexpensive, valve failures can cause costly shutdowns in addition to safety hazards in certain applications. Flow-induced vibration is an important concern for the operation of spring-loaded valves, as it can not only shorten the life of the valve but also affect its performance during operation due to oscillations of the flow area. As such, valve vibrations have been an ongoing subject of inquiry for over a half-century. Early researchers investigated stability problems in hydraulic control valves (Kasai, 1968). Subsequent investigations mainly provided steady response modelling of valves subjected to flow (Killmann, 1972; Tsui et al., 1972) or performed a linear analysis of valve vibrations suitable for small amplitude oscillations (Kolkman, 1976). Certain studies considered nonlinearities in the structure of the valve, namely nonlinear gasket stiffness (Nayfeh and Bouguerra, 1990). Others provided physical descriptions of the interaction between the structure of the valve and the flow-field by simplifying the complex flow geometry. Such investigations presented by Weaver and Ziada (1980) as well as D'Netto and Weaver (1987) provide useful prediction capabilities for check and poppet valves. Additional experimental work done by Ziada et al. (1986) on multi-ring disk valves used in reciprocating compressors has exposed some important features of the excitation mechanism and showed that the vibration persists even under steady flow conditions. The vibration frequencies were different from the natural frequency of the valve, which would be due to the valve plate inertia

and valve spring stiffness. The influence of the upstream and downstream piping was also observed, with oscillations observed to occur at frequencies close to the acoustic plane wave modes of the pipes. Finally, the work of Habing and Peters (2006) revealed that gas forces applied to spring-loaded valves in compressors behave in a quasi-steady fashion, while the same cannot be said for the discharge through the valve, especially when the valve virtually closes during vibration.

When acoustic effects are present, previous studies have shown the existence of an interaction mechanism between the structural properties of the valve, the acoustic properties of the piping system, and the fluid flow through the valve. One such study was completed by Baldwin and Simmons (1986), who provided a case study of dynamic instability of pressure relief valves in operation in various locations in steam power plants, and investigated their operational conditions to determine factors affecting instability. Other researchers (Ziada et al., 1987) conducted series of experiments for the purpose of selecting a suitable spring stiffness for a particular valve design in order to mitigate the severity of the self-excited oscillations and demonstrated coupling with the acoustic properties of the piping. Moussou et al. (2010) also considered the effect of reflected acoustic waves at the upstream pipe on the valve's dynamic instability for water flow through a particular safety relief valve. The instability frequencies were found to be a function of the valve geometry and its hydraulic properties. More recently, Allison and Brun (2016) conducted testing on a pilot operated relief valve and found similar acoustic coupling.

Some knowledge of the valve behaviour coupled with a downstream piping system may be gained from the study of musical wind instruments, where the conditions under which dynamic instability occurs need to be understood in order to produce pleasant sounds. The self-excited phenomenon can be considered similar to the spring-loaded valve case as the instrument player applies a pressure differential across the reed, which

will oscillate at frequencies that are believed to depend on the boundary conditions of the tube. However, these studies tend to focus more on the sound resonant and sound radiation capabilities of the instrument rather than the oscillation characteristics of the reed. Wilson and Beavers (1974) experimentally investigated the effects of reed damping on the excited mode of the tube in a clarinet. Atig et al. (2004) provided a numerical analysis of the linear and nonlinear acoustic losses that cause a clarinet to saturate at certain frequencies but excessively attenuate the sound at others, defining its timbre and playing range.

While the above literature about spring loaded valves provides some valuable insight into valve vibration, a generalised description of the valve dynamics that accounts for the effects of the unsteady characteristics of the flow, the valve geometry, and fully defines the influence of the acoustic properties of the piping system remains elusive. To this effect, the current study aims to provide a foundation of experiments on a model spring-loaded valve that can be used to describe the self-excited instability behaviour of spring-loaded valves found in use in the industry, specifically as observed by Ziada et al. (1986, 1987). This will provide a reliable datum against which a simplified model of the unsteady hydrodynamics, the valve structural oscillations, and the acoustic pressure in the piping system could be validated in order to predict and design against flow induced vibration of spring-loaded valves.

3.2 Experimental Methodology

The test facility used for this investigation is shown in Fig. 3.1. The design of the model valve involved several assumptions. A bell-mouth entrance is used for a smooth entrance of the air flow. The flow is then directed through a pipeline of variable length (140 mm in diameter) upstream of the valve test section. The test section

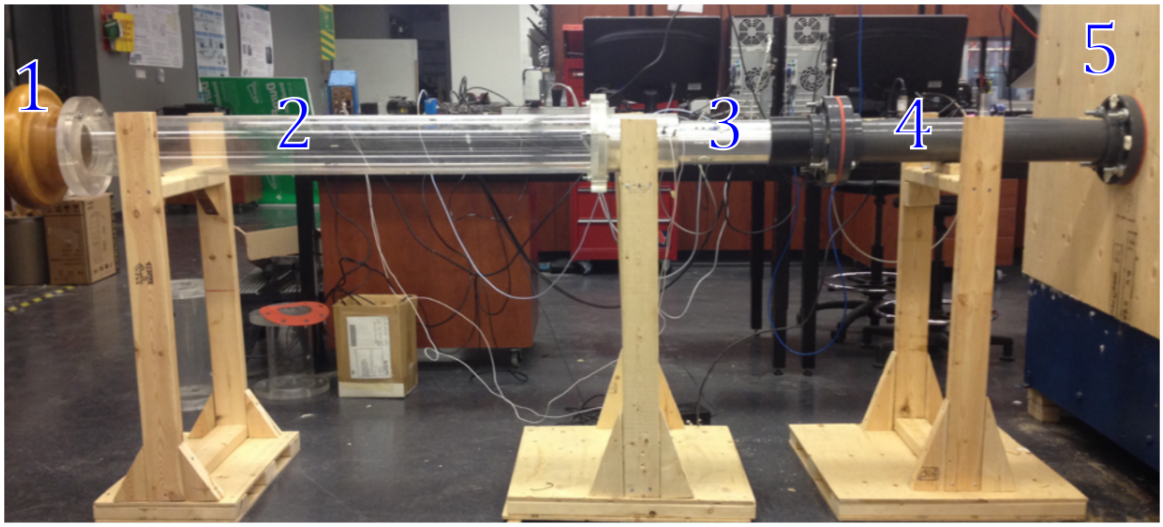

Figure 3.1: Spring-loaded valve test facility. 1- Bellmouth entrance, 2- Upstream piping, 3- Valve test section, 4- Downstream piping, 5- Settling chamber.

contains a spring-loaded valve. Subsequently the flow is guided through additional piping (102 mm in diameter) of variable length to a settling chamber of a Roots blower operating in suction. This blower is manufactured by Cycloblower and driven by a 20 hp (15 kW) Westinghouse AC induction motor with a variable frequency drive unit supplied by ABB (AC S550 series). A schematic of the cross-section of the test rig in

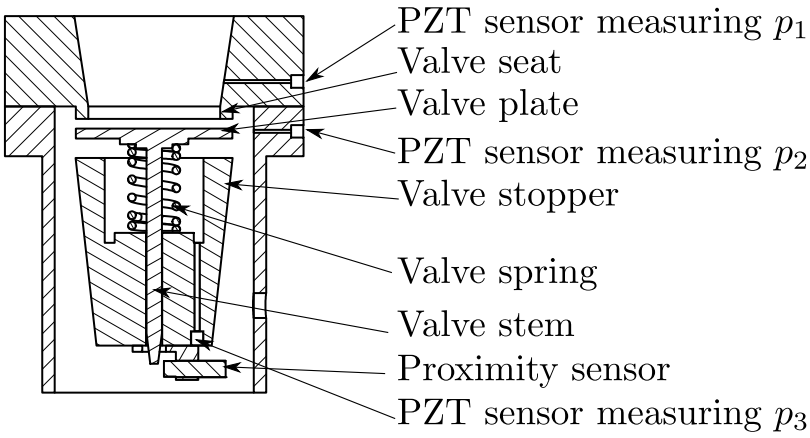

Figure 3.2: Flow channel in the model valve.

the vicinity of the valve is provided in Fig. 3.2. While multi-ring disk valves used in reciprocating compressors usually allow the valve plate to tilt, it is assumed here that the instability only occurs when the valve plate is parallel to its seat and moves in a purely translational motion. This is a fair assumption based on the findings of Ziada et al. (1986). Consequently, the valve model shown in Fig. 3.2 is fitted with a frictionless linear bearing that houses the valve stem such that the valve plate is only allowed translational motion in the axial direction. Furthermore, the test section is fitted with PCB 112A21 PZT high-resolution fluctuating pressure transducers connected to a KISTLER Type 5134 signal conditioner. Hence, p_1 corresponds to a tap in the wall of the pipe before the valve inlet, p_2 corresponds to a tap in the wall of the pipe after the valve inlet, and p_3 corresponds to a pressure collected in the area behind the valve plate. Although the transducers are not flush-mounted, cavity lengths are all short enough such that the lowest cavity mode is 1100 Hz, well above the 30–80 Hz oscillations observed throughout this study. The valve stem is fitted with a Bently Nevada 3300 XL proximity sensor to measure the valve plate displacement. A Validyne DP-15 diaphragm pressure transducer is used with a Validyne CD-15 carrier demodulator unit to measure the static pressure across the whole system. The instruments are connected to a National Instruments PCI-DAQ NI-6221. The acquisition is conducted through a LabView virtual instrument interface.

Several parameters are varied throughout these tests. The valve spring stiffness is varied from 1400 N/m to 4400 N/m. The maximum valve lift is varied between 5 and 10 mm. The valve plate is made of High Density Polyethylene (HDPE) such that it reflects mass ratios similar to the ones seen in production valves. Consequently, the valve plate and stem assembly has a mass of 0.1 kg. The valve plate has a diameter of 80 mm, and a thickness of 8 mm. Additionally, the geometry around the valve inlet consists of sharp edges. Finally, several combinations of piping lengths upstream and

downstream are considered, from cases of no piping to a length of 2.7 m. The tests are conducted by increasing the blower speed, and incidentally the pressure drop, in steps and collecting sensor data over 30 seconds until the valve is completely open.

Data processing is conducted through MATLAB by considering both time and frequency domain signals. Frequency spectra are obtained through a Fast Fourier Transformation (FFT) of the time domain signals over the full 30 second duration. A Hamming window is applied in order to minimise the effects of spectral leakage. Valve vibration signals are decomposed into a mean (time-independent) component and perturbation or fluctuation component. While the signal tends to be sinusoidal for the self-excited case without impact, the occurrence of impact distorts the waveform, and a more suitable way to compare the severity of the vibration is by considering the RMS of the aforementioned perturbation component. When it is necessary to compare different stiffness cases, a non-dimensional quantity needs to be used for the static pressure drop across the valve, as stiffer valves require proportionally higher pressure differentials to open. Similarly, when cases with different maximum lift values are compared, a normalised valve lift quantity needs to be defined. The non-dimensional fluid force F^* and valve lift x^* are defined by:

$$F^* = \frac{\Delta P A_v}{k x_{max}} \tag{3.1}$$

$$x^* = \frac{x}{x_{max}} \tag{3.2}$$

With ΔP the static pressure drop across the system, A_v the valve plate area, k the valve spring stiffness, and x_{max} the maximum valve lift. As can be seen, F^* represents the ratio between the steady fluid force and the maximum valve spring force.

3.3 Theoretical Background

A comprehensive model of the investigated system would require describing the complex interaction mechanisms between the valve structure, the acoustic field, and the hydrodynamic field. The details involved in the modelling and numerical computation for this system are treated in greater detail in a separate publication (El Bouzidi et al., 2017). The following theory is provided as a basis to analyse and understand the experimental results. It relies on a few fundamental assumptions. First, the motion of the valve plate is purely translational, as the instability mechanism is manifested with the valve plate always parallel to its seat in compressor valves Ziada et al. (1986). Second, the flow in the vicinity of the valve is assumed to be mainly one-dimensional. While the flow patterns in multi-ring disk valves and safety relief valves can be quite complex, they are not believed to be the root cause of the self-excited instability in valves. Finally, the instability occurring in steady flow is assumed to be caused by the same mechanism that is seen in reciprocating compressors where the flow is pulsating. This is not an unreasonable assumption as shown by experimental investigations of Ziada et al. (1987). The equation of motion of the valve plate may then be stated as:

$$\begin{cases} m\ddot{x} + c\dot{x} + k\left(x - \delta_0\right) = F_{hyd} + F_{ac}, & x \in [0, x_{max}] \\ m\ddot{x} + c\dot{x} + k\left(x - \delta_0\right) = F_{hyd} + F_{ac} + F_{imp}, & x \notin [0, x_{max}] \end{cases} \tag{3.3}$$

where m is the mass of the valve, k the stiffness of the valve spring, and c is the damping coefficient. F_{imp} represents the net impact force on the valve which is generated during contact with the seat or limiter. δ_0 is the pre-load deflection on the spring. F_{hyd} and F_{ac} are respectively the net hydrodynamic and acoustic forces on the valve plate, which are motion dependent. They will be described in further detail in the remainder of

this section.

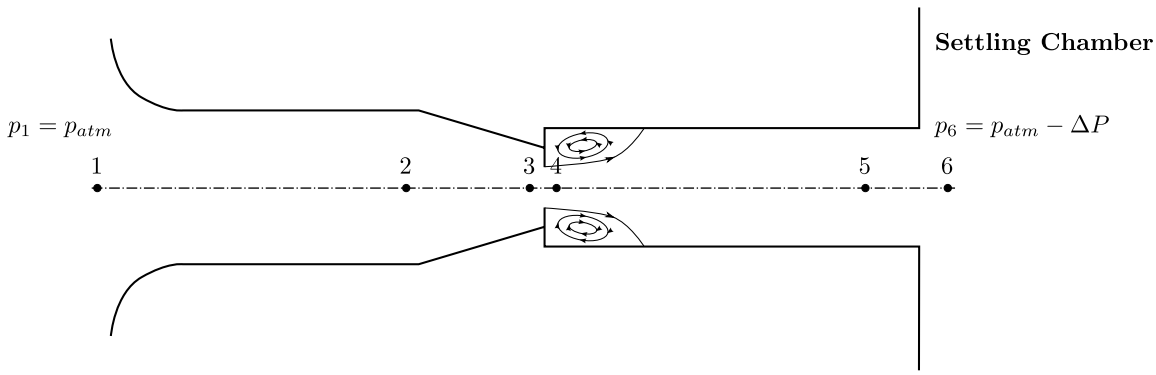

Figure 3.3: Hydrodynamic configuration of the valve.

The hydrodynamic force can be determined through knowledge of the unsteady flow conditions acting upon the valve. For this purpose, great insight can be gained by following the approach of Weaver and Ziada (1980). Such an approach is illustrated by Fig. 3.3 and can be briefly explained by stating that the flow between any two stations i and j can be described by the unsteady Bernoulli equation:

$$\frac{p_i}{\gamma} + \frac{V_i^2}{2g} = \frac{p_j}{\gamma} + \frac{V_j^2}{2g} + h_{L_{ij}} + I_{ij}\frac{dQ}{dt} \tag{3.4}$$

where p is the static pressure, γ is the specific weight of the fluid, V is the mean velocity, and Q is the flow rate or discharge through the system. All non-orifice related losses between stations i and j are assumed to be turbulent and are accounted for within the head loss term $h_{L_{ij}}$. The inertance of the fluid, I_{ij}, represents the pressure differential required to accelerate the fluid through the system. Solution of the above equation coupled with the equation of motion of the valve can yield the instantaneous hydrodynamic force acting upon the valve.

The acoustic system is represented in Fig. 3.4 for the upstream pipe, assuming a driver-pipe configuration as described by Kinsler et al. (1999). For the scenario where

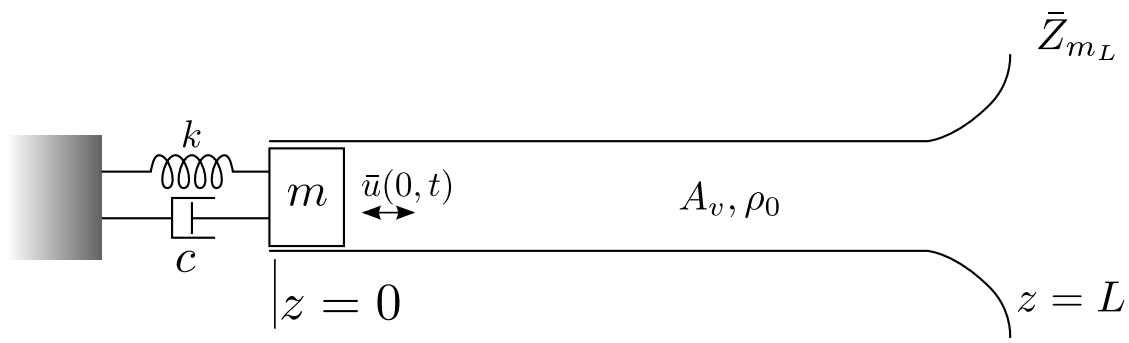

Figure 3.4: Valve–pipe configuration of the valve.

the driver (mass-spring-damper) is only interacting with the pipe, and is subjected to a harmonic external force ($\boldsymbol{f} = Fe^{j\omega t}$) that is only dependent on time, the equation of motion may be given as:

$$m\ddot{x} + c\dot{x} + kx + A_v\boldsymbol{p}(0,t) = Fe^{j\omega t} \tag{3.5}$$

where $\boldsymbol{p}$ is the complex acoustic pressure. Hence the oscillating valve is only subjected to two forces in this case: a hypothetical harmonic load and the acoustic pressure at $z = 0$. From Fig. 3.4, it can be assumed that the valve plate velocity $\dot{x}$ is equal to the acoustic particle velocity at $z = 0$, *i.e.* $\boldsymbol{u}(0,t) = \dot{x}$. Hence, by substituting the acoustic particle velocity into Equation (3.5), the following relationship may be obtained:

$$c + j\left(\omega m - \frac{k}{\omega}\right) + \frac{A_v\boldsymbol{p}(0,t)}{\boldsymbol{u}(0,t)} = \frac{\boldsymbol{f}}{\boldsymbol{u}(0,t)} \tag{3.6}$$

Thus, it can be said that the applied harmonic force driving the combined system sees the impedance of both the valve structure and the connected pipe. Additionally, the resonant frequencies can be found by equating the imaginary part of Equation (3.6) to zero. This means that:

$$Im\{\boldsymbol{Z}_{mv} + \boldsymbol{Z}_{m0}\} = 0 \tag{3.7}$$

where the first term $\boldsymbol{Z}_{mv}$ is the mechanical impedance of the valve whereas the second term $\boldsymbol{Z}_{m0}$ is the inlet impedance of the pipe. A solution of Equation (3.7) provides the eigenvalues of the fully coupled structural–acoustical system.

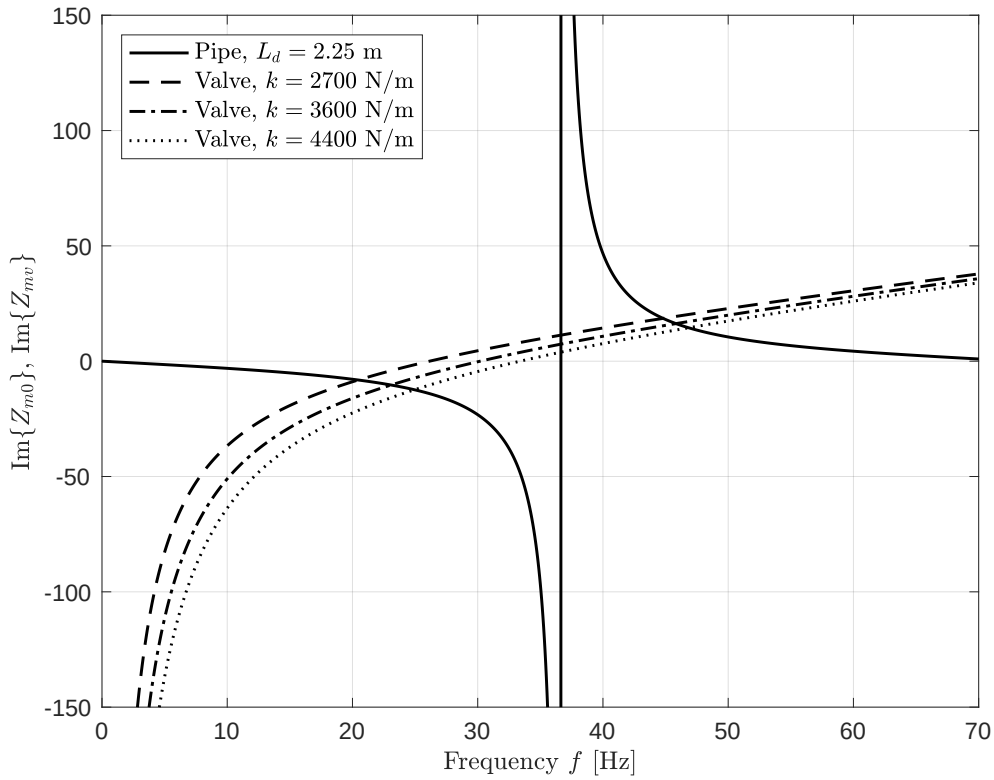

Figure 3.5: Graphical solution of Eq. (3.7) for $L_d = 2.25$ m.

A sample solution to Eq. (3.7) is provided in Fig. 3.5 for one of the unstable cases. The imaginary part of the pipe inlet impedance is plotted for a 2.25 m long pipe with an inner diameter of 102 mm (4 in). The intersection between the impedance plots for the valve structure and pipe represents the combined modes of the system. The intersection point around 43 Hz appears to be the dominant mode for experiments with a downstream pipe length of 2.25 m. The above procedure can be used to predict possible oscillation frequencies of the coupled system for different pipe lengths.

3.4 Results & Discussion

General dynamic behaviour

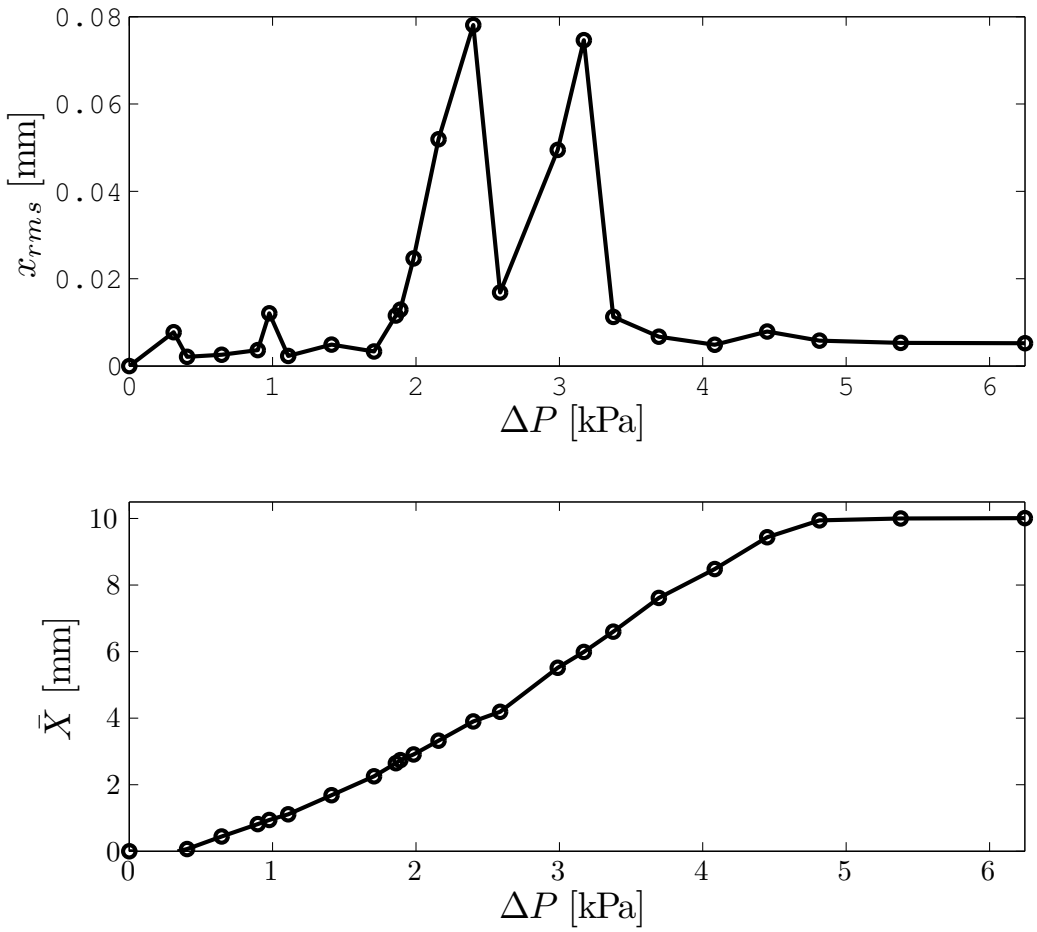

Figure 3.6: Mean and fluctuating valve lift for a *stable case* vs. total pressure drop with $k = 2700$ N/m, $x_{max} = 10$ mm, $L_d = 0.75$ m, $\delta_0 = 1$ mm. Top: RMS of the valve lift oscillation, Bottom: Mean valve lift.

Figure 3.6 shows the valve opening and oscillation characteristics for a stable case. While the top figure shows the RMS vibration amplitude plotted against the pressure

drop across the whole system, the bottom figure shows the mean valve position. It is seen that the valve opens almost linearly after the pressure drop overcomes the initial spring preload, until it reaches the maximum allowable lift of 10 mm in this case. Despite the presence of a pipe downstream with a length of 0.75 m, no instability is observed, as the fluctuations only cause slight deviations from the nominal lift at any given pressure. As is evident from the valve vibration RMS amplitude which does not exceed 0.08 mm, this small amplitude oscillation is likely caused by the flow turbulence. Similar results were observed for spring stiffness values of 3600 and 4400 N/m. The valve was also seen to be stable with a downstream pipe length of 1.6 m, albeit with slightly higher vibration amplitude (8% of max. valve lift).

When the downstream pipe length is increased to 2.25 m, the valve can be seen to experience severe vibrations. Figure 3.7 illustrates this case, where the highest RMS amplitude shown is 3.55 mm corresponding to a sinusoidal amplitude of 5 mm. The valve plate is hence impacting on both the seat and limiter. Furthermore, the onset of instability appears to be sudden, where the valve transitions abruptly from a stable state with barely any oscillation to severe vibrations, as can be seen around 2.71 kPa. A similarly sudden transition is seen from the instability state back to a stable state once the pressure exceeds 4 kPa. Additionally, it can be seen that there is a pressure recovery when the valve transitions from its unstable to stable state, as can be seen through the sudden decrease in the pressure differential. Samples of time domain signals during excitation for this case when $\Delta P = 2.71$ kPa are shown in Fig. 3.8 for a few cycles over a duration of 0.1 seconds.

For the static pressure difference prescribed in this case, the valve is seen to oscillate almost sinusoidally at a frequency near 35 Hz with a peak-to-peak displacement of 6 mm, which is very large considering the maximum allowable motion is 10 mm. Visual inspection shows that the fundamental frequency is the same for all the plots shown

in Fig. 3.8. A spectral analysis over the whole measurement window of 30 seconds indicated that this fundamental frequency is 34.7 Hz, seen across all plots. Higher harmonics can also be seen in the plot of p_1 which are found to occur at frequencies of 69.4 Hz and 103.5 Hz. Furthermore, one can notice a significant increase in the amplitude of the pressure fluctuation going from p_1 to p_3, where p_3 is the pressure measured behind the valve plate. One may also note the phase lag between the net pressure across the valve Δp_{13} and the valve displacement x.

When the static pressure difference is increased to 3.6 kPa the valve can be seen to impact upon its seat and limiter. The sharp corners at the lowest and highest points of the oscillation signal shown in Fig. 3.9 demonstrate this feature. Inspection of the FFT plots indicates that the dominant frequency is 41 Hz, suggesting a slight change in the frequency of oscillation even though the valve's stiffness remains the same. This is likely due to impact which truncates the oscillation cycle and reduces the period of oscillation.

Figure 3.10 shows the unsteady pressure difference across the valve between locations 1 and 3, where 1 is the pressure tap prior to the valve inlet and 3 is the pressure tap in the valve backplate area. The unsteady pressure is shown against the valve displacement. Figure 3.10 is a convenient way to illustrate work done over a cycle. The figure presents a case where the valve is self-excited without the occurrence of impact. The solid line shows 7 cycles of the valve's oscillations while the dashed line shows an averaged cycle over 24 cycles. Based on the orientation of the curve (as indicated by the arrows) one can notice the presence of hysteresis as more work is done during the opening phase of the valve compared with the closing phase.

While Fig. 3.10 is an indicator for the work done over a cycle, Fig. 3.11 shows the energy added over a cycle of oscillation, as it presents the unsteady pressure as a function of the valve plate velocity. The averaged curve shown by a dashed line in

Fig. 3.10 is used for its computation. The first and third quadrants of the cycle are the ones where energy is transferred from the fluid to the valve structure, while the second and fourth quadrants dissipate energy from the structure to the fluid. From the size of the first and third quadrants it can hence be seen that there is a net addition of energy from the fluid to the structure of the valve over a cycle of oscillation. While operating conditions described thus far either result in a convergence towards a stable equilibrium or sustained self-excited oscillations, there were marginal instability cases where the oscillatory behaviour of the valve resulted in periodic pulses of wavelets, as can be seen in Fig. 3.12. For this case, this behaviour determines a transitioning static pressure between unstable self-excited oscillations and stable dynamic valve behaviour once this pressure is sufficiently exceeded.

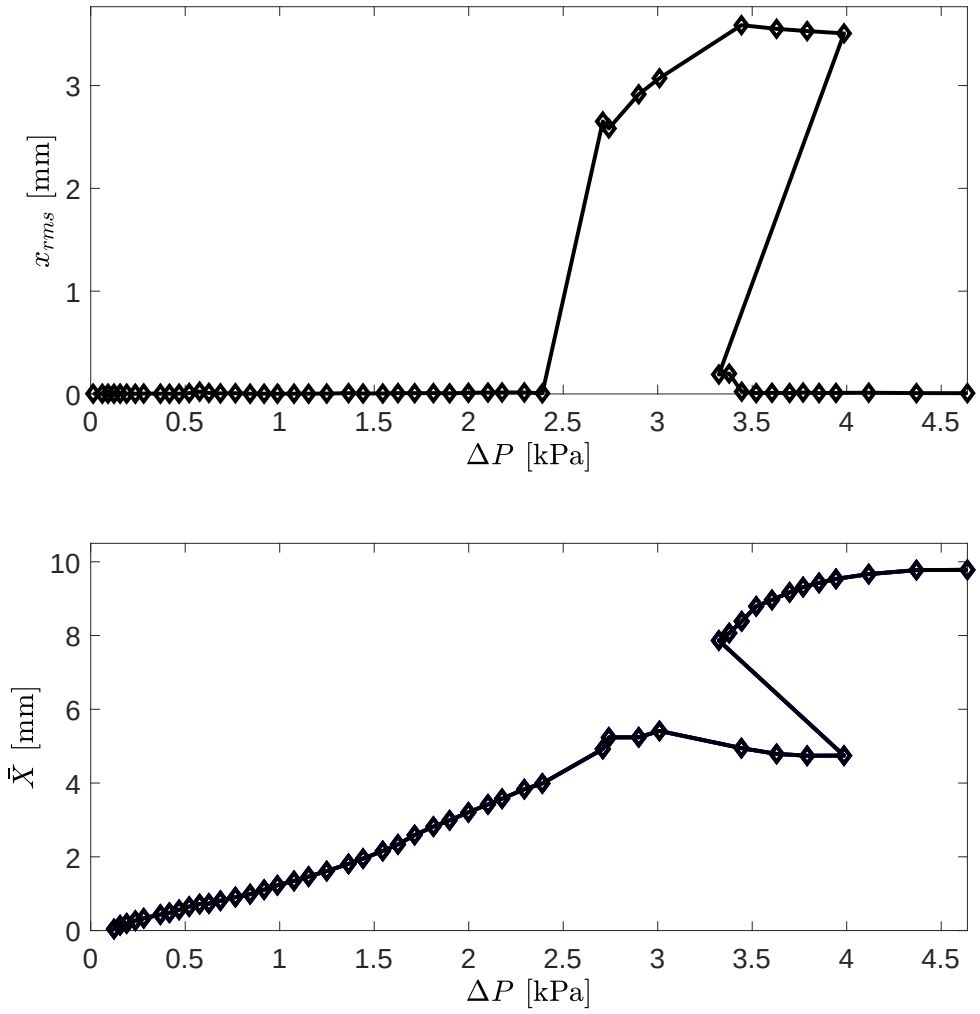

Figure 3.7: Mean and fluctuating valve lift for *an unstable case* vs. total pressure drop with $k = 2700$ N/m, $x_{max} = 10$ mm, $L_d = 2.25$ m, $\delta_0 = 1$ mm. Top: RMS of the valve lift oscillation, Bottom: Mean valve lift.

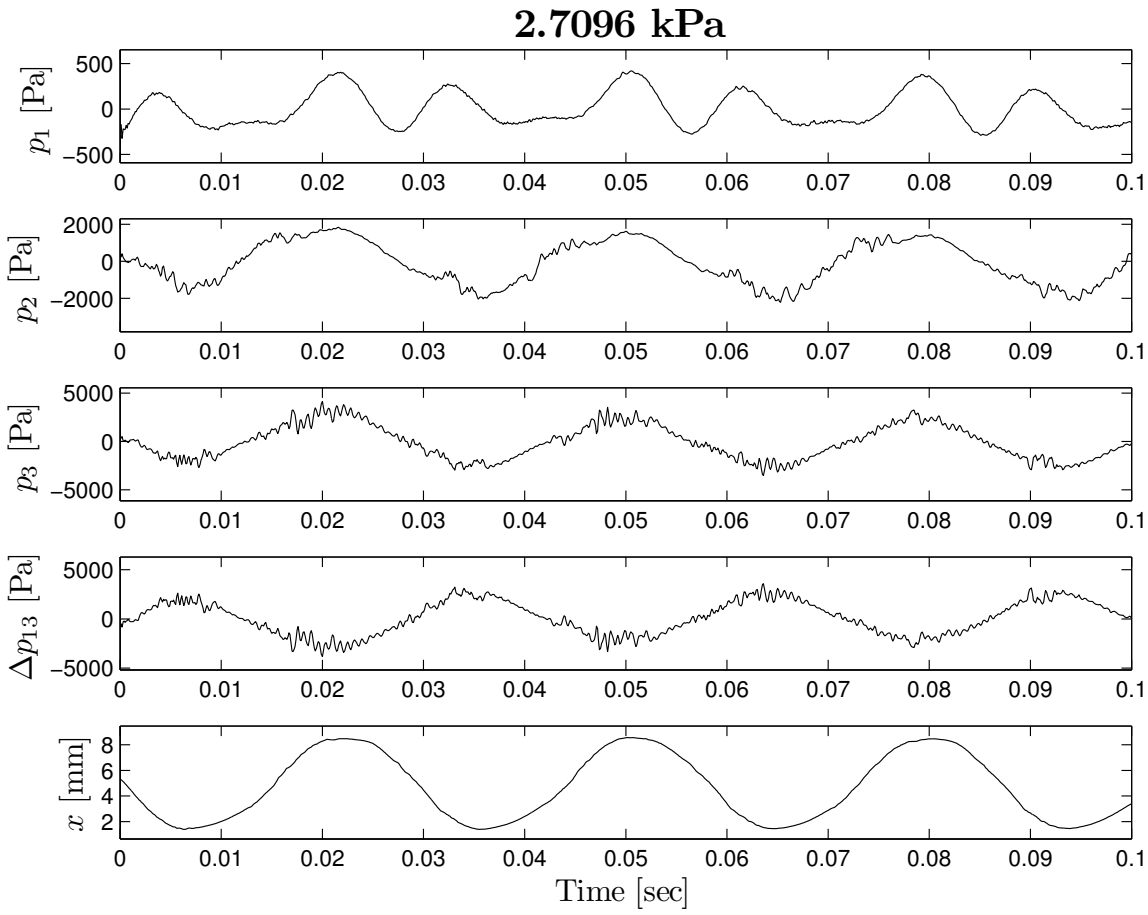

Figure 3.8: Time domain signals for unsteady pressure and valve displacement with $k = 2700$ N/m, $x_{max} = 10$ mm, $L_d = 2.25$ m, $\Delta P = 2.71$ kPa , $\delta_0 = 1$ mm. p_1: Valve inlet pressure, p_2: Pressure beside valve plate, p_3: Valve backplate pressure, Δp_{13}: Net pressure acting upon valve, x: Valve displacement.

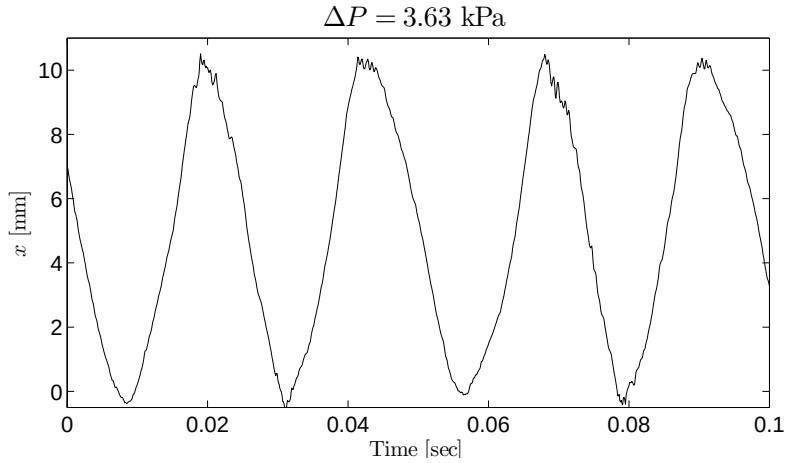

Figure 3.9: Time domain signals for the valve displacement during impact conditions with $k = 2700$ N/m, $x_{max} = 10$ mm, $L_d = 2.25$ m, $\Delta P = 3.6$ kPa.

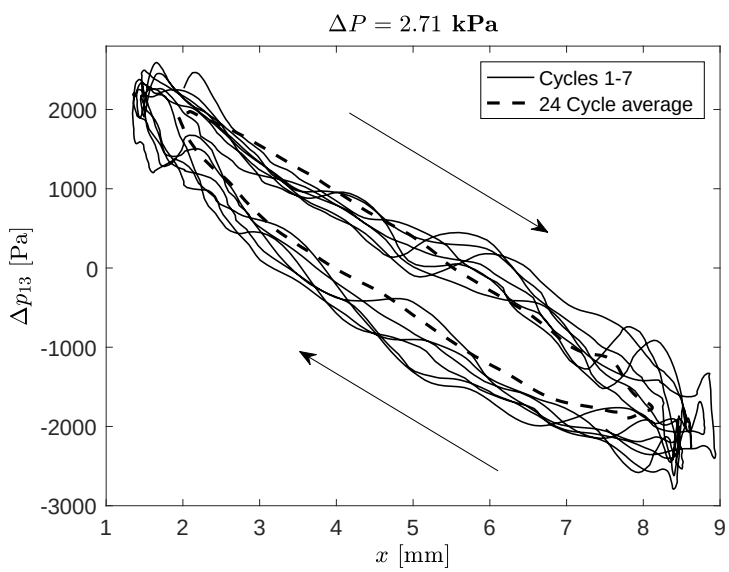

Figure 3.10: Instantaneous pressure difference across the valve Δp *vs.* Valve lift x. $\Delta P = 2.71$ kPa, $x_{max} = 10$ mm, $L_d = 2.25$ m, $\delta_0 = 1$ mm.

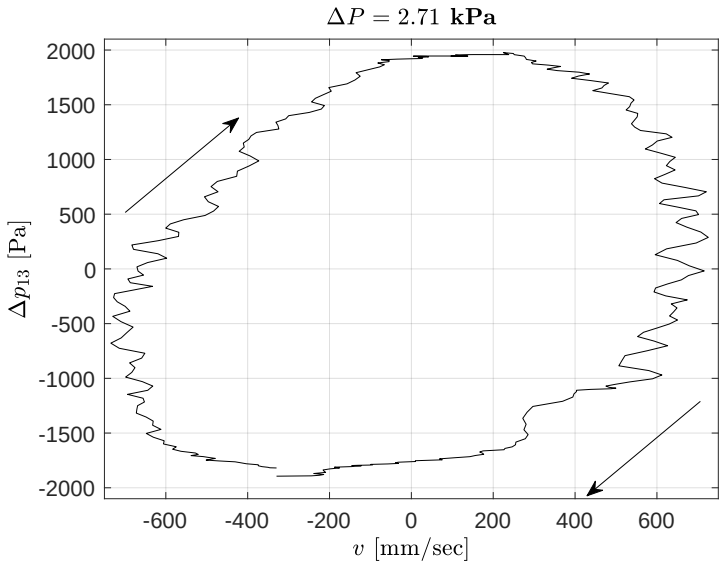

Figure 3.11: Instantaneous pressure difference across the valve Δp against valve plate velocity $\dot{x}$ computed from the average trajectory from 24 cycles. $\Delta P = 2.71$ kPa, $x_{max} = 10$ mm, $L_d = 2.25$ m, $\delta_0 = 1$ mm.

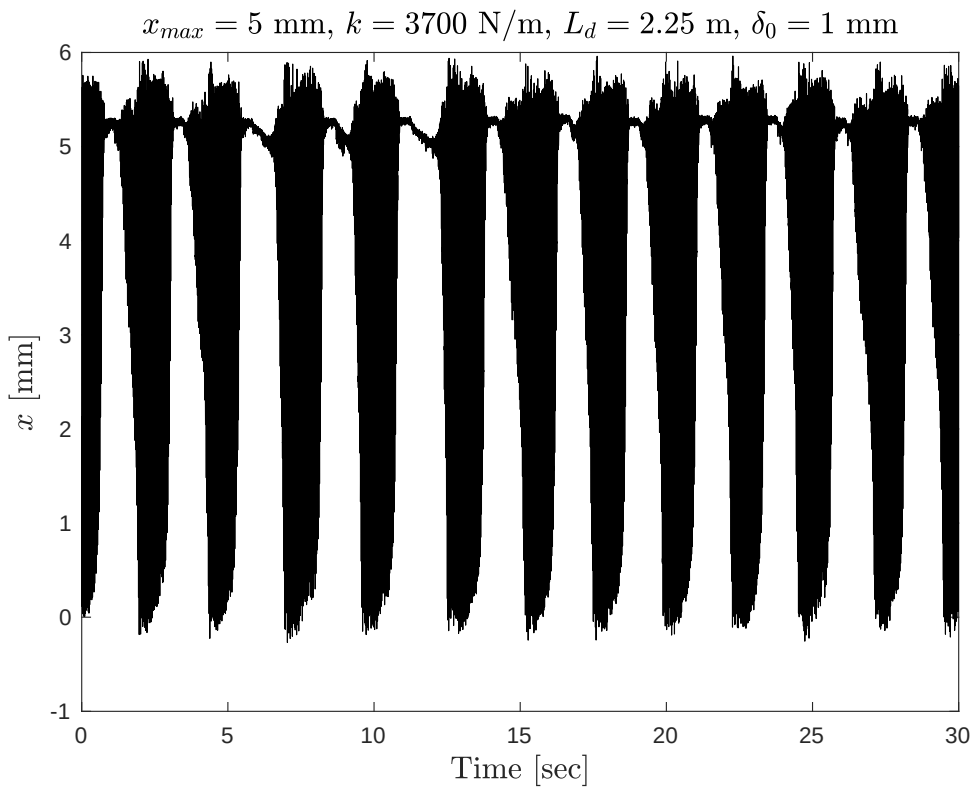

Figure 3.12: Time response for a marginally unstable case: $x_{max} = 5$ mm, $k = 3700$ N/m, $L_d = 2.25$ m, $\delta_0 = 1$ mm.

Limit cycle behaviour

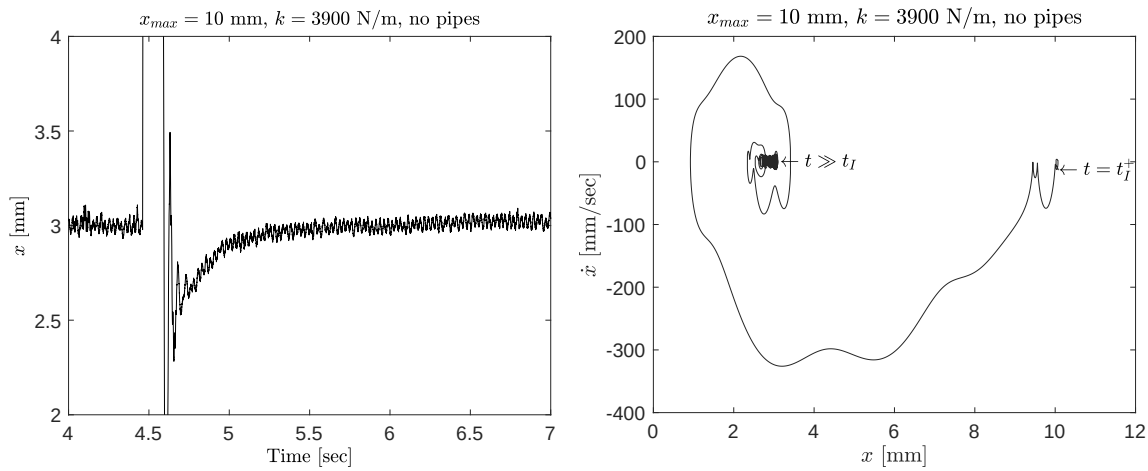

(a) Time response (b) Phase portrait

Figure 3.13: Impulse response tests of the valve for a stable case: $\Delta P = 3.54$ kPa, $x_{max} = 10$ mm, $k = 3900$ N/m, $\delta_0 = 1$ mm.

Figure 3.13a shows the response of the valve plate for a case subjected to an impulse while under a static pressure difference of 3.54 kPa, corresponding to a stable opening at 3 mm for the selected spring stiffness. In this particular configuration, the valve test section is directly connected to the settling chamber and the Roots blower without any piping at its upstream nor downstream ends. It can be seen that when subjected to a disturbance, the valve (without piping) will promptly return to its initial steady-state position in a stable fashion without showing significant oscillatory behaviour. This stable dynamic behaviour can be represented using a phase portrait, as shown in Fig. 3.13b. The valve velocity is plotted against its position starting at a time shortly after the impulse ($t = t_I^+$), once it has reached its maximum position. The valve velocity is computed numerically using a first order approximation, and the valve displacement time history is filtered to exclude frequencies higher than 50 Hz to enhance the legibility of the phase portrait. A spiral towards the valve's equilibrium

position with zero velocity can then be seen, which is characteristic of a stable damped oscillatory system. After a sufficiently large time duration ($t \gg t_I$) the valve converges towards its stable equilibrium state at a position $x \approx 3$ mm and zero velocity.

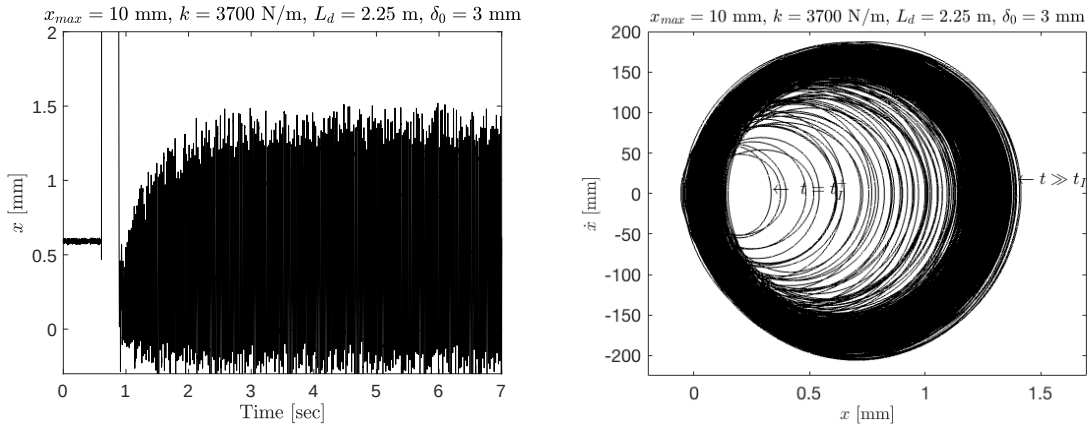

(a) Time response (b) Phase portrait

Figure 3.14: Impulse response tests of the valve for an unstable case: $\Delta P = 2.28$ kPa, $x_{max} = 10$ mm, $k = 3700$ N/m, $\delta_0 = 3$ mm, $L_d = 2.25$ m.

Figure 3.14a shows the time response under a static pressure difference of 2.28 kPa with a downstream length of 2.25 m resulting in a self-excited case upon an applied impulse. It can be seen that the oscillation amplitude is not limited by the valve stopper. Following the impulse, the vibration amplitude grows until the energy added to the structure of the valve is balanced by the energy dissipated through impact on the seat, dissipative flow effects, and acoustic losses. This appears to occur when the peak-to-peak displacement reaches approximately 1.5 mm which manifests itself through a stable limit cycle. A phase portrait (with a 50 Hz low-pass filter applied to the time signal) is provided in Fig. 3.14b to better showcase the limit cycle behaviour of the valve. Shortly following the applied impulse ($t = t_I$), the phase trajectory starts as a small spiral that grows in radius as the self-excited oscillations are sustained. As time significantly exceeds the moment the impulse is applied ($t \gg t_I$), the phase trajectory settles into a circle representing its limit cycle. One may note a growing spiral typical

of stable limit cycles. As a concluding remark, pipe acoustics appear to be essential for the production of valve vibration, as limit cycle oscillations only occurred when piping was connected to the model valve, whereas self-excited oscillations were absent when sufficient piping was not attached.

Effect of stiffness

Figure 3.15 shows normalised oscillation amplitudes as a function of the normalised static pressure difference for various valve spring stiffness values. It can be seen that the increase in spring stiffness has a destabilising effect, as seen through the initial increase and then persistence of large amplitude vibration. As observed in Fig. 3.15 variations in valve spring stiffness can drastically alter the dynamic behaviour of the valve, from localised small amplitude oscillations for $k = 1400$ N/m to full range seat-to-limiter oscillations over a wide range of operating conditions for $k = 4400$ N/m.

This is counter-intuitive as the theory of vibration would suggest that oscillation amplitudes should decrease when spring stiffness is added. This effect could be explained due to a valve structure natural frequency shift towards a plane wave mode of the downstream pipe. Alternatively, the increase in stiffness would require a higher dynamic head to open, which could result in higher excitation forces. Furthermore, it is seen that changing the spring stiffness has little effect on the vibration frequency beyond perhaps selecting the dominant mode of oscillation of the driver-pipe system. This was predicted by means of the fully coupled analytical solution plotted in Fig. 3.5.

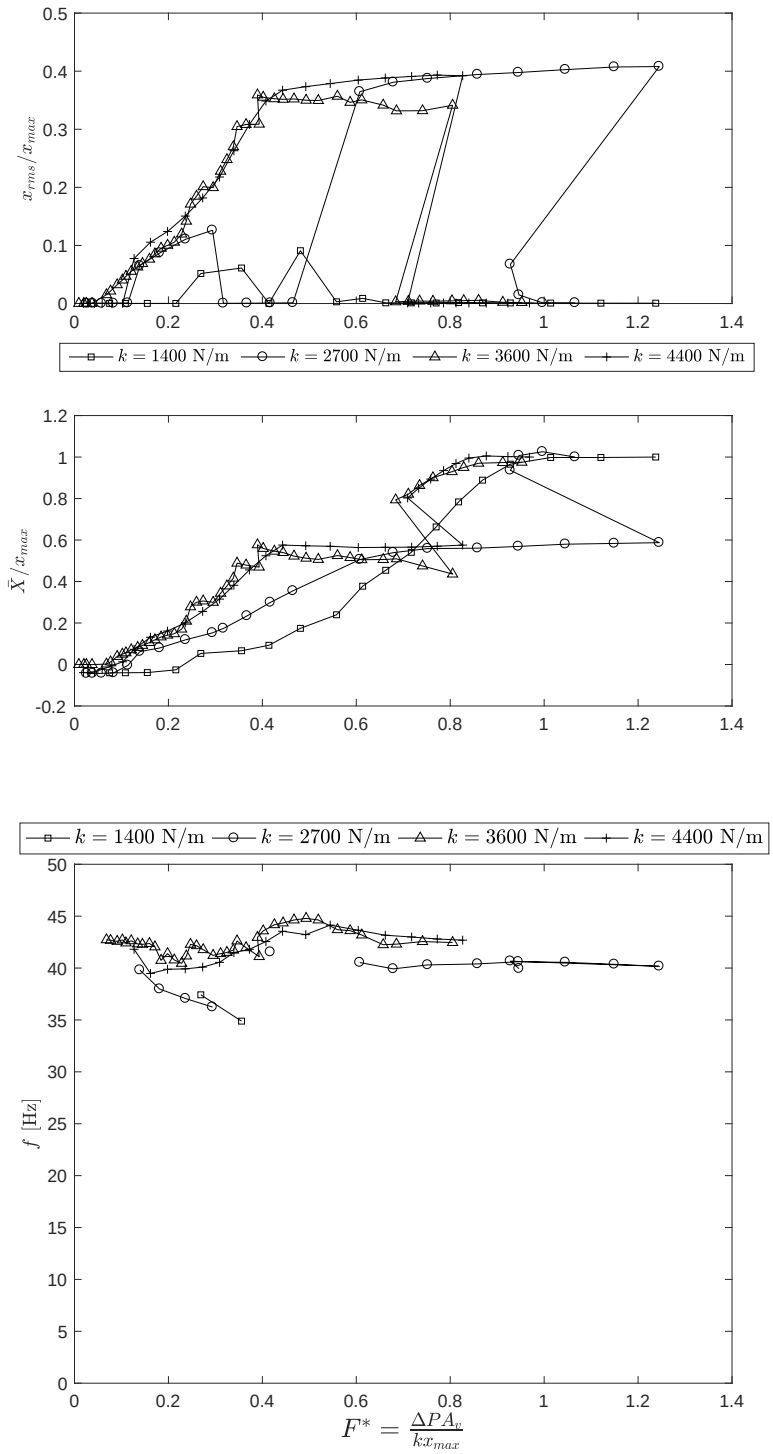

Figure 3.15: Effect of stiffness on amplitude and frequency of oscillation. $x_{max} = 10$ mm, $\delta_0 = 1$ mm.

Effect of pipe length

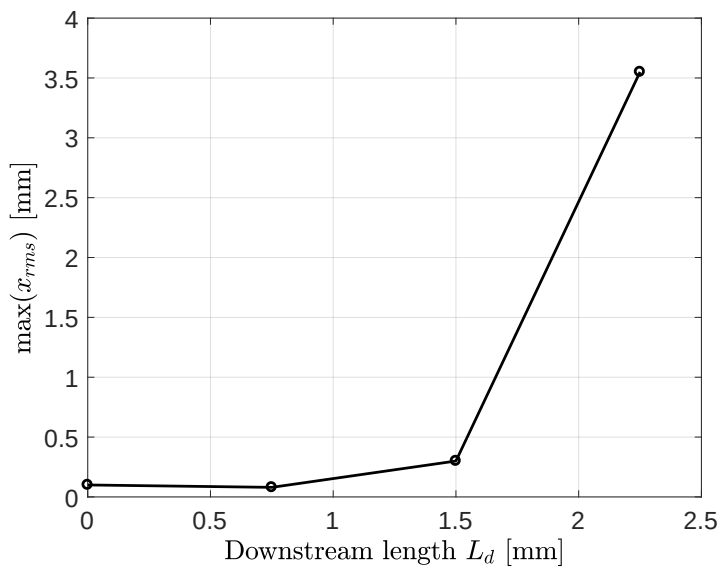

Figure 3.16: Maximum RMS amplitude of valve vibration as a function of downstream pipe length. $x_{max} = 10$ mm, $k = 2700$ N/m.

Figure 3.16 shows the maximum RMS amplitude of the valve vibration recorded over the whole opening range of the valve for various lengths of the downstream pipe. The valve properties (stiffness and maximum lift) are kept the same but only the downstream pipe length is changed in these tests. It is seen that an increase in the piping length positively correlates with the vibration amplitude of the valve plate. One may also note that, prior to a length of 2.25 m, the oscillation is not significant, whereas at 2.25 m vibrations occur with impact on both the seat and limiter. Similar behaviour was observed for all spring stiffness values considered, for both upstream and downstream pipes. It may hence be said that acoustic interaction between the valve and piping is necessary in order to sustain the unstable oscillations of the spring-loaded valves.

Table 3.1: Predicted and observed frequencies for selected pipe lengths. L_d: Downstream piping length, L_u: Upstream piping length.

Length	**Predicted Freq.**	**Observed Freq.**
$L_d = 0.75$ m	78 Hz	71-74 Hz
$L_d = 1.50$ m	54 Hz	58 Hz
$L_d = 2.25$ m	43 Hz	35, 41–44 Hz
$L_u = 2.70$ m	32 Hz	35 Hz

The effect of the pipe length is not only to sustain the oscillation of the valve, but it also controls the oscillation frequency, in conjunction with the valve stiffness and mass, as part of the driver-pipe system described earlier. Through a numerical solution of Equation 3.7, it is possible to predict theoretical frequencies of the valve and compare them with the measured oscillation frequencies of the valve. Examples are shown in Table 3.1.

It can be seen that there is a reasonable agreement between the combined valve–pipe model predictions of the oscillation frequencies and the observed oscillation frequencies in the experiments. Differences may be introduced by the simplifying assumptions of the valve geometry and by ignoring the flow effects in the analytical solution.

Effect of vibration amplitude

To further emphasise the case that non-linear effects alter the dynamic behaviour of the valve, Fig. 3.17 presents the dominant oscillation frequency for unstable cases plotted against the RMS vibration amplitude. When the valve is oscillating at a peak-to-peak amplitude lower than its whole opening range, an increase in vibration amplitude is correlated with a slight drop in frequency of oscillation. On the other hand, when the amplitudes are so large that the valve is impacting, the oscillation cycle is abruptly shortened (frequency increases). While in a purely linear system, oscillation frequency should not depend on the vibration amplitude. In the current

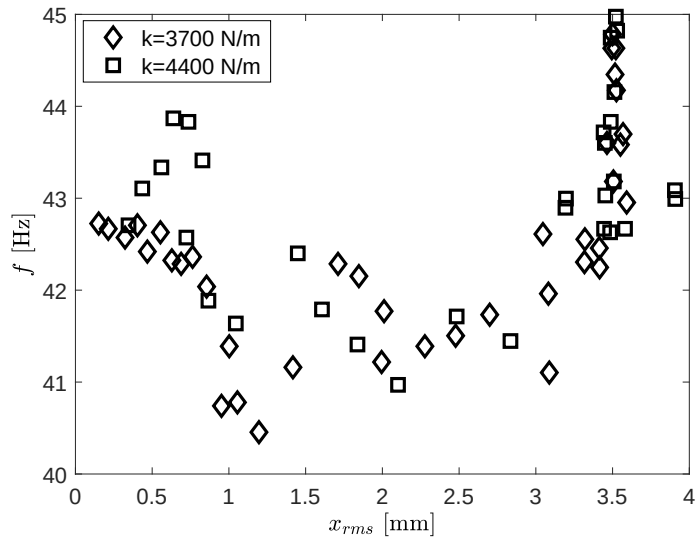

Figure 3.17: Dominant frequency of oscillation as a function of vibration amplitude for valve spring stiffness values of 3700 N/m and 4400 N/m.

context of a complex non-linear system, these results make sense. The initial drop in frequency can be attributed to flow inertia, which has the effect of elongating the oscillation cycle, whereas the sharp rise in frequency is due to a shortening of the oscillation due to impact. This can be observed through the time signals of the valve displacement at increasing amplitudes. This is provided in Fig. 3.18 for $k = 4400N/m$. As the valve plate oscillation grows with increasing static pressure, a plateau is seen in the top portion of the oscillation that results in the elongation of the period due to flow inertia. A further increase in the static pressure results in a shortening of the period due to the non-linear effects of impact.

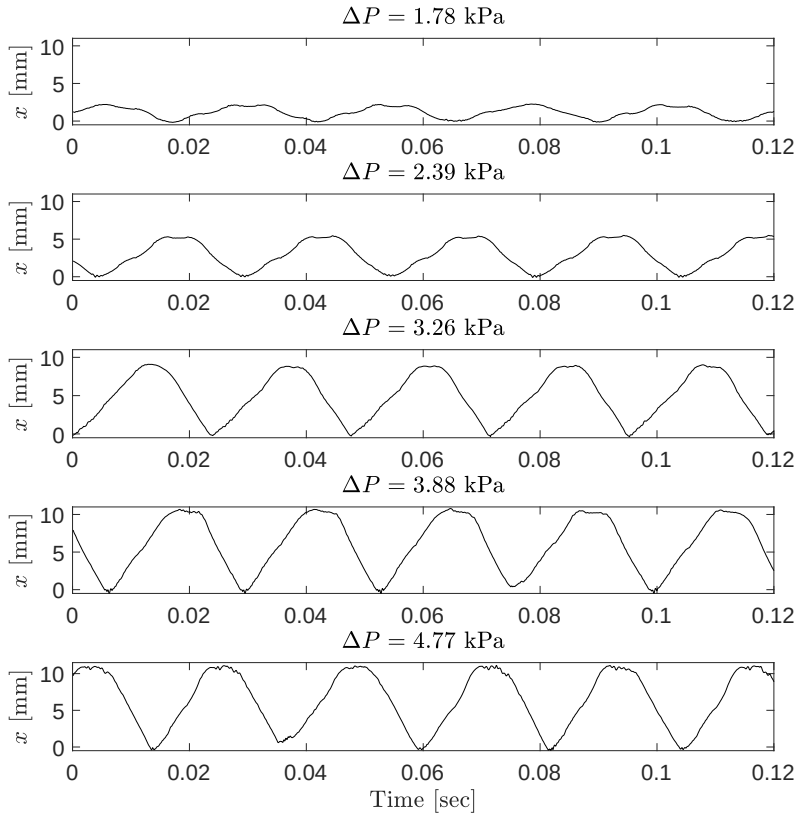

Figure 3.18: Time domain signals for the valve displacement at various static pressure drop values for $k = 4400$ N/m, $x_{max} = 10$ mm, $L_d = 2.25$ m, $\delta_0 = 1$ mm.

Effect of valve spring initial compression

In an investigation of coupled oscillations of a specific spring-loaded multi-ring disk valve used in gas compressors, Ziada et al. (1987) determined that a softer spring combined with a higher initial spring force was an effective means of attenuating the self-excited oscillations of the valve during operation. The specific effect of the initial spring compression was not investigated. Figure 3.19 shows the valve's steady and unsteady opening characteristics as well as its modal characteristics with initial spring

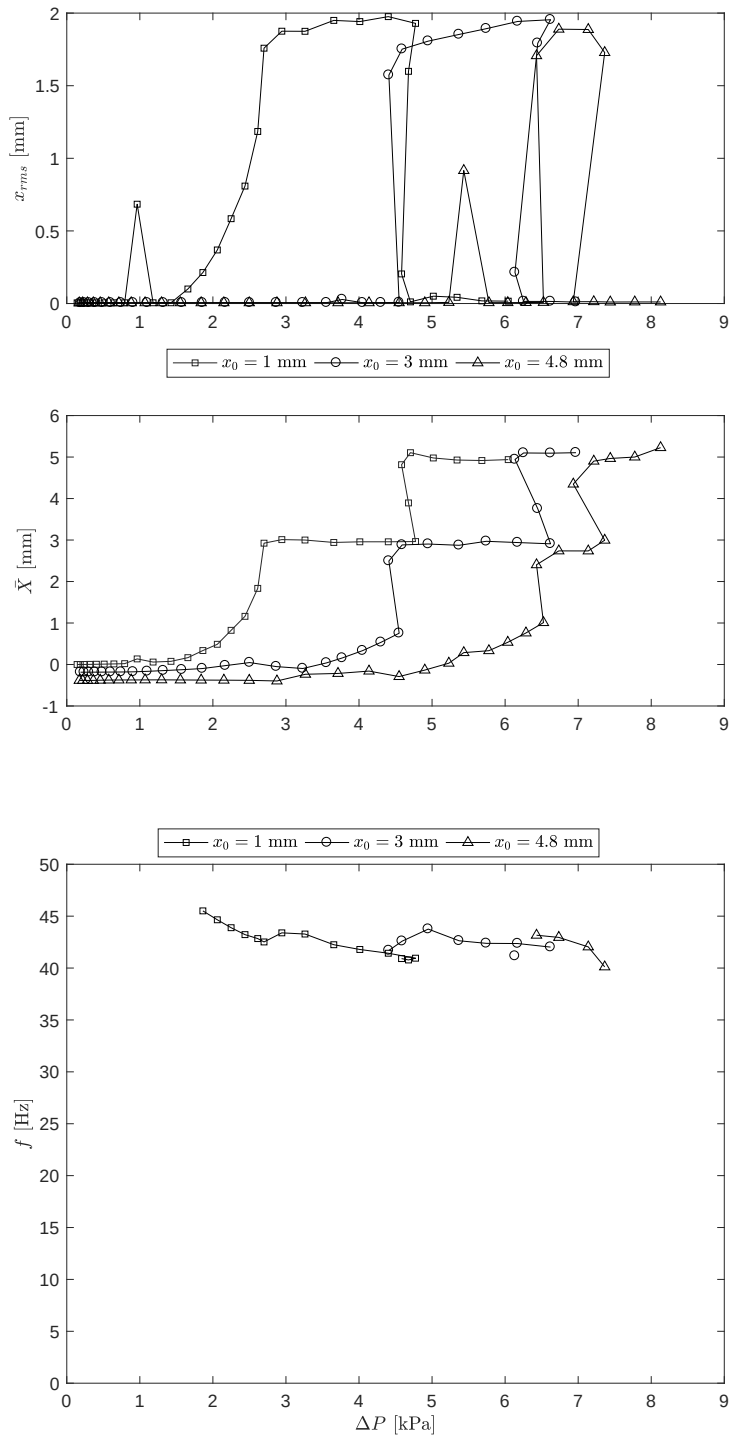

Figure 3.19: Effect of spring preload force on valve instability. $x_{max} = 5$ mm, $k = 3700$ N/m. $\delta_0 = 1 - 5$ mm.

compressions of 1 - 4.8 mm for a maximum valve lift $x_{max} = 5$ mm and a spring stiffness $k = 3700$ N/m. It can be seen that as far as the steady opening characteristics are concerned (mean valve opening $\bar{X}$), increasing the initial compression has the expected effect of delaying the valve opening. Furthermore, when instability occurs, the valve still oscillates at the frequency of the combined valve-piping system rather than the valve structure. In addition, one can see that increasing the spring initial compression has the effect of narrowing the range of static pressures that can experience self-excited vibrations. Despite this effect, severe oscillations are still present even in high initial compression cases.

3.5 Conclusions

This experimental investigation sought to provide a characterization of the self-excited vibration behaviour of spring-loaded valves used extensively as flow control valves in reciprocating compressors and safety relief valves in nuclear power plants. A simplified model valve was manufactured, instrumented, and tested under steady pressure drop to investigate the effect of valve spring stiffness, pipe length, and initial spring compression on the stability of spring-loaded valves.

A key finding was the necessity of acoustic interaction for the self-excited instability mechanism to prevail. In the extensive sets of parameters tested, no instability occurred without upstream or downstream piping and thus without acoustic interaction. Furthermore, while the modal characteristics of the oscillation depended on several factors, a major one was the natural frequency of the combined valve-piping system, agreeing with the postulate that acoustic interaction played a large role in this dynamic instability mechanism. Other parameters merely modulated the oscillation frequency around the combined frequency resulting from the acoustic interaction of the valve and

piping system. Another finding, counter-intuitive to the fundamentals of vibrations, was that an increase in spring stiffness resulted in higher vibration amplitudes. In addition, whereas an increase in the initial spring compression reduced the range of static pressures that result in instability, it did not suppress or attenuate the oscillations.

This investigation provides experimental data about the dynamic instability mechanism of spring-loaded valves which can be used in the development of theoretical models that can be instrumental in the design of durable hydraulic control devices, crucial to the safe and efficient operation of industrial processes.

Bibliography

Allison, T. C., & Brun, K. (2016). Testing and modeling of an acoustic instability in pilot-operated pressure relief valves. *Journal of Engineering for Gas Turbines and Power*, *138*, 052401.

Atig, M., Dalmont, J.-P., & Gilbert, J. (2004). Saturation mechanism in clarinet-like instruments, the effect of the localised non-linear losses. *Applied Acoustics*, *65*, 1133–1154.

D'Netto, W., & Weaver, D. S. (1987). Divergence and limit cycle oscillations in valves operating at small openings. *Journal of Fluids and Structures*, *1*, 3–18.

El Bouzidi, S., Hassan, M., & Ziada, S. (2017). Characterization of flow-sound-structure coupling in spring-loaded valves. In *Proceedings of the 2017 ASME Pressure Vessels and Piping Conference, Waikoloa Village, Hawaii, USA, July 2017* PVP2017-65767. Waikoloa, Hawaii, USA.

Habing, R. A., & Peters, M. C. A. M. (2006). An experimental method for validating compressor valve vibration theory. *Journal of Fluids and Structures*, *22*, 683–697.

Kasai, K. (1968). On the stability of a poppet valve with an elastic support: 1st report, considering the effect of the inlet piping system. *Bulletin of JSME*, *11*, 1068–1083.

Killmann, I. (1972). Aerodynamic forces acting on valve discs. In *International Compressor Engineering Conference*.

Kolkman, P. A. (1976). *Flow-induced gate vibrations*. Technische Hogeschool Delft.

Moussou, P., Gibert, R. J., Brasseur, G., Teygeman, C., Ferrari, J., & Rit, J.-F. (2010). Instability of pressure relief valves in water pipes. *Journal of Pressure Vessel Technology*, *132*, 041308.

Nayfeh, A., & Bouguerra, H. (1990). Non-linear response of a fluid valve. *International Journal of Non-Linear Mechanics*, *25*, 433–449.

Tsui, C., Oliver, C., & Cohen, R. (1972). Discharge phenomena of a two-dimensional poppet-type valve. In *Internal Compressor Engineering Conference*. Purdue, Indiana: Purdue University.

Weaver, D. S., & Ziada, S. (1980). A theoretical model for self-excited vibrations in hydraulic gates, valves and seals. *Journal of Pressure Vessel Technology*, *102*, 146–151.

Wilson, T. A., & Beavers, G. S. (1974). Operating modes of the clarinet. *The Journal of the Acoustical Society of America*, *56*, 653–658.

Ziada, S., Shine, S., & Bühllmann, E. (1986). Self-excited vibrations of reciprocating compressor plate valves. In *International Compressor Engineering Conference*.

Ziada, S., Shine, S., & Buhlmann, E. (1987). Tests on the flutter of a multi-ring plate valve. In *Proceedings of the International Conference on Flow Induced Vibrations* (pp. 393–402). Bowness-on-Windermere, England: BHRA.

Chapter 4

Self-Excited Vibrations of Spring-Loaded Valves Operating at Small Pressure Drops

Complete Citation:

El Bouzidi, S., Hassan, M., & Ziada, S. A Theoretical Model For The Self-Excited Vibrations of Spring-Loaded Valves. *Initially submitted on March 25, 2018 to the Journal of Fluids and Structures. Revised manuscript submitted on June 27, 2018.*

Relative Contributions:

S. El Bouzidi: Developed the theoretical model. Conducted analysis, simulations, and interpretation of results. Prepared manuscript for publication.
M. Hassan: Co-supervisor of S. El Bouzidi. Provided guidance on modelling methodology, results, and feedback on manuscript.

S. Ziada: Co-supervisor of S. El Bouzidi. Provided guidance on modelling methodology, results, and feedback on manuscript.

Abstract

Flow-induced vibration is a major issue for spring-loaded valves. However, their complex geometry, combined with their diversity of operational conditions, creates a significant challenge for modelling their dynamic response to potential excitation mechanisms. This paper proposes an analytical framework to describe flow-sound-structure coupling in spring-loaded valves operating at subcritical conditions, therefore without the occurrence of choking at the *vena contracta*. The model consists of a single-degree of freedom model of the valve structure, a pseudo-force implicit algorithm to calculate impact forces, a one-dimensional unsteady Bernoulli model to describe the flow, and a one-dimensional wave propagation finite difference scheme to account for the acoustic feedback. The model has shown excellent agreement with experimental results as well as promising predictive capabilities for valve life and wear assessment.

Keywords

flow-induced vibration, spring-loaded valves, acoustic feedback, self-excited vibrations, theoretical modelling, computational techniques, non-linear dynamics

4.1 Introduction

Flow-induced vibration failures present serious concerns for industrial and power plant equipment. Under favourable conditions, components in plants experience oscillations that can cause either rapid degradation or shorten the operational life of the equipment.

This is especially true for spring-loaded valves, which upon failing require costly shutdowns of pipelines. Based on the aforementioned motivations, a vast body of literature has emerged in order to investigate the excitation and instability sources in spring-loaded valves over the past fifty years. Initial interest in the subject was spurred by stability considerations in hydraulic control valves (Kasai, 1968). Studies that followed provided steady-state characteristics of the fluid flow loading (Killmann, 1972; Tsui et al., 1972). A comprehensive investigation into sources of instability for hydraulic valves and gates based on a classification of their operational characteristics was then provided by Kolkman (1976). However, its assumption of small amplitude oscillations and reliance on a linear analysis of the modelled system narrows its applicability to cases where the valve oscillation is small compared to its maximum opening. To overcome this limitation, Weaver and Ziada (1980) provided a physical description of the interaction mechanism for a check valve in a water pipeline. Their model, which relies on simplifying the complex flow geometry around the check-valve, showed that the unsteady Bernoulli description of the flow provides reasonable predictions of the instability conditions. Experiments on production multi-ring disk valves (Ziada et al., 1986) revealed additional features of the self-excited oscillation mechanism, showing that vibrations occurred under steady flow. Furthermore, modal characteristics of the vibration appeared to depend on the acoustic properties of the piping system rather than the structural properties of the valve. Based on this insight, Oengören (1987) and Shine (1987) ran tests on a particular disk valve design to select an appropriate spring stiffness that would attenuate or suppress the self-excited oscillations. In this process, they confirmed the coupling of the valve structure with the plane wave acoustic modes of the piping system. Moussou et al. (2010) later investigated self-excited instability issues in a safety relief valve and considered the effect of the reflected acoustic wave at the upstream pipe for water flow. They found that the oscillation frequency depended

on the geometry and flow characteristics of the valve. More evidence of acoustic coupling in spring-loaded valves was demonstrated by Bazsó and Hős (2013), whose experimental study of a spring-loaded poppet relief valve exhibited chaotic behaviour, which they identify as Hopf Bifurcation, with valve oscillations occurring at the first acoustic resonance mode of the piping.

Thus far, it has become clear that a reliable model must make several considerations that pertain to three areas: structural modelling, fluid loading, and acoustic interaction. The first area involves taking into account nonlinearities inherent to the valve's structural geometry and installation conditions. Nayfeh and Bouguerra (1990) provided a model for the effect of a nonlinear gasket on valve dynamics during closing. Habing and Peters (2006) provided a theoretical model of a spring-loaded valve under impact with an elastic coefficient of restitution. The second area involves developing a model for computing flow behaviour and the resulting forces in complex flow geometries at large oscillation amplitude conditions. Weaver and Ziada (1980) developed a 1D unsteady Bernoulli model of the flow where dynamic behaviour of the flow is dependent on viscous loss characteristics of the system, flow inertia due to the piping length, and discharge properties of the valve for a given opening. Some insight can be gained through reviewing modelling techniques intended for vocal folds, which operate under similar conditions, whereby their oscillations typically result in interruption and re-establishment of the flow through cycles of opening and closing. To this effect, Deverge et al. (2003) investigated the suitability of several standard fluid flow models for this application. They found that a steady Bernoulli solution corrected for friction performed adequately when compared to experimentally (*in vitro*) obtained time domain signals of the net pressure across the glottis. The final area to consider is the acoustic interaction mechanism, which requires devising a model that incorporates the influence of the valve plate motion on the acoustic pressure in the piping system, as

well as boundary conditions that allow for a time domain solution of the acoustic force acting on the valve plate. While Moussou et al. (2010) uses a convolution method to determine the reflected acoustic pressure acting upon a valve, it is challenging to implement it in a time domain model with nonlinear conditions such as impact.

Further work on pressure-relief valves by Darby (2013) and later Darby and Aldeeb (2014) sought to provide a model for valve dynamics that accounted for nonlinear effects of the gas flow. This was accomplished by utilizing an analytical solution of structural motion subjected to a step, albeit while neglecting the effects of impact and opting instead to limit the valve's motion to a prescribed range. Consequently, the model's predicted instability frequencies significantly differed from their test data. Hős et al. (2014, 2015) coupled a gas-dynamics model to a single-degree-of-freedom model of structural motion to explain chatter instability in pressure-relief valves. The acoustic effects of this model are incorporated into the gas-dynamics equation, which creates a challenge in attempting to assess the influence of acoustic interaction on the instability. They further demonstrate that a single-mode expansion of the gas-dynamics based on acoustic interaction, which they call the quarter-wave model (QWM), may be utilized to predict the onset of instability as well as severity for low-amplitude oscillations. Later on, Erdődi and Hős (2017) compared the effectiveness of the QWM against CFD simulations and demonstrate that reduced-order models can be used to capture the main features of dynamic instability in valves.

Research into musical reed instruments has revealed some similarities to the spring-loaded valve case investigated in this study, however the aims of such studies are typically to understand the sound resonant and sound radiation features of the instrument rather than the reed oscillation characteristics. In one particular study, Atig et al. (2004) conducted a numerical investigation of the acoustic losses causing a clarinet to saturate at certain frequencies while suppressing sound at others.

The purpose of the current study is to develop a theoretical model that is representative of the complex interaction mechanisms between the fluid flow, acoustic field, and valve structure. This will provide an analytical context to explain the spring-loaded valve instability features described in previous experimental work on a spring-loaded valve in air flow (El Bouzidi et al., 2018). The theoretical model consists of a structural dynamic model of the valve, including nonlinear impact forces expressed using a pseudo-force method. Hydrodynamic forces are determined through simultaneous solution of the unsteady Bernoulli equation with turbulent viscous losses. Acoustic forces are determined through a solution of the one-dimensional wave equation and coupled to the valve structure using the Euler force equation. The proposed framework seeks to provide modelling tools for spring-loaded valves experiencing small pressure drops with rapid transients, large amplitude vibrations with impact, and low viscous losses.

4.2 Model Description

General approach & assumptions

The modelling approach was developed to describe the flow-sound-structure interaction present in *multi-ring disk valves, used in reciprocating gas compressors.* Typical operational conditions for these compressor valves involve small openings, low pressure drops across the valve, as well as rapid transients due to the low mass of the valve plate. When the instability mechanism prevails, the valve may also experience vibrations over the entire opening range of the valve, resulting in repetitive impacts on the seat and limiter. Despite its operation at small openings, the numerous concentric flow channels in the valve provide a large flow area that allows for high flow rates at rather

small pressure drops. This allows the gas to discharge from the cylinder into the delivery pipe with very small losses. The flow is assumed compressible and subsonic, while it is conjectured that these compressibility effects are wholly encompassed within the acoustic field modelling. This is unlike safety-relief valves in high-pressure gas service which may experience choking at overcritical pressure drops and would therefore require additional specialized treatment.

However, the methodology is highly relevant to spring-loaded valves in other applications. Valves often feature complex geometries, with complex flow profiles that can be challenging to model. In the case of multi-ring disk valves, the valve plate is supported using multiple springs, allowing for possible tilting. In addition, the valve plate is usually made of thin metal, resulting in a flexible structure. Furthermore, compressor valves may feature manifolds of intricate geometry, which may prove challenging to model from an acoustic standpoint. Hence, the purpose of this theoretical model is not to reproduce the dynamic response of this complex coupled system with high fidelity. Rather, the aim is to provide insight into the flow-sound-structure coupling phenomenon. The model should also be capable of predicting the dominant characteristics of the dynamic response. Therefore, some simplifications are necessary.

First, as demonstrated by Ziada et al. (1986), the self-excited instability only occurs when the valve plate is parallel to its seat. Hence, its motion can be considered to be purely translational, with the valve plate rigid, resulting in one-dimensional motion. Flexibility of the structure is accounted for either through the valve spring stiffness, or the impact stiffness during contact. In addition, the instability was seen to persist under steady pressure drop conditions (El Bouzidi et al., 2018). It should hence be possible to simulate the self-excited instability for a given case at a constant pressure difference across the system. Also, the density changes resulting from pressure differences are neglected, and the fluid is assumed to be a single-phase gas (in this

case air). Moreover, it is assumed that compressibility effects can be accounted for through modelling of the acoustic field. Further, the acoustic effects are assumed to be principally due to the plane wave propagation in the upstream and downstream pipes.

Thus, a reduced-order model is proposed. This model consists of three sub-models to address the dynamic behaviour of the valve, the fluid flow, and the acoustic field. The following sub-sections provide further details into the sub-models.

Valve plate motion and impact modelling

The valve may be modelled as a single degree of freedom system, subjected to hydrodynamic, acoustic, and impact forces. The equation of motion for such a system can be stated as:

$$m\ddot{x} + c\dot{x} + k_s(x - x_0) = F_{imp}(t) + F_h(t) + F_a(t) \tag{4.1}$$

where m, c, and k_s are respectively the valve mass, damping coefficient, and stiffness. x is the valve position with respect to its seat. Impact is accounted for using a pseudo-force method. Hence, F_{imp} is the impact force, calculated as:

$$\begin{cases} F_{imp}(t) = 0, & x \in [0, x_{max}] \\ F_{imp}(t) = -\left(K_{imp}\delta + 1.5\alpha\dot{\delta}\left|K_{imp}\delta\right|\right), & x \notin [0, x_{max}] \end{cases} \tag{4.2}$$

where x_{max} is the maximum valve opening, δ is the overlap distance between the valve plate and the seat or limiter, and K_{imp} is the impact stiffness. α represents material damping as defined by Hunt and Crossley (1975). An iterative computation of the impact force is required in order to determine an accurate overlap distance. This method for computing impact forces has proven to be reliable in other applications,

such as modelling the dynamics of heat exchanger tube bundles in loose supports (Johansson, 1997; Hassan et al., 2002). Finally, the other two forces (F_a and F_h) appearing in Eq. (4.1) are the acoustic and hydrodynamic forces, respectively. They are discussed in further detail in the following sub-sections.

Hydrodynamic modelling

Figure 4.1 illustrates the piping system to be described by the hydrodynamic model. Based on the approach initially developed by Weaver and Ziada (1980), one may state the unsteady Bernoulli equation between any two points i and j as follows:

$$\frac{p_i}{\gamma} + \frac{V_i^2}{2g} = \frac{p_j}{\gamma} + \frac{V_j^2}{2g} + h_{L_{ij}} + I_{ij}\frac{dQ}{dt} \tag{4.3}$$

p and V are the pressure and velocity at the location. Q is the flow rate or discharge of the system. γ and g are the specific weight and the acceleration of gravity, respectively. $h_{L_{ij}}$ is the head loss between points i and j, while I_{ij} is the inertance of the pipe length between those two points, defined as:

$$I_{ij} = \frac{L_{ij}}{gA_{ij}} \tag{4.4}$$

with L_{ij} as the pipe length between points i and j, and A_{ij} being the flow area.

One may then obtain a first order differential equation describing the discharge in the system:

$$\frac{dQ}{dt} = \frac{1}{\sum I}\left[\frac{\Delta P}{\gamma} - \sum \frac{K_{ij}}{A_i^2}\frac{Q^2}{2g}\right] \tag{4.5}$$

The above equation may then be solved simultaneously with the equation of motion of the valve stated in (4.1) using a 4th order Runge-Kutta scheme. The structural coupling in the hydrodynamic equation comes from the effect of the plate motion on

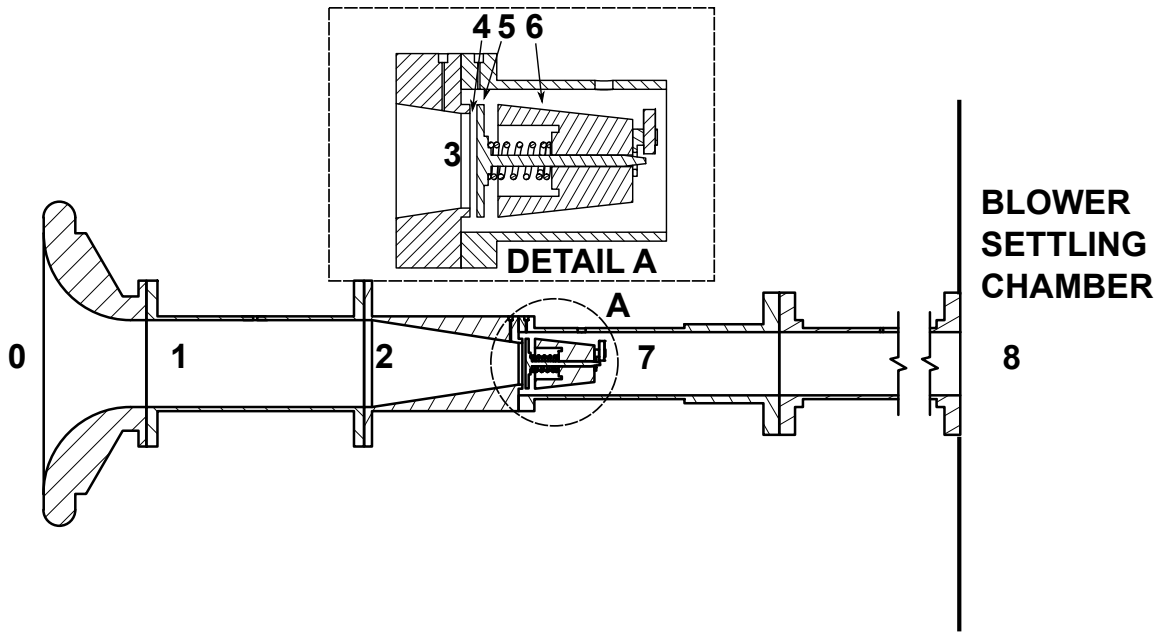

Figure 4.1: Modelled geometry of the flow – locations 0 to 8 represent possible i and j indices in Eq. (4.3).

certain loss coefficients K_{ij} and the flow areas A_i, namely $A_4(x)$, $K_{34}(x)$, and $K_{45}(x)$. On the other hand, the fluid coupling in the differential equation of the structure originates from the influence of the discharge Q and its rate of change on the pressure difference across the valve ($\Delta p_{35} = p_5 - p_3$), and incidentally on the hydrodynamic force acting on the valve F_h. Equation (4.3) can be written between locations 3 and 5 in order to solve for the dynamic pressure difference across the valve:

$$\Delta p_{35} = \frac{\rho}{2}\left(\left(\frac{1}{A_5^2} - \frac{1}{A_3^2}\right)Q^2 + \sum_{i=3,j=i+1}^{i=5} \frac{K_{ij}}{A_i^2}Q^2\right) \tag{4.6}$$

Equation (4.6) may then be integrated over the valve area in order to obtain the effective hydraulic force acting on the valve at a given time, such that:

$$F_h(t) = \int_{A_v} \Delta p_{35} dA \tag{4.7}$$

Table 4.1: Loss coefficients used in hydrodynamic model.

Coefficient	**Description**	**Value**
K_{01}	Well-rounded entrance	0.05
K_{12}	Upstream pipe length	$0.0015L_u/d$
K_{23}	Gradual area contraction	$1.18 - \left(\frac{A_3}{A_2}\right)^2$
K_{34}	Elbow and expansion	$1.1 + \frac{1}{2}\left(1 - \frac{A_4(x)}{A_3}\right)^2$
K_{45}	Elbow and contraction	$1.1 + \frac{1}{2}\left(1 - \frac{A_4(x)}{A_5}\right)^2$
K_{56}	Gradual area expansion	$\left(\frac{A_5}{A_6}\right)^2 - 0.89$
K_{67}	Downstream pipe length	$0.0015L_d/d$
K_{78}	Sudden expansion	$\left(1 - \frac{A_7}{A_8}\right)^2$

Finally, the minor loss coefficients K_{ij} are associated with the irregularities in the flow. Those coefficients can be found in standard handbooks. For this model, they are sourced from Blevins (1984), and are described in Table 4.1.

Acoustic interaction modelling

The acoustic interaction between the valve and the piping system is modelled using the 1D wave equation:

$$\frac{\partial^2 p}{\partial z^2} = \frac{1}{c_0^2}\frac{\partial^2 p}{\partial t^2} \tag{4.8}$$

where p is the acoustic pressure, z is the position along the pipe, t is time, and c_0 is the acoustic wave propagation speed. The wave equation is discretized using a central difference method in space and time. The acoustic pressure p at a future time-step $k+1$ may be calculated as:

$$p_n^{k+1} = Co^2 p_{n+1}^k + 2(1 - Co^2)p_n^k + Co^2 p_{n-1}^k - p_n^{k-1} \tag{4.9}$$

where n is the spatial index and Co is the Courant number ($Co = c_0 \Delta t / \Delta z$). The equation describing the interaction with the valve is expressed as a Von Neumann boundary condition using the Euler force equation (Kinsler et al., 1999), such that:

$$\left.\frac{\partial p}{\partial z}\right|_{z=0} = -\rho \left.\frac{\partial u}{\partial t}\right|_{z=0} \tag{4.10}$$

It may be recalled that u is the acoustic particle velocity, and at $z = 0$ it is equal to the valve plate velocity $\dot{x}$. Hence, Eq. (4.10) becomes:

$$\left.\frac{\partial p}{\partial z}\right|_{z=0} = -\rho \ddot{x} \tag{4.11}$$

The left hand side of the above equation may then be discretized using a first order finite difference scheme, allowing for implementation in the 1D wave equation. Furthermore, knowledge of the acoustic pressure at the boundary may be used to compute the force resulting from the acoustic pressure acting on the valve.

In addition, the acoustic boundary condition at $z = L$ is considered to be an open pipe, such that:

$$p(L, t) = 0 \tag{4.12}$$

To account for the fact that in reality the pipe is flanged to the settling chamber, an end correction is applied by increasing the length L of the pipe to $L + \frac{8r}{3\pi}$, where r is the pipe radius.

4.3 Model Validation & Parameter Estimation

Contact model parameters

The contact model requires certain impact properties of the system to be known. Namely, it is dependent on the impact stiffness K_{imp} and the material damping α. In order to determine K_{imp}, static Finite Element Analysis (FEA) is conducted. A geometry is generated to represent the loading case of the valve plate during impact on the valve seat. The plate is 8 mm thick with a 80 mm diameter, and is made of high density polyethylene (HDPE) with a Young's modulus of $E = 1.2$ GPa. The FEA solution is computed with a total number of elements of 10,483. A downward

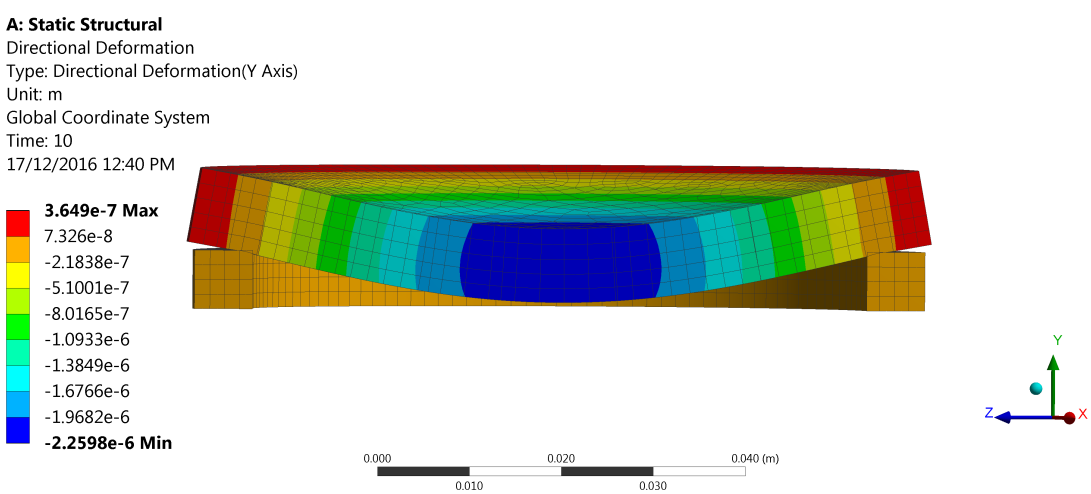

Figure 4.2: Structural Finite Element Analysis (FEA) simulation of the valve plate and seat.

point load is applied at the centre of the plate of magnitude $F = 10$ N. Since this is a steady-state simulation, the time duration needs to be long enough to allow the system to reach an equilibrium point. Consequently, the simulation is run for a duration of 10 seconds, with a timestep $\Delta t = 1$ sec. The maximum deflection δ_{max}, occurring at the

centre of the valve plate δ and the applied load F are used to determine an effective impact stiffness $K_{imp} = 4.425 \times 10^6$ N/m.

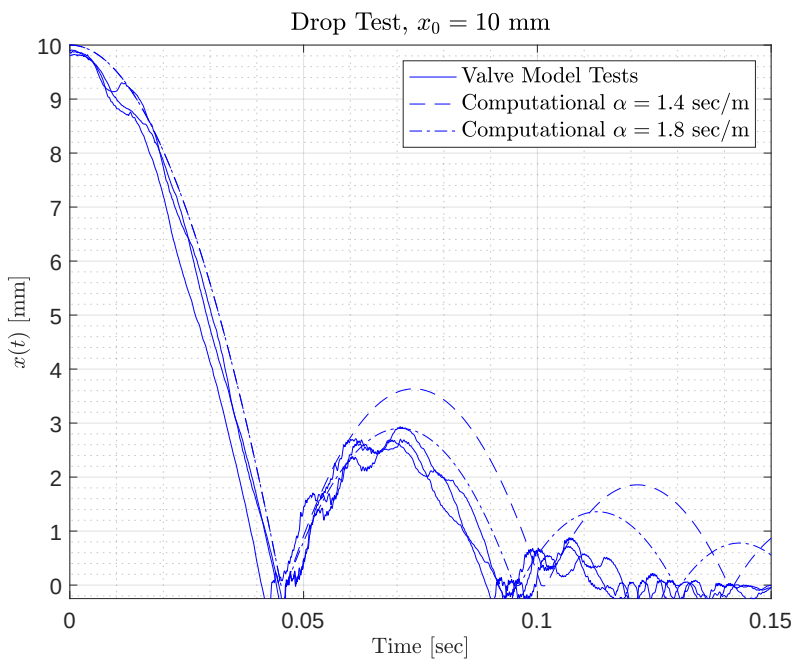

Figure 4.3: Valve drop-tests to determine material damping properties during contact.

The next challenge concerns obtaining an acceptable value for α. The analysis of Hunt and Crossley (1975) defines the material damping α as being related to the coefficient of elastic restitution e and the velocity prior to impact v_i as:

$$e = 1 - \alpha v_i \tag{4.13}$$

The energy dissipated during contact is defined as ΔE, such that:

$$\Delta E = \frac{1}{2} m \left(v_i^2 - v_o^2 \right) \tag{4.14}$$

with v_o the velocity after impact, defined according to classical elastic impact physics

as:

$$v_0 = ev_i \tag{4.15}$$

Typically, α is determined empirically, as it is material dependent. For the current case, the valve plate is made from high density polyethylene (HDPE), whereas its seat and limiter are constructed using aluminium. To measure α, the valve spring is removed, and the test section is positioned vertically. The valve plate is set to its maximum opening, then released and allowed to drop. Multiple tests are conducted to ensure repeatability, as can be seen in Fig. 4.3 (solid-line plots). Equation (4.1) is numerically solved (with F_a and F_h set to zero) using the impact stiffness value K_{imp} previously found through FEA, and α is varied until a value that reflects the actual behaviour of the valve best is found. In addition, a forcing term is added to account for the effect of gravity. It can be seen that $\alpha = 1.4$ sec/m results in insufficient energy dissipation during impact, while $\alpha = 1.8$ sec/m replicates the contact dynamics of the valve satisfactorily, albeit only for the first bounce. The experimental tests show that higher frequency oscillations are present following impact, due to excitation of the higher plate modes. The single degree of freedom model of the valve is not capable of accounting for the higher mode plate deflections. Fortunately, they can be neglected as the effect is only dominant for small opening oscillations, whereas the interest of this study is to model large amplitude oscillations in valves.

Finally, it may be worth comparing the pseudo-force method's prediction to a simpler contact dynamics model. Figure 4.4 provides such a comparison with the more commonly used elastic restitution model of impact. In the elastic restitution model, the velocity following impact v^- related to the velocity prior to impact v^+ using the following relationship:

$$v^+ = e_r v^- \tag{4.16}$$

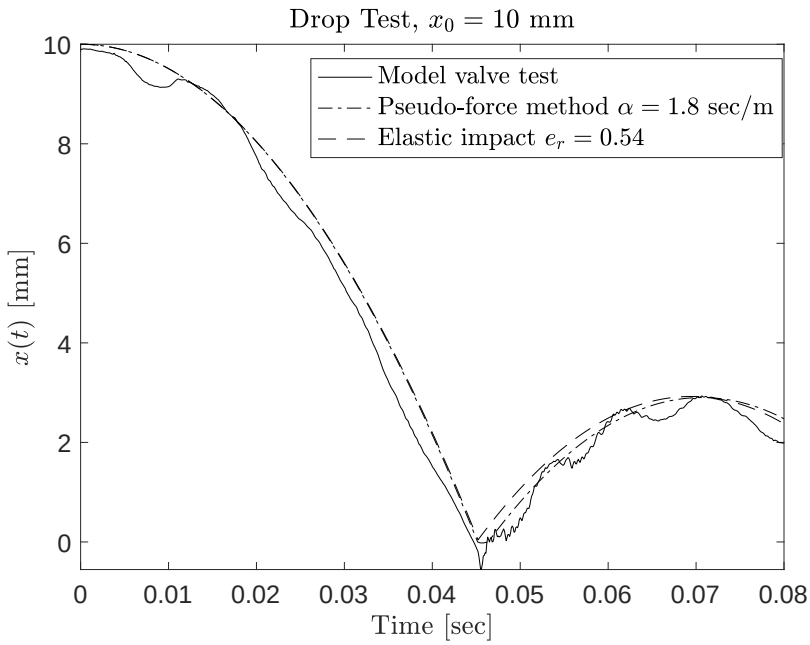

Figure 4.4: Impact model comparison.

where e_r is the coefficient of momentum restitution. In this model, the duration of contact is assumed instantaneous. Figure 4.4 shows a comparison of an experimental drop-test using the model valve, overlaid with simulated time traces of the valve displacement using the elastic impact model and the pseudo-force method. It can be seen that following impact, neither impact model is capable of reproducing the plate mode oscillations of the valve, which cause the valve displacement signal to oscillate around the idealized paths predicted computationally. Furthermore, it can be seen in Fig. 4.4 that the elastic impact model assumes an instantaneous restitution of momentum, resulting in a sharp corner in the displacement time trace at the moment of impact, which would be manifested in steps in the velocity response of the valve, with the acceleration reaching infinity at that instant. This is of course unrealistic as it would not be physical to achieve such accelerations. This is in contrast with the pseudo-force method, where the instantaneous impact assumption is not present,

resulting in finite acceleration values during contact. This is not a trivial aspect, as the acoustic field modelling is reliant on knowledge of the valve's instantaneous acceleration as a prerequisite for computing the boundary condition at $z = 0$. Finally, the chosen method provides the ability to compute contact forces acting on the valve, a capability which is simply not possible with the elastic impact model.

Numerical procedure test

In the current framework, the structural model of the valve is interacting with the acoustic field in a flanged pipe. This case is similar to the driver-pipe mechanism presented by Kinsler et al. (1999), with the valve plate acting as the driver and a minor difference in boundary conditions as Kinsler et al. (1999) considers the case of a rigidly closed pipe. This theoretical framework is insightful as it provides analytical validation means for the acoustic interaction model. The coupling between the valve and pipe is shown in Fig. 4.5, where the valve plate is represented by a mass-spring-damper system, and allowed to oscillate in the axial direction at the inlet of a flanged pipe. The valve is subjected to a harmonic excitation force of constant amplitude. The equation of motion may then be stated in complex exponential form as:

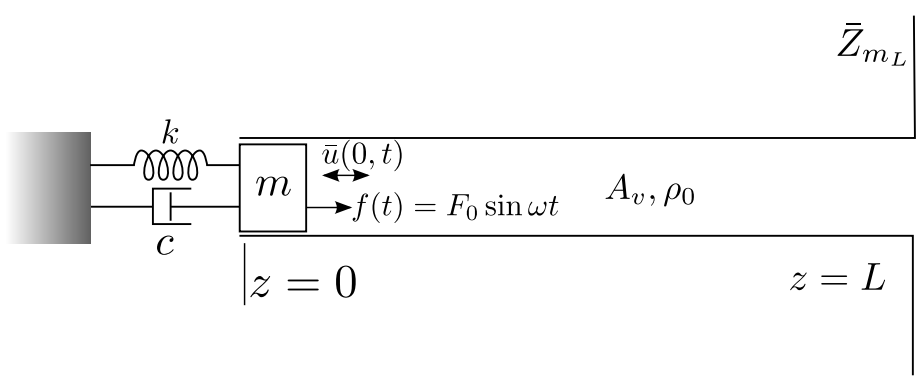

Figure 4.5: Acoustic coupling model for the spring-loaded valve.

$$m\ddot{\boldsymbol{x}} + c\dot{\boldsymbol{x}} + k_s\boldsymbol{x} + A_v\boldsymbol{p}(0,t) = Fe^{j\omega t} \tag{4.17}$$

where $\boldsymbol{p}$ is the complex acoustic pressure. The oscillating valve is only subjected to two forces in this case: a hypothetical harmonic load $\boldsymbol{f} = Fe^{j\omega t}$ and the acoustic pressure at $z = 0$. Since Eq. (4.17) is stated in its complex form, it is possible to express the acceleration $\ddot{\boldsymbol{x}}$ and the valve position $\boldsymbol{x}$ as a function of the valve velocity $\dot{\boldsymbol{x}}$. That is:

$$jm\omega\dot{\boldsymbol{x}} + c\dot{\boldsymbol{x}} + \frac{k_s}{j\omega}\dot{\boldsymbol{x}} + A_v\boldsymbol{p}(0,t) = Fe^{j\omega t} \tag{4.18}$$

From Fig. 4.5, it is clear that the valve plate velocity $\dot{x}$ is equal to the acoustic particle velocity at $z = 0$, *i.e.* $\boldsymbol{u}(0,t) = \dot{x}$. Hence, by substituting the acoustic particle velocity into Equation (4.18), we obtain the following relationship:

$$jm\omega\boldsymbol{u}(0,t) + c\boldsymbol{u}(0,t) + \frac{k_s}{j\omega}\boldsymbol{u}(0,t) + A_v\boldsymbol{p}(0,t) = Fe^{j\omega t} \tag{4.19}$$

The final steps are to ensure that all imaginary terms appear in the numerator, separate the real and imaginary parts on the left-hand side, and divide both sides of Eq. (4.19) by $\boldsymbol{u}(0,t)$, resulting in:

$$c + j\left(\omega m - \frac{k_s}{\omega}\right) + \frac{A_v\boldsymbol{p}(0,t)}{\boldsymbol{u}(0,t)} = \frac{\boldsymbol{f}}{\boldsymbol{u}(0,t)} \tag{4.20}$$

In the above relationship, one may identify two key quantities on the left hand side. The first represents the mechanical impedance of the valve structure, defined as:

$$\boldsymbol{Z}_{mv} = c + j\left(\omega m - \frac{k_s}{\omega}\right), \tag{4.21}$$

and the second represents the input mechanical impedance of the pipe, which can be

stated as:

$$\boldsymbol{Z}_{m0} = \frac{A_v \boldsymbol{p}(0,t)}{\boldsymbol{u}(0,t)} \tag{4.22}$$

In addition, an accepted way of expressing the input mechanical impedance (at $z = 0$) consists in relating it to the impedance at the end of the pipe section (at $z = L$), as provided by Kinsler et al. (1999):

$$\boldsymbol{Z}_{m0} = \rho c_0 A_v \frac{(\boldsymbol{Z}_{mL}/\rho c_0 A_v) + j \tan k_n L}{1 + j\,(\boldsymbol{Z}_{mL}/\rho c_0 A_v) \tan k_n L} \tag{4.23}$$

The relationship above allows for an expression of the acoustic influence at $z = 0$ due to a given condition at $z = L$. In this case, the condition at $z = L$ is that of an open-flanged pipe, for which it is assumed that acoustic radiation is the dominant effect. The end impedance $\boldsymbol{Z}_{mL}$ should then equal the radiation impedance $\boldsymbol{Z}_r$ of an open-flanged pipe, which according to Kinsler et al. (1999) is as follows:

$$\boldsymbol{Z}_{mL} = \boldsymbol{Z}_r = \rho c_0 A_v \left(\frac{1}{8}(k_n d)^2 + j \frac{4 k_n d}{3\pi} \right) \tag{4.24}$$

Where d is the pipe diameter at the flange. Knowledge of the mechanical impedance values for this system is equivalent to solving the differential equation given in (4.17), allowing for computation of the displacement and velocity amplitudes using the following relations:

$$X(\omega) = \frac{F}{Z_{mv}(\omega) + Z_{m0}(\omega)} \tag{4.25}$$

$$X(\omega) = \frac{U(\omega)}{j\omega} \tag{4.26}$$

The above relations can be used to calculate expected amplitudes of oscillation for a given frequency. This driver response is then obtained for a unit harmonic force

applied to the driver. This is shown in Figs. 4.6 and 4.7 for a light and flexible driver, then heavy and stiff driver, respectively. The horizontal axis is shown as a non-dimensionalized frequency term kL, with $k = \omega/c$ the wave number. The definition

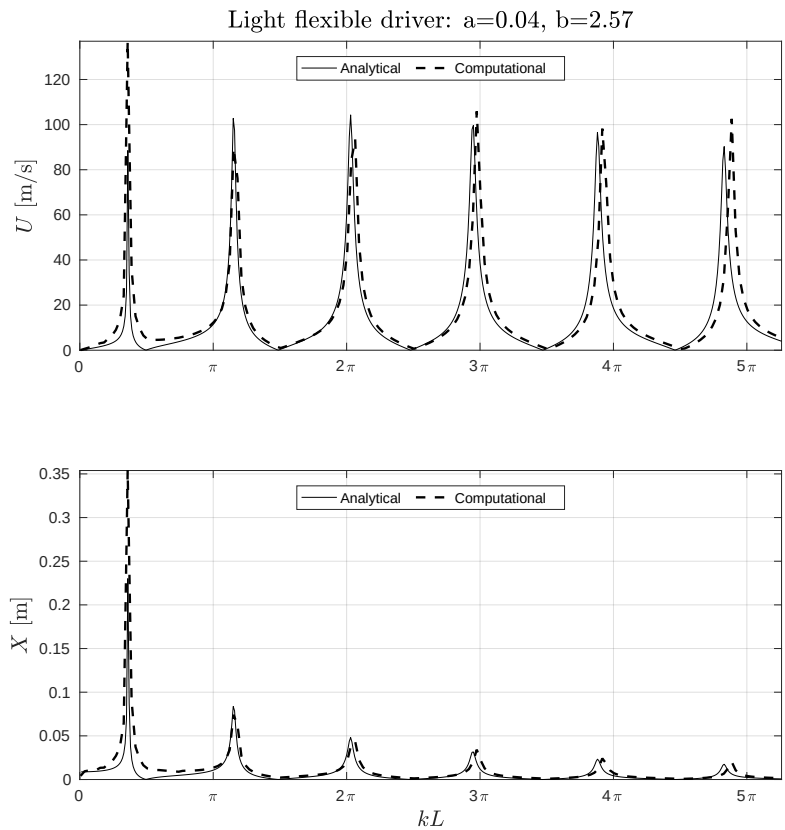

Figure 4.6: Driver position (top) and velocity (bottom) as computed theoretically (solid line) and numerically (dashed line). Case of a light and flexible driver.

of a light and flexible (or heavy and stiff) driver is consistent with Kinsler et al. (1999), based on the non-dimensional parameters a and b defined as:

$$a = \frac{m}{A_v \rho L} \tag{4.27}$$

$$b = \frac{k_s L}{A_v \rho c_0^2} \tag{4.28}$$

The acoustic description of the system presented herein concurs with the hypothesis of Hős et al. (2014), who propose a standing quarter-wave as a model of the acoustic pressure distribution in the upstream piping of pressure relief valves.

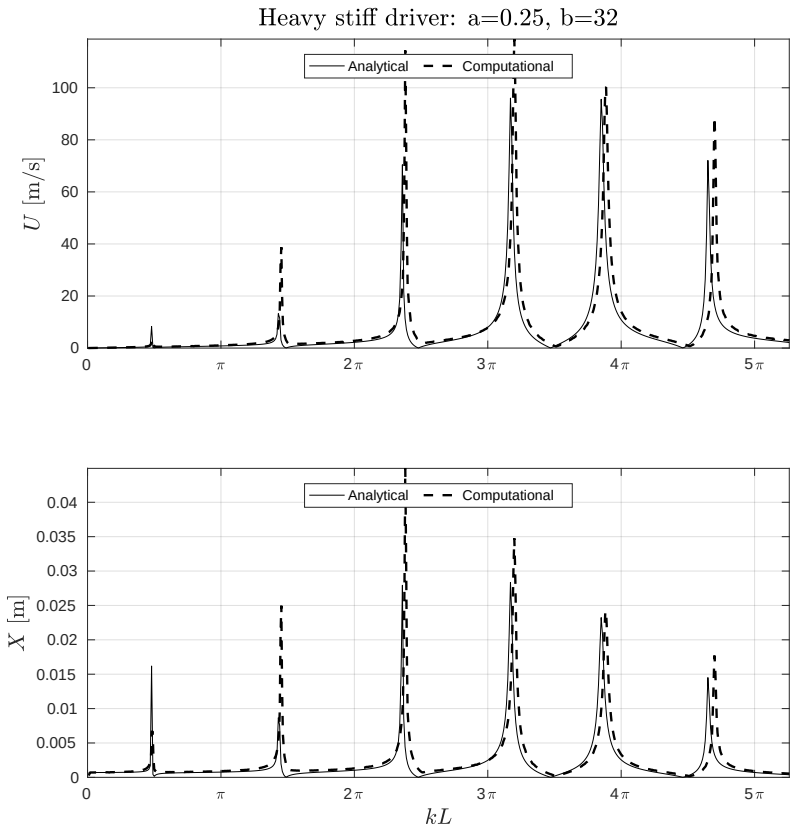

Figure 4.7: Driver position (top) and velocity (bottom) as computed theoretically (solid line) and numerically (dashed line). Case of a stiff and heavy driver.

The numerical technique described in Sec. 4.2 is used to compute the valve position and velocity for the above cases, shown with a dotted line in Figs. 4.6 and 4.7. It can be seen that the numerical technique shows great agreement with the theoretical model of the driver-pipe interaction mechanism for a flanged pipe. Typical to discretization models of Eigenvalue problems, higher modes are predicted with less accuracy, which isn't a concern for the frequency ranges of interest for this study.

4.4 Experimental Setup

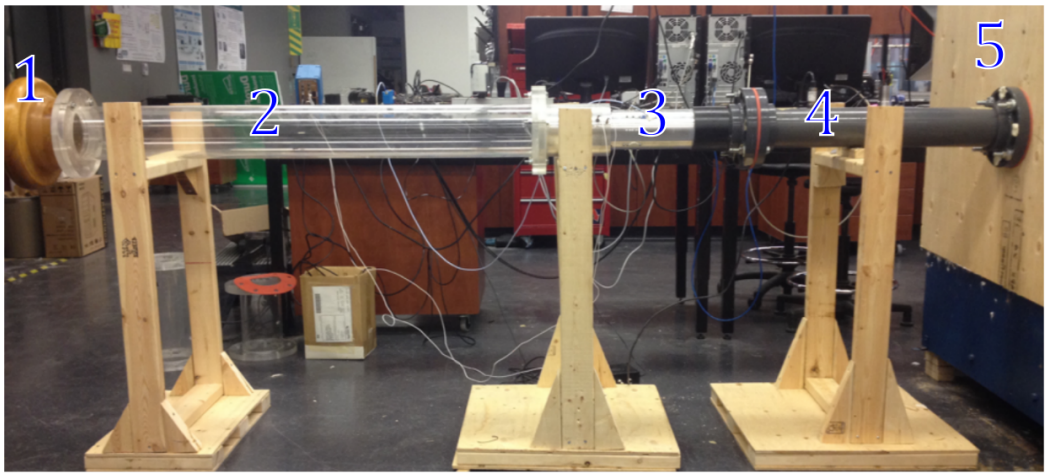

Figure 4.8: Experimental facility used for validation experiments. 1- Bellmouth entrance, 2- Upstream pipe length. 3- Spring-loaded valve test section, 4- Downstream pipe, 5- Settling chamber.

The test facility used for the validation of the model is shown in Fig. 4.8. The setup is described in detail in a previous publication (El Bouzidi et al., 2018). Briefly, the flow enters through a bell-mouth (1), and exits to a settling chamber (5) to which a 20 hp variable speed Roots blower is connected in suction. The test section (3) can be attached to upstream pipes of length L_u (2) and downstream pipes of length L_d (4). The system is in an open-loop configuration, with the flow entering the test-section at room temperature and pressure conditions. A static pressure transducer is used to measure the total pressure drop across the system. The valve position $x(t)$ is determined by a magnetic dynamic proximity transducer reading, which produces a voltage proportional to the distance to the tapered tip of the valve stem. Additionally, the model valve as well as the positions of the dynamic pressure transducers can be seen in greater detail in Fig. 4.9.

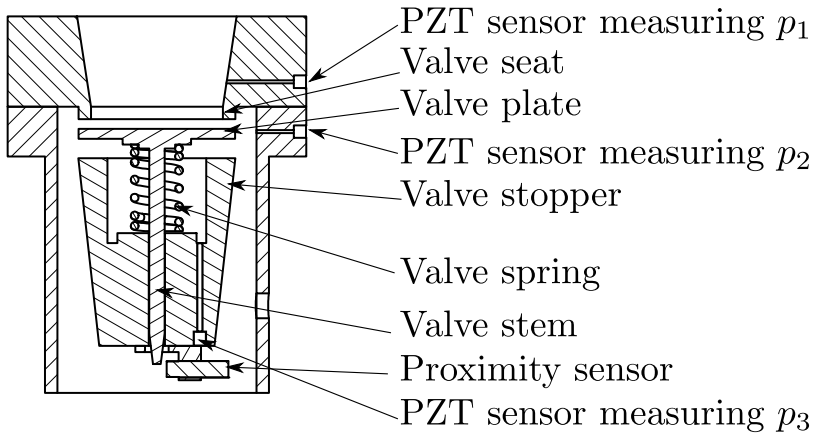

Figure 4.9: Sketch showing important features in the model valve.

4.5 Results & Discussion

Uncoupled hydrodynamic response

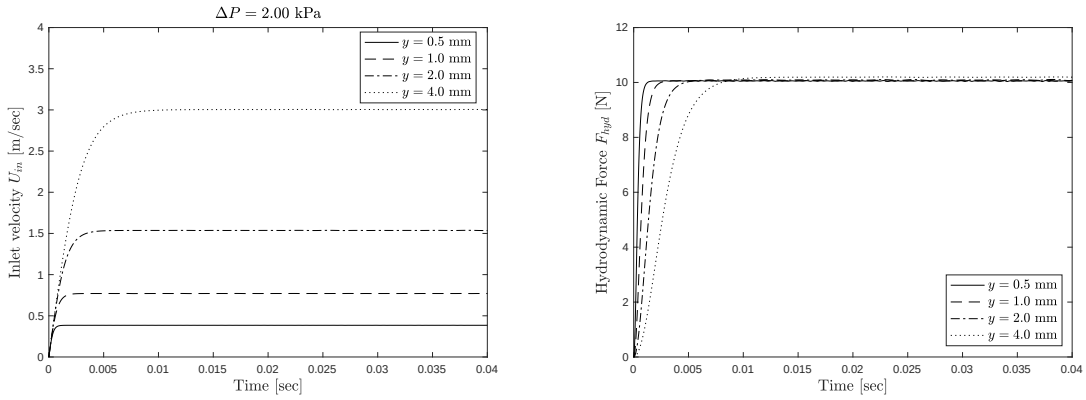

(a) Flow velocity (b) Hydrodynamic force

Figure 4.10: Step response of the hydrodynamic model at various valve openings.

Some uncoupled unsteady simulations were conducted with the hydrodynamic model alone, in order to gain some insight about the characteristics of the system. Solutions were obtained by applying a fixed valve opening, a fixed static pressure difference (*e.g.*

$\Delta P = 2.0$ kPa) and numerically solving Eqs. (4.3) and (4.6) for the instantaneous flow rate through the system and the unsteady pressure across the valve, respectively. These quantities are in turn utilized to compute the valve inlet velocity U_{in} and the hydrodynamic force F_{hyd}, which are shown in Fig. 4.10. It can be seen that the increase in valve opening allows for higher flow velocities at the inlet, due to significant losses at small valve opening. It can also be seen that the transient behaviour corresponding to the establishment of the flow at a given opening shows similar features to a first order system. However, one may notice that the time constant for each opening is different, whereby an increase in opening appears to increase the time to steady-state. This is more evident in the hydrodynamic force plot (shown in Fig. 4.10b), where steady state is reached at different times, despite an identical equilibrium point for a given ΔP value. The transient step response for the hydrodynamic system is demonstrating strong non-linear behaviour. Further manifestation of this non-linearity can be observed in sinusoidal response simulations.

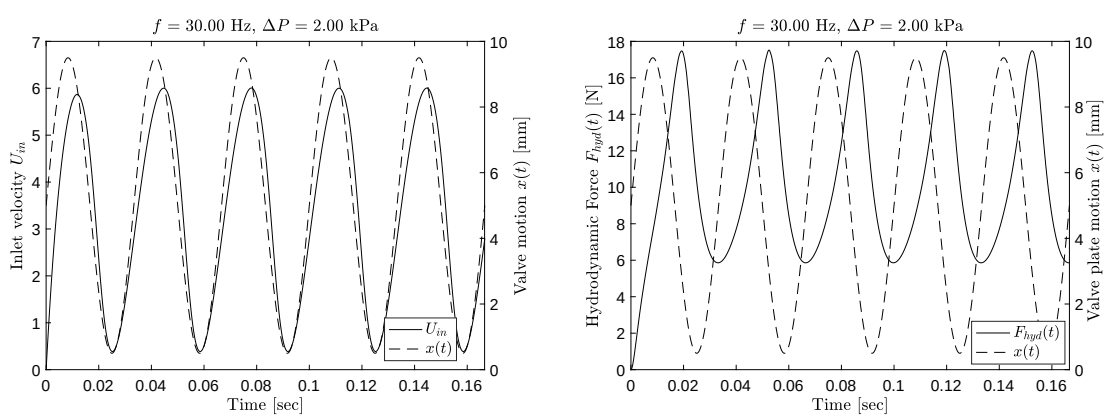

(a) Flow velocity (b) Hydrodynamic force

Figure 4.11: Sinusoidal response of the hydrodynamic model. $f = 30$ Hz. $\Delta P = 2.00$ kPa.

Figure 4.11 shows the response of the hydrodynamic model to a prescribed sinusoidal motion of the valve plate at a frequency of 30 Hz. The flow velocity (Fig. 4.11a) is

seen to lag behind the valve motion during the opening portion of the cycle, whereas it tracks it during closing. This showcases the hysteretic behaviour of the flow in the valve channel over a cycle of oscillation. This type of behaviour cannot be reproduced using a quasi-steady model of the flow, which has been the norm in this type of modelling, as seen in the work of Habing and Peters (2006) and Moussou et al. (2010). Furthermore, the hydrodynamic force (Fig. 4.11b) is showing a sharper peak when it is at maximum compared to when it is at minimum. This shows that the unsteady behaviour of the flow during the opening of the valve is governed by the inertia of the flow, whereas during closing it is controlled by the valve plate motion.

Hydrodynamic coupling

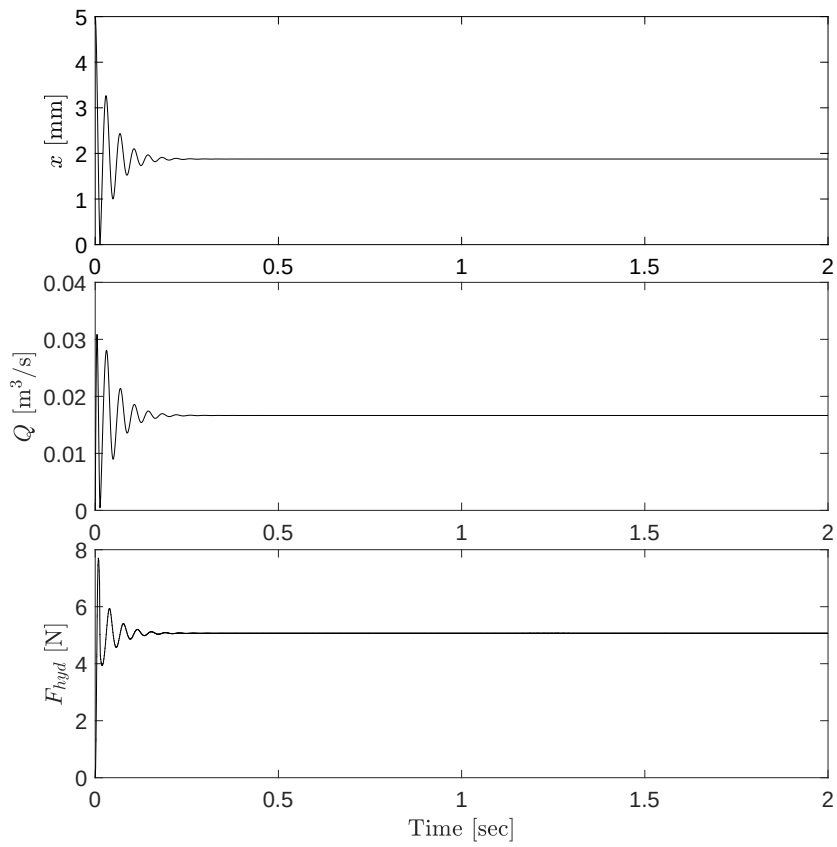

Figure 4.12: Simulated time signals for a case with no acoustic feedback. Top: valve displacement, middle: flow rate, bottom: hydrodynamic force. $\Delta P = 1$ kPa, $k = 2700$ N/m, $L_d = 2.25$ m, $x_{max} = 10$ mm. $\Delta t = 5 \times 10^{-5}$ sec, $T_f = 2$ sec.

The hydrodynamic model described by Eq. (4.3) is then utilized to calculate the forces acting on the valve, while the valve plate dynamics are calculated using Eq. (4.1), with acoustic effects neglected for the time being (*i.e.* $F_{ac}(t) = 0$). A long pipe case, which has experimentally shown severe oscillations is considered, where $k = 2700$ N/m, $x_{max} = 10$ mm, $L_d = 2.25$ m. Simulations are conducted by setting the initial

valve position to $0.5x_{max}$ at ΔP increments and simulating 2 seconds of the coupled response.

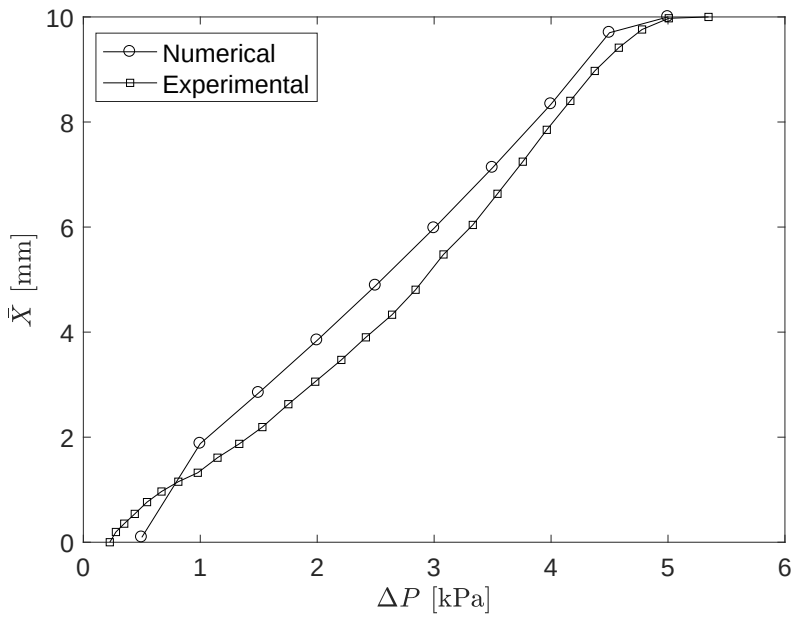

Figure 4.13: Simulated mean displacement of the valve for case with no acoustic feedback. $k = 2700$ N/m, $L_d = 2.25$ m, $x_{max} = 10$ mm.

Sample results are shown in Fig. 4.12, where it can be seen that for the given prescribed pressure difference ($\Delta P = 1.0$ kPa), the valve plate will oscillate about its equilibrium point, impacting on its seat, prior to settling at its steady-state opening. The flow rate and hydrodynamic force show similarly stable behaviour. Simulations are conducted over the entire range of opening of the valve. A summary of the results is provided in Fig. 4.13, which shows the mean opening of the valve plotted against the static pressure difference across the system. The simulation results are compared against an experimental case where acoustic feedback is suppressed using an acoustic device (concentric cavity resonator). It can be seen that the simulations show remarkable agreement with the experimental case. Furthermore, without acoustic

feedback, instability does not occur in either case. This lack of instability when acoustic forces are neglected is manifested for both short and long pipes.

To gain further insight into the dynamics of this coupled system, simulations are conducted with a unit sinusoidal force, and a frequency sweep is conducted at various static pressure difference values.

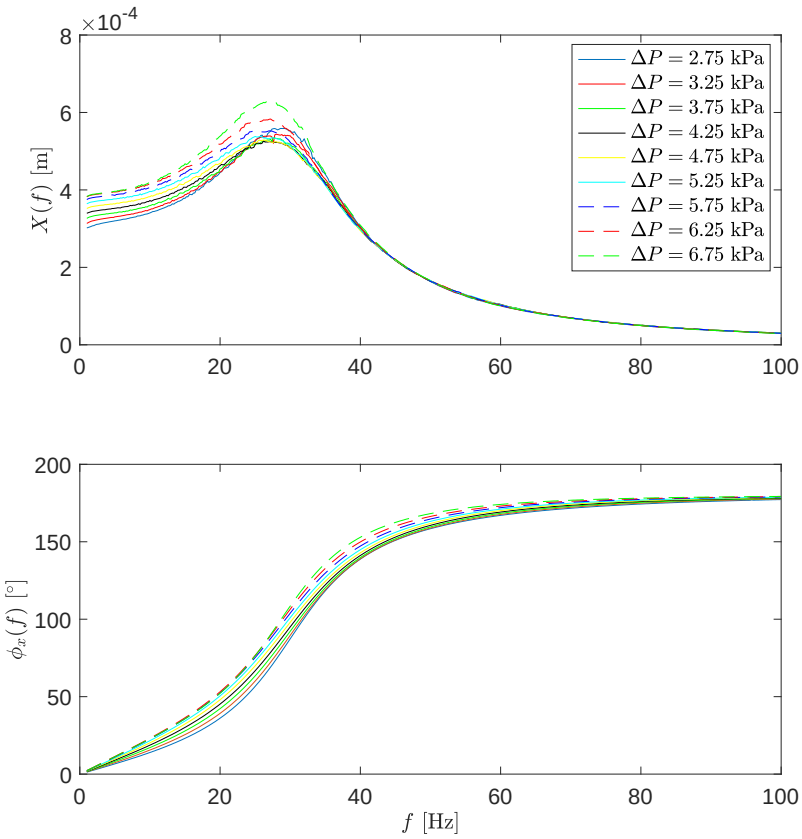

Figure 4.14: Hydrodynamic coupling response to a sinusoidal frequency sweep with a unit force. $k = 3600$ N/m.

Displacement amplitude and phase response plots are provided in Fig. 4.14. It can be seen that the sinusoidal steady state behaviour of this system at a given pressure difference is dominated by the second order system properties of the valve structure. The more interesting aspect revealed by these series of simulations is the shift of the

natural frequency of the coupled system as a result of the static pressure difference. Figure 4.15 provides a more convenient visualization of this phenomenon.

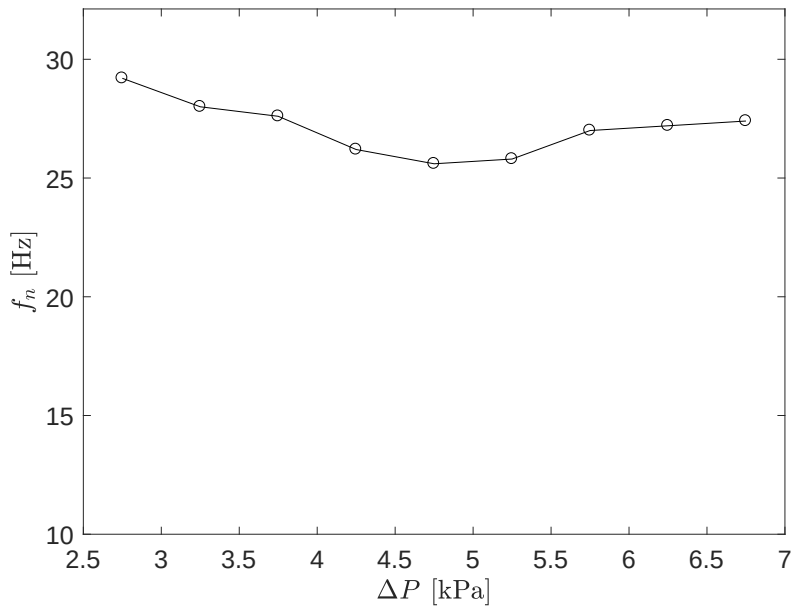

Figure 4.15: Simulated resonance frequency of the hydrodynamic-structural system *vs.* static pressure difference across the system.

It can be seen that the hydrodynamics have an added mass effect or added stiffness effect, which is responsible for a 3 Hz deviation from the structural frequency.

Influence of acoustic feedback

Fully coupled simulations are also conducted by including the forces due to the acoustic interaction mechanism. It can be seen that this is the critical feature that causes the valve to experience severe unstable oscillations. Sample time traces are provided in Fig. 4.16. Given an initial position away from its closed equilibrium ($x_0 = 5$ mm), the valve oscillations grow in amplitude until the seat-to-limiter vibrations occur, at a frequency of 39 Hz. This frequency does not correspond to the structure's natural

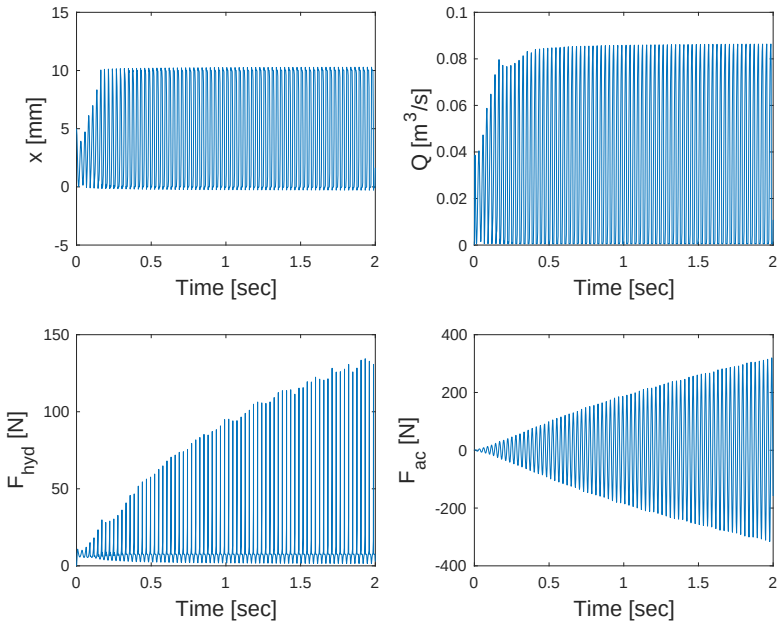

Figure 4.16: Simulated time traces for an unstable case. $k = 3600$ N/m, $x_{max} = 10$ mm, $L_d = 2.25$ m, $\Delta P = 1.5$ kPa.

frequency (29 Hz). Rather, it is the resonance frequency of the combined structural-acoustic system. The feedback mechanism can be observed through the simultaneous exponential growth of the amplitude of the acoustic force and the valve displacement. This provides further evidence that the acoustic feedback is essential to the instability.

As far as the waveform of the valve plate oscillation is concerned, the model is able to reproduce its main characteristics reasonably well. The valve plate position, predicted by the model for an unstable case, is shown for five cycles in Fig. 4.17. It can be seen that the predicted frequencies of oscillation are relatively close (around 39 Hz). In addition, the predicted behaviour during valve closing is reproduced adequately. On the other hand, while the reduced-order model does not replicate the intricate details of the valve plate motion when it impacts upon its stopper, it does predict the presence of a plateau, due to unsteady flow effects. Hence, this demonstrates that the

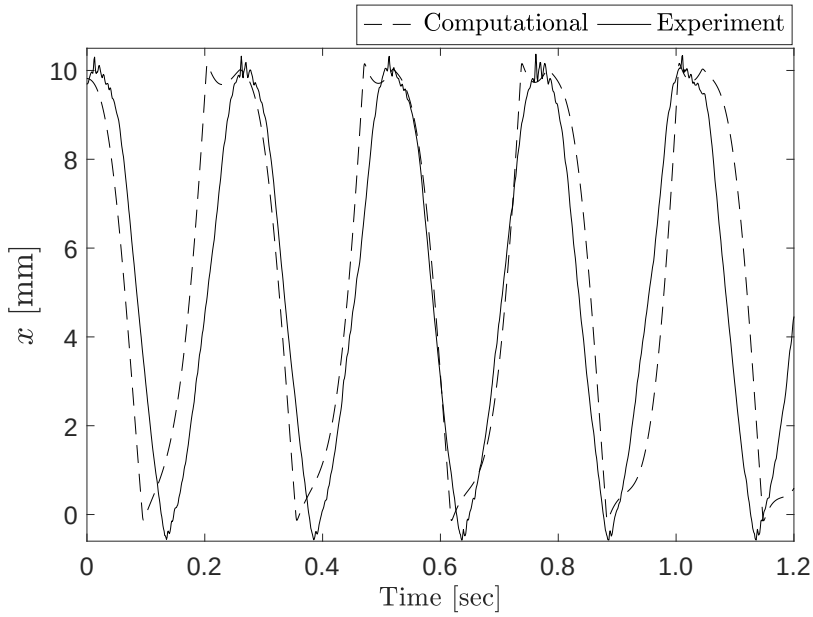

Figure 4.17: Simulated and experimental valve plate position for an unstable cae. $k = 2700$ N/m, $x_{max} = 10$ mm, $L_d = 2.25$ m, $\Delta P = 3.16$ kPa.

simplifications undertaken thus far do not compromise the model's ability to capture the essence of the instability mechanism, as well as the unsteady characteristics of the flow manifested through the delayed response of the flow and the complex behaviour during valve closing.

Effect of pipe length

In prior experiments, it was seen that the effect of downstream pipe length had two major effects. The first one was to change the oscillation frequency, due to the resulting change of the acoustic resonance frequency in the downstream pipe. This effect can be seen in Fig. 4.18, where the dominant frequency of oscillation predicted in the simulations can be seen, plotted against the experimental validation data. The negative correlation between frequency and length is present in both experimental and numerical results. This is not surprising, since the acoustic interaction model has

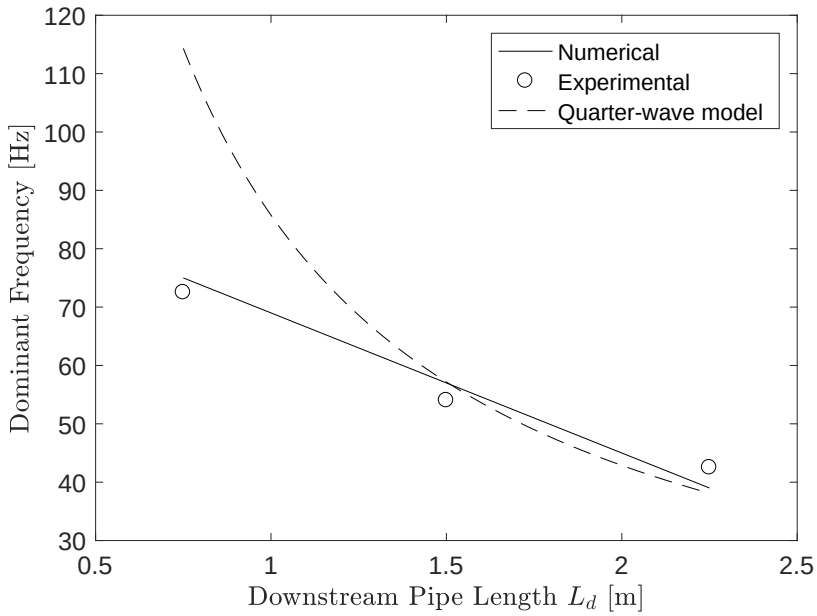

Figure 4.18: Dominant frequency of valve plate oscillation.

shown great agreement with the driver-pipe analytical model of Kinsler et al. (1999), which has previously shown great agreement with the experimental data (El Bouzidi et al., 2018). This demonstrates that the proposed model is able to replicate the modal characteristics of this system, despite the simplifications involved in formulating the reduced order model.

A third frequency prediction based on the acoustic resonance characteristics of the pipe alone (assuming closed-open boundary conditions) is provided. For such a configuration, the first mode consists in a quarter sine wave establishing itself as the standing wave in the downstream pipe. It can be seen that for a sufficiently long pipe (longer than 1.5 m for the considered geometry), the frequencies predicted using this model are quite close to the experimentally predicted frequencies, justifying the use of this model by Hős et al. (2015) for those circumstances. For short pipes (shorter than 1.5 m for the considered geometry), the experimentally observed frequencies are

significantly over-predicted by the quarter wavelength model of acoustic feedback. On the other hand, the model proposed within this article provides an accurate description of the modal characteristics of the system, as can be seen through the numerical solution results in Fig. 4.18.

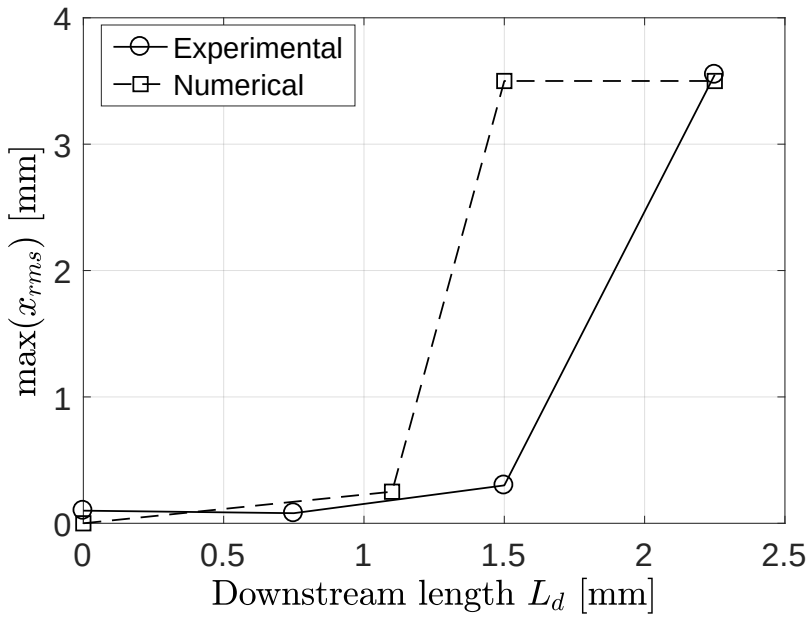

Figure 4.19: Maximum RMS amplitude of valve plate oscillation observed.

The second major effect that was seen in experiments was on oscillation amplitude. That is, a very short pipe caused small amplitude oscillations, which were seen to increase drastically in amplitude as the pipe length was increased. This effect was thought to be due to the stronger coupling that occurs when the plane wave mode of the pipe is closer to the structural natural frequency of the valve. This feature is present in the numerical simulations, as can be seen in Fig. 4.19. It is shown that the valve transitions from stable to unstable as pipe length is increased. The numerical model appears to make conservative predictions, as it predicts instability at a shorter pipe length than is seen in experiments. This stability threshold behaviour demonstrated

by the experimental results and predicted by the proposed model indicates the presence of a critical pipe-length that causes the system to undergo unstable oscillations, similar to the prediction of the Quarter-Wave Model of Hős et al. (2015) for pressure-relief valves.

Effect of stiffness

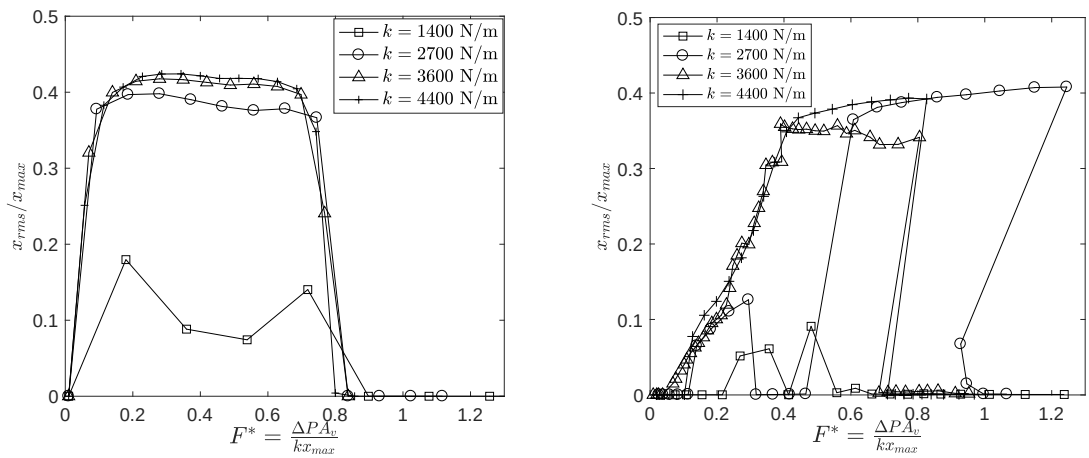

(a) Computational (b) Experimental

Figure 4.20: Valve stiffness effect as predicted by theoretical model compared to experimental results.

Figure 4.20 shows normalised oscillation RMS amplitudes as a function of the normalised static pressure difference for various valve spring stiffness values, over the range 1400–4400 N/m. The results obtained using the proposed model are shown in Fig. 4.20a and show great agreement with experimental data, shown in Fig. 4.20b. In both instances, it is observed that an increase in stiffness has a destabilising effect. The proposed model exhibits this effect through an increase in the RMS amplitude of the valve plate oscillation. For the experimental case, this destabilising effect is manifested through an increase in vibration amplitude when stiffness is increased from 1400 to 2700 N/m, as well as an early onset of the instability when stiffness

is further increased to 3600 N/m. Finally, the experimental case shows an increase in RMS amplitude when the stiffness is once again increased to 4400 N/m. The overall resulting trend that is reproduced by the theoretical model is the stronger coupling, manifested through higher amplitude or earlier onset of instability, when valve spring stiffness is increased. Furthermore, it can be seen that while comparable, the computationally predicted vibration amplitude is higher than experiments reports, further demonstrating the conservative nature of the proposed model, as losses are underestimated in the system. Moreover, it can be seen that due to the uncoupled nature of the outlet pressure boundary condition in the computational method, the theoretical model does not exhibit the pressure recovery that is seen in experiments when the blower speed is increased such that the valve is past its instability range.

Valve life & wear

A crucial advantage of the pseudo-force method used to model impact for this valve is the ability to predict contact forces acting on the valve. The force amplitude can be used to compute the stresses acting on the valve, which may in turn be used to conduct high-cycle fatigue analysis. Furthermore, this information is also instrumental for crack propagation simulations. This is a valuable design tool for engineers, as it can enhance structural valve design and material selection. In addition, it would provide a maintenance engineer a valuable tool for scheduling preventative maintenance in industrial plants.

Sample results are seen in Fig. 4.21 for an unstable case for a few cycles of oscillation. As expected, the impact forces appear during the contact portion of the cycle. It can be seen that since they occur over a small time duration, the peak force is quite high.

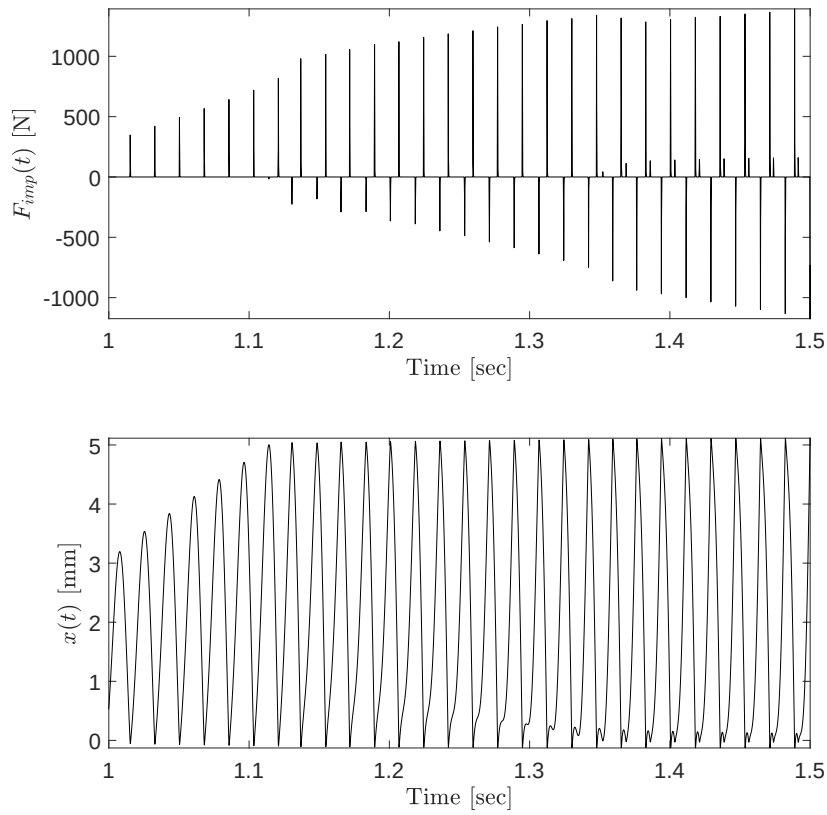

Figure 4.21: Impact forces acting on valve. Top: Impact force acting on valve, bottom: Valve plate displacement. $k = 3600$ N/m, $L_d = 1.50$ m, $x_{max} = 5$ mm, $\Delta P = 500$ Pa.

4.6 Conclusion

The aim of this paper is to propose a theoretical model of spring-loaded valves that can simulate the self-excited instability due to flow-sound-structure coupling. The original approach undertaken involved the use of a reduced order model of the structure that takes into account non-linear impact, a hydrodynamic model of the flow that incorporates unsteady effects, and a model of the acoustic field that accounts for the coupling with structural oscillations.

The model showed a remarkable ability to reproduce the governing features of this

self-excited instability. The necessity for acoustic feedback to trigger the instability was confirmed. Furthermore, the effect of pipe length on the amplitude of oscillation was also seen to agree with experimental data. In addition, the modal characteristics of the system were correctly predicted by this reduced order model. Also, the model provided useful insight on the non-linear aspects of the hydrodynamic model, such as the ability of the pressure difference across the system to alter its natural frequency. Finally, the predictive capability of the model was emphasized with computations of impact forces acting on the valve, which can be instrumental when assessing the life of a plant component.

Future work could involve extending this computational approach to more complex geometries. The ability to resolve the acoustic field for a more complex geometry would be useful as compressor manifolds and piping systems in plants are usually more complex than the straight pipe considered in this model. Furthermore, a more detailed model of the hydrodynamics could allow for a better description of the flow conditions.

Acknowledgements

The authors wish to acknowledge the support of the Natural Sciences and Engineering Research Council (NSERC) of Canada.

Bibliography

Atig, M., Dalmont, J.-P., & Gilbert, J. (2004). Saturation mechanism in clarinet-like instruments, the effect of the localised non-linear losses. *Applied Acoustics*, *65*, 1133–1154.

Bazsó, C., & Hős, C. (2013). An experimental study on the stability of a direct spring loaded poppet relief valve. *Journal of fluids and structures*, *42*, 456–465.

Blevins, R. D. (1984). *Applied fluid dynamics handbook*. New York: Van Nostrand Reinhold Co.

Darby, R. (2013). The dynamic response of pressure relief valves in vapor or gas service, part i: Mathematical model. *Journal of loss prevention in the process industries*, *26*, 1262–1268.

Darby, R., & Aldeeb, A. (2014). The dynamic response of pressure relief valves in vapor or gas service. part iii: Model validation. *Journal of Loss Prevention in the Process Industries*, *31*, 133–141.

Deverge, M., Pelorson, X., Vilain, C., Lagrée, P.-Y., Chentouf, F., Willems, J., & Hirschberg, A. (2003). Influence of collision on the flow through in-vitro rigid models of the vocal folds. *The Journal of the Acoustical Society of America*, *114*, 3354–3362.

El Bouzidi, S., Hassan, M., & Ziada, S. (2018). Experimental characterisation of the self-excited vibrations of spring-loaded valves. *Journal of Fluids and Structures*, *76*, 558–572.

Erdődi, I., & Hős, C. (2017). Prediction of quarter-wave instability in direct spring operated pressure relief valves with upstream piping by means of cfd and reduced order modelling. *Journal of Fluids and Structures*, *73*, 37–52.

Habing, R. A., & Peters, M. C. A. M. (2006). An experimental method for validating compressor valve vibration theory. *Journal of Fluids and Structures*, *22*, 683–697.

Hassan, M., Weaver, D., & Dokainish, M. (2002). A simulation of the turbulence response of heat exchanger tubes in lattice-bar supports. *Journal of Fluids and Structures*, *16*, 1145–1176.

Hős, C., Champneys, A., Paul, K., & McNeely, M. (2014). Dynamic behavior of direct spring loaded pressure relief valves in gas service: Model development, measurements and instability mechanisms. *Journal of loss prevention in the process industries*, *31*, 70–81.

Hős, C., Champneys, A., Paul, K., & McNeely, M. (2015). Dynamic behaviour of direct spring loaded pressure relief valves in gas service: Ii reduced order modelling. *Journal of Loss Prevention in the Process Industries*, *36*, 1–12.

Hunt, K., & Crossley, F. (1975). Coefficient of restitution interpreted as damping in vibroimpact. *Journal of applied mechanics*, *42*, 440–445.

Johansson, L. (1997). Beam motion with unilateral contact constraints and wear contact sites. *Journal of Pressure Vessel Technology*, *119*, 105–110.

Kasai, K. (1968). On the stability of a poppet valve with an elastic support: 1st report, considering the effect of the inlet piping system. *Bulletin of JSME*, *11*, 1068–1083.

Killmann, I. (1972). Aerodynamic forces acting on valve discs. In *International Compressor Engineering Conference*.

Kinsler, L. E., Frey, A. R., Coppens, A. B., & Sanders, J. V. (1999). *Fundamentals of acoustics* volume 1 of *ISBN 0-471-84789-5*. (4th ed.). Wiley-VCH.

Kolkman, P. A. (1976). *Flow-induced gate vibrations*. Technische Hogeschool Delft.

Moussou, P., Gibert, R. J., Brasseur, G., Teygeman, C., Ferrari, J., & Rit, J.-F. (2010). Instability of pressure relief valves in water pipes. *Journal of Pressure Vessel Technology*, *132*, 041308.

Nayfeh, A., & Bouguerra, H. (1990). Non-linear response of a fluid valve. *International Journal of Non-Linear Mechanics*, *25*, 433–449.

Oengören, A. (1987). *Experimental Investigation of Valve Plate Flutter on a Compressor Under Actual Working Conditions*. Technical Report 3503 Sulzer Laboratorium für Schwingungen und Akustik.

Shine, S. (1987). *Experimental Investigation on Self-Excited Vibrations of Reciprocating Compressor Multi-ring Plate valves*. Technical Report 3450 Sulzer Laboratorium für Schwingungen und Akustik.

Tsui, C., Oliver, C., & Cohen, R. (1972). Discharge phenomena of a two-dimensional poppet-type valve. In *Internal Compressor Engineering Conference*. Purdue, Indiana: Purdue University.

Weaver, D. S., & Ziada, S. (1980). A theoretical model for self-excited vibrations in hydraulic gates, valves and seals. *Journal of Pressure Vessel Technology*, *102*, 146–151.

Ziada, S., Shine, S., & Bühllmann, E. (1986). Self-excited vibrations of reciprocating compressor plate valves. In *International Compressor Engineering Conference*.

Nomenclature

A_v	Valve plate area.
A_{ij}	Cross-sectional area from location i to j.
Co	Courant number.
c	Viscous damping of the valve structure.
c_0	Sound propagation speed in the medium.
d	Pipe diameter.
E	Young's modulus.
F^*	Ratio of the fluid force to spring force at maximum opening.
F_a	Acoustic force acting on the valve.
F_h, F_{hyd}	Hydrodynamic force acting on the valve.
F_{imp}	Impact force acting on the valve.
g	Acceleration of gravity.
$h_{L_{ij}}$	Viscous loss coeffiecient between locations i and j.
I_{ij}	Inertance of the pipe length between locations i and j.
K_{ij}	Loss coefficient between location i and j.
K_{imp}	Impact stiffness.
k_s	Valve spring stiffness.
k	Plane wave number.
L	Pipe length.
L_{ij}	Pipe length from location i to j in the hydrodynamic system.
l_{eq}	Equivalent resonator neck length.
m	Valve plate mass.
ΔP	Static pressure difference across the system.

Nomenclature (continued)

p_i	Instantaneous pressure at location i.
Q	Instantaneous flow rate.
$\bar{u}(0,t)$	Acoustic particle velocity at the valve.
U_{in}	Inlet velocity.
V_i	Flow velocity at location i.
x	Valve plate displacement.
x_{max}	Maximum valve opening.
x_{rms}	RMS value of the valve plate oscillation.
$\bar{X}$	Mean valve opening.
z	Axial location along the pipe.
$\boldsymbol{Z}_{m0}$	Inlet mechanical impedance of the pipe.
$\boldsymbol{Z}_{mL}$	Mechanical impedance at the flanged outlet.
$\boldsymbol{Z}_{mv}$	Mechanical impedance of the valve.
α	Material damping coefficient during contact.
δ	Contact overlap distance.
γ	Specific weight.
ρ	Density of the propagation medium in the pipe.

Chapter 5

Acoustic Methods to Suppress Self-Excited Oscillations in Spring-Loaded Valves

Complete Citation:

El Bouzidi, S., Hassan, M., & Ziada, S. Acoustic Methods to Suppress Self-Excited Oscillations in Spring-Loaded Valves. *Submitted on March 20, 2018 to the Journal of Fluids and Structures.*

Relative Contributions:

S. El Bouzidi: Performed experimental work. Conducted analysis and interpretation of results. Prepared manuscript for publication.

M. Hassan: Co-supervisor of S. El Bouzidi. Provided guidance on experimental work and feedback on manuscript.

S. Ziada: Co-supervisor of S. El Bouzidi. Provided guidance on experimental work and feedback on manuscript.

Abstract

Spring-loaded valves have been reported to experience self-excited vibration in reciprocating compressor installations as well as in safety relief devices of pressurized systems. Prior work by the authors has provided an experimental characterization (El Bouzidi et al., 2018) and a theoretical model (El Bouzidi et al., 2017) of the flow-sound-interaction mechanism which causes the self-excited vibration. It was found that the vibration occurred only when the fluid-structure interaction at the valve is coupled with acoustic reflections in the associated piping system. In other words, coupling with the pipe acoustics was essential for the initiation of the self-excited valve vibration.

This investigation evaluates the effectiveness of three acoustic devices in suppressing the self-excited vibrations. The objective is to dampen the sound waves in the piping system and weaken its coupling with the valve oscillations. A concentric Helmholtz-type cavity resonator, an orifice plate, and an anechoic termination are placed at the downstream side of a model valve which exhibited strong self-excited vibration in previous investigations. The orifice plate was successful in eliminating the oscillation frequency, but its placement at the acoustic pressure node was critical. The concentric cavity resonator dampened the oscillations to very small amplitudes, but a knowledge of the oscillation frequency was necessary. Finally, the anechoic termination was also successful in suppressing the oscillation, but its practicality is rather limited in industrial pipelines.

Keywords

flow-induced vibration, spring-loaded valves, fluid-structure interaction, acoustic filters

5.1 Introduction

Spring-loaded valves are widely used in industrial applications. Their self-acting ability, which allows them to open or close based on pressure conditions, makes them particularly instrumental in safety-relief applications for nuclear power plants. In these cases, valves open systematically as an emergency measure if the pressure in the pipeline exceeds operational specifications. They are also often used as directional valves in reciprocating compressors. In gas compression and safety relief applications alike, traditional valve design has mainly relied on steady, time-independent characteristics of the system. However, dynamic fluid loading can result in vibrations that severely hinder the operation of the valve either by reducing its performance or through premature wear. Furthermore, interaction with the acoustic properties of the piping can exacerbate these issues by introducing an additional factor that is also typically omitted in valve design. This specific failure mode has been seen in several cases reported in the industry, for both reciprocating compressor valves (Ziada et al., 1986) as well as safety relief valves (Baldwin and Simmons, 1986).

Over nearly half a century, a great deal of literature has emerged to characterize various aspects of spring-loaded valve dynamic instability. While some investigations attempted to determine the nature of fluid loading present (Killmann, 1972; Tsui et al., 1972), others sought to provide linear stability analysis for these types of systems (Kolkman, 1976). Later studies aimed to provide a comprehensive overview of the flow-sound-structure interaction mechanism either through experimental (Ziada et al.,

1986; Moussou et al., 2010; El Bouzidi et al., 2018; Habing and Peters, 2006) or numerical means (Erdődi and Hős, 2017; El Bouzidi et al., 2017). On the other hand, existing literature on suppressing the vibration of the valves has usually focused on altering structural parameters of the valve, such as the spring stiffness (Ziada et al., 1987), or through minimizing the fluid-resonant vortex-shedding mechanism in safety relief valves (Baldwin and Simmons, 1986). Despite the principal role that acoustic interaction plays in the onset of this dynamic instability, little experimental work has been conducted to determine whether attenuating these acoustic plane waves would suppress the valve plate oscillations. This gap in the literature provides an opportunity to uncover potential methods that can mitigate the destructive effect of the self-excited oscillations, which is the objective of this investigation.

With this stated purpose, the current study aims to suggest solutions that could eliminate valve flutter due to flow-sound-structure coupling without altering the design of the spring-loaded valve, which may already be in operation. Rather, the proposed devices can be conveniently added to the piping system in the plant. Three solutions are experimentally assessed for a case that has previously shown severe vibrations. First, an anechoic termination is connected, to demonstrate that attenuating the acoustic plane wave by reducing the magnitude of the reflected pressure wave is able to suppress the vibrations. Second, an orifice plate is tested, due to its ease of manufacturing and installation while being an effective solution. Finally, a Helmholtz-type concentric cavity resonator is designed, built, and assessed, in order to provide a solution with minimal hydraulic losses. The suggested approach is a novel method to address these types of concerns for spring-loaded valves.

5.2 Theoretical Background

Coupled Valve-Pipe Interaction Mechanism

The acoustic interaction phenomenon for the coupling between the spring-loaded valve and connected piping is best described by the driver-pipe mechanism presented by Kinsler et al. (1999). A treatment of this theoretical framework as it applies to a spring-loaded valve, as well as a time-domain implementation are presented in previous work by the authors (El Bouzidi et al., 2017, 2018). Briefly, the acoustic interaction between the valve and downstream pipe can be schematically represented as shown in Fig. 5.1. In such a system, the sum of the reactive parts of the inlet impedance $\boldsymbol{Z}_{m0}$ of

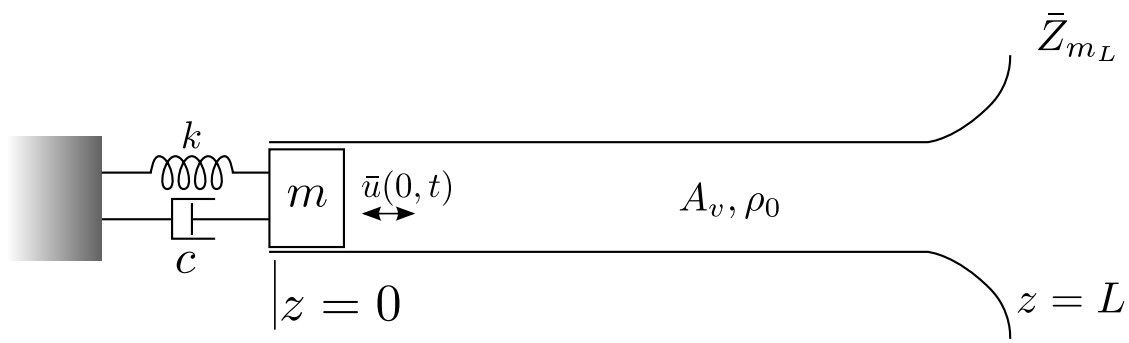

Figure 5.1: Valve–pipe configuration of the valve.

the pipe at $z = 0$ and the mechanical impedance of the valve $\boldsymbol{Z}_{mv}$ is zero at resonance, such that:

$$Im\{\boldsymbol{Z}_{mv} + \boldsymbol{Z}_{m0}\} = 0 \tag{5.1}$$

Hence, a solution of the above equation yields the dominant frequencies of oscillation during instability for this system. A graphical solution method is illustrated in a previous publication (El Bouzidi et al., 2018). Any remedial measure to mitigate this instability needs to take into account the characteristics of this system. To this respect,

three solutions are devised, operating on different aspects of the acoustic coupling present between the valve and piping, and are described in the subsequent subsections.

Anechoic Termination

An anechoic termination aims to prevent the establishment of a standing wave in a pipe through elimination of the reflected wave. While such a description only strictly holds for an ideal termination, practically, it is still possible to achieve significant attenuation of the reflected wave over a wide frequency spectrum. Terminations can be manufactured inexpensively and achieve an average pressure reflection coefficient below 10% over a wide range of audible frequencies.

Orifice Plate

The purpose of placing an orifice plate in the downstream pipe is to introduce a source of losses through attenuation of the acoustic particle velocity. Consequently, a suitable location is critical to the performance of this device. The orifice will be most effective at the acoustic particle velocity antinode (*i.e.* the acoustic pressure node). Furthermore, it should be mentioned that the orifice plate behaves as an amplifier of acoustic energy over a certain Strouhal number range, while it acts as a dissipater outside this range. The exact nature of this amplitude *vs.* frequency relationship depends on non-dimensional quantities such as the Reynolds number, Mach number, and thickness-to-diameter ratio. Fortunately, the existing literature (Karthik et al., 2008; Testud et al., 2009; Lacombe et al., 2011) provides adequate guidance in order to design an orifice plate that will perform as a dissipater when placed in the piping system. The final aspect to consider is that the orifice plate is inherently a hydraulic loss device. As such, the area ratio must be selected in order to minimize the losses

caused by its insertion.

Concentric Cavity Resonator

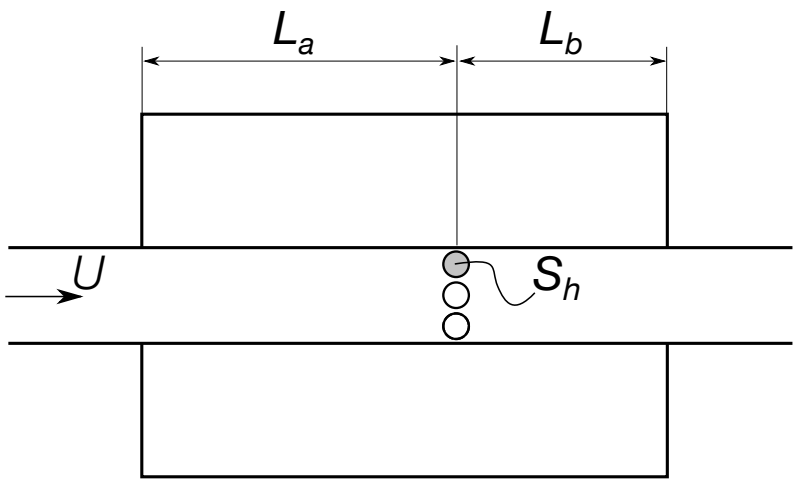

Figure 5.2: Sketch of a concentric cavity resonator.

The concentric cavity resonator is a device similar to a Helmholtz resonator, operating based on the same principle. It is more practical than the latter for use in piping systems, and is often a component of automotive exhaust mufflers. When placed in a piping system, the concentric cavity resonator behaves as a notch filter (Munjal, 2014), by preventing the transmission of the propagating acoustic plane wave downstream. The device consists of an outer annular cavity connected at a specified location on the downstream pipe, and a hole pattern on the inner pipe. An illustration is provided in Fig. 5.2. The design of the device relies on selecting parameters such that the following equation is satisfied:

$$\frac{1}{n_h}\frac{\omega l_{eq}}{S_h} = \frac{\rho_0 c_0 / S_c}{\tan\left(k_0 L_a\right) + \tan\left(k_0 L_b\right)} \tag{5.2}$$

where n_h is the number of holes, ω is the filter design angular frequency, S_h is the area

per drilled hole, ρ_0 the density of the medium, c_0 the sound propagation speed, S_c the transverse area of the concentric cavity resonator, and $L_a + L_b$ is its length.

The design of this acoustic filter based on Eq. (5.2) is a reasonably achievable task, as the problem is usually under-constrained due to the large number of parameters. Hence, it is often possible to adjust some of the parameters to overcome design constraints, which are typically a fixed inner pipe diameter, the total resonator length, and the maximum outer-pipe diameter. On the other hand, the range of frequencies suppressed around the target frequency may often be too narrow for practical purposes, as it may not be possible to know the instability frequencies exactly. As a remedy, steel wool may be inserted in the holes to broaden the range of frequencies attenuated.

5.3 Experimental Methodology

Testing Facility and General Parameters

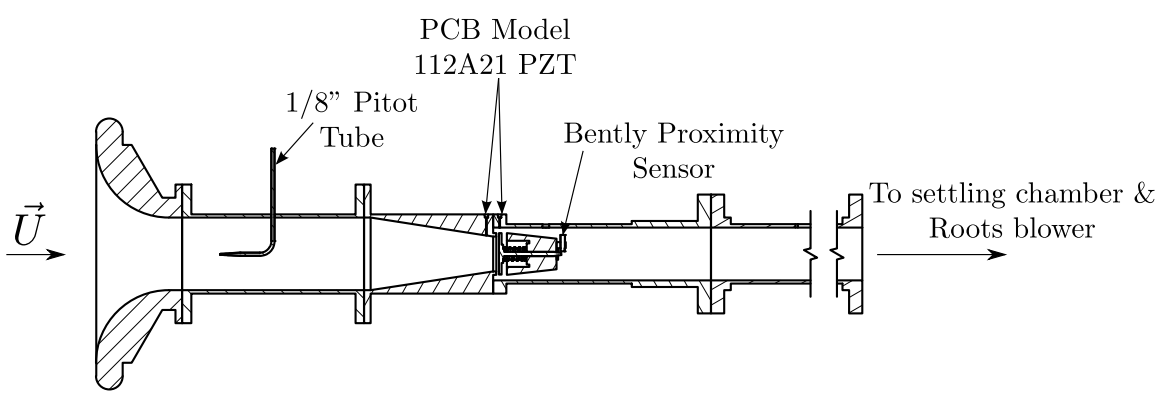

Figure 5.3: Sketch of the spring-loaded valve testing apparatus.

The test facility used for the validation of the model is shown in Fig. 5.3. The rig is described in further detail by El Bouzidi et al. (2018). To summarize, air flow enters through a bell-mouth, and exits to a settling chamber to which a Roots blower

is connected in suction, driven by a 20hp 3-phase AC motor and its speed is controlled by a variable-frequency drive. The system is in an open-loop configuration, with the flow entering the test-section at room temperature and pressure conditions. A static pressure transducer is used to measure the total pressure drop across the system. The valve position $x(t)$ is determined directly by using a magnetic proximity transducer that produces a voltage proportional to the displacement of the valve plate. This direct displacement measurement method provides a significant advantage compared to using an accelerometer, especially in cases with impact. The flow geometry and instrument arrangement surrounding the valve can be seen in greater detail in Fig. 5.4.

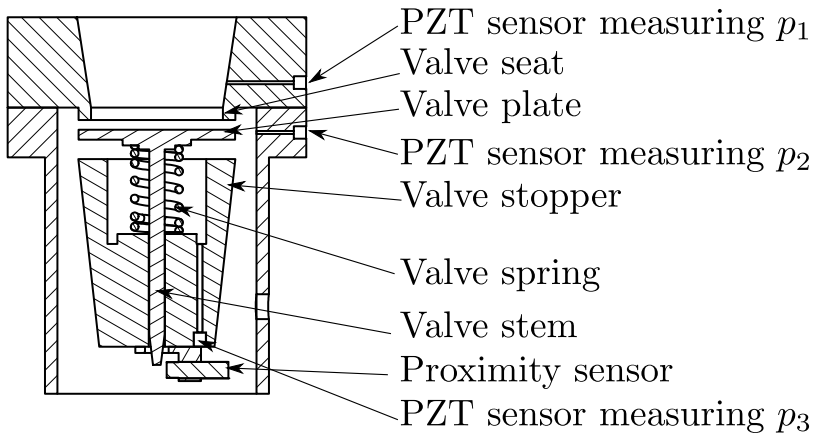

Figure 5.4: Flow channel in the model valve.

For this testing routine, the system parameters were selected for a case that previously exhibited strong self-excited oscillations with repeated impacts on the valve seat and limiter (El Bouzidi et al., 2018). This provides a challenging case where the ability of the countermeasures to mitigate the self-excited oscillations can be assessed. Hence, the spring stiffness value is taken as $k = 2700$ N/m, while the initial spring pre-load $x_0 = 0.6$ mm. Meanwhile, the downstream piping length and the maximum

valve opening are respectively set to 2.25 m and 10 mm. Experiments are conducted by first testing a datum case without any acoustic devices, then in subsequent tests adding them to assess their effectiveness.

Finally, results are non-dimensionalized such that they are independent of pressure drop, stiffness, and maximum valve opening. Valve plate fluctuations are normalized with respect to the maximum valve lift (x_{max}). In addition, a non-dimensional quantity F^* is established to represent the total static pressure difference across the system. This quantity is expressed as:

$$F^* = \frac{\Delta P A_v}{k x_{max}} \tag{5.3}$$

where ΔP is the pressure difference across the system, A_v is the valve plate area, k is the spring stiffness, and x_{max} is the maximum valve lift. For cases where the valve is the dominant source of pressure losses, the non-dimensional quantity represents the ratio of the fluid forces acting on the valve plate to the spring force at maximum opening. For this investigation, this characterization holds for all cases other than the orifice, as this device introduces significant losses. Nevertheless, F^* will henceforth be referred to as the fluid force ratio for the remainder of this article.

Anechoic Termination Parameters

The 1.5 m long anechoic termination is manufactured using a PVC pipe with a 98 mm inner diameter, and is connected downstream of a 0.75 m long pipe of identical inner diameter, resulting in a total downstream length of 2.25 m. The characteristics of the anechoic termination used for this experimental investigation can be seen in Fig. 5.5. The plot provides an overview of the spectral characteristics of the pressure transmission ratio. The ratio between the reflected and emitted wave is equal or less than 0.2 for frequencies below 100 Hz, while it is less than 0.1 for frequencies between

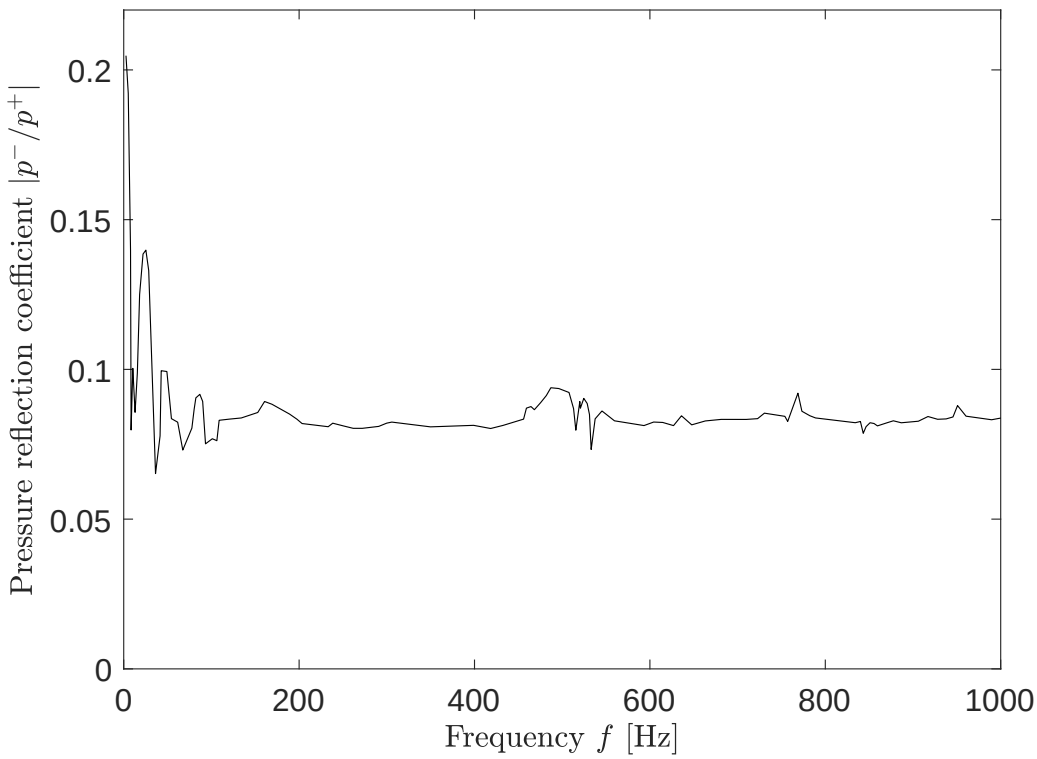

Figure 5.5: Spectral characteristics of the pressure reflection coefficient for the anechoic termination. Reproduced with data from Madani (2002)

100 Hz and 1000 Hz. As previously mentioned, the frequency range of interest is 35 Hz to 45 Hz, and it is expected that a dissipation of 80% of the acoustic pressure amplitude should be sufficient to impede the onset of instability for the valve.

Orifice Plate Parameters

The orifice plate was manufactured from a 4.8 mm thick PVC plate with an area ratio of 0.52, resulting in a thickness-to-diameter ratio of 0.07. The trailing edge of the orifice is tapered, to reduce the likelihood of flow reattachment. A sketch is provided in Fig. 5.6.

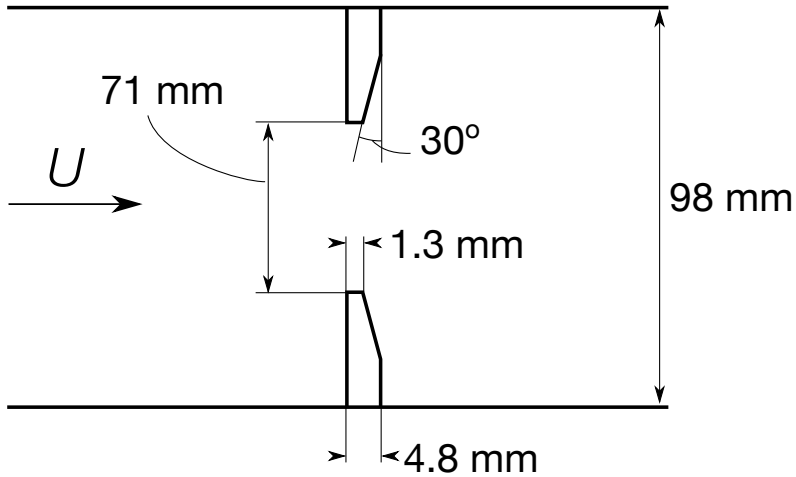

Figure 5.6: Characteristics of the orifice plate designed (Not to scale).

The downstream pipe is 2.25 m long. However, the pressure node occurs at $z = 2.29$ m, which is the effective acoustic length of this pipe ($L_e = L + \frac{4}{3\pi}d$) due to the flanged termination into the settling chamber. Placement at the end of the downstream pipe ($z/L_e = 0.98$) should produce the most acoustic losses for this system. Other locations ($z/L_e = 0, 0.33, 0.66$) are also investigated to gain a more comprehensive understanding of the influence of the orifice plate.

Concentric Cavity Resonator Parameters

As was mentioned earlier, the concentric cavity resonator provides a great deal of flexibility in its design due to its under-constrained nature. The device was sized for a target frequency of 35 Hz, which is on the low range of the frequencies observed for the 2.25 m downstream pipe case (typically 35 Hz to 44 Hz). Choosing the lower bound as the target frequency allowed for further tuning by reducing the concentric cavity volume through addition of sand. Given the constraints of the experimental facility, stock materials available, and using Eq. 5.2, the parameters selected are given in Table 5.1.

Table 5.1: Parameters selected for the concentric cavity resonator.

Performance Specification	**Value**
Design frequency	35 Hz
Resonator length ($L_a + L_b$)	500 mm
Number of holes	6, 60° spacing
Hole diameter	7 mm
Hole neck length	25 mm
Inner pipe inner diameter	98 mm
Inner pipe outer diameter	114 mm
Outer pipe inner diameter	254 mm

5.4 Results and Discussion

Reference Case

A datum case was selected on the basis that it had previously shown severe oscillations. This case is then tested by progressively increasing the Roots blower speed, and collecting time signals for 30 seconds. A sample summary of the results is shown in Fig. 5.7. The top graph provides a plot of the RMS of the unsteady component of the valve plate displacement time signal over the acquisition duration vs. the fluid force ratio, while the bottom graph provides a plot of the mean component of the displacement time signal.

It can be seen that the reference case shows little oscillation below $F^* = 0.35$, beyond which point the vibrations increase in amplitude until impact on both the seat and limiter occurs at $F^* \approx 0.6$. On the mean displacement graph it can be seen that once the initial spring preload is overcome, the valve opening increases linearly until impact occurs, at which point a plateau is seen. Frequency spectra indicate that the frequencies of oscillation are around 35 Hz prior to impact and 40 Hz thereafter, while the valve's structural natural frequency is 26 Hz. While the peak-to-peak amplitude of oscillations over $F^* \approx 0.6$ to 1.1 are unchanged, due to the occurrence of impact,

the RMS amplitude continues to increase, as the waveform of the signal varies. More details regarding this are provided by El Bouzidi et al. (2018). In addition, experiments show that although the fluid force exceeds the maximum spring force (when $F^* > 1$), the severe seat-to-limiter oscillations with impact result in a mean opening around $0.5x_{max}$. The blower speed is then increased until the instability disappears, which also corresponds to a decrease in the static pressure drop across the system. This is due to the valve producing more losses when it is oscillating compared to when it is stable. Time domain signals during impact are provided in Fig. 5.8 to demonstrate the waveform captured by the normalized RMS values of the perturbation (as plotted in Fig. 5.7). The nearly sinusoidal oscillations, with sharp edges due to impact on the seat and limiter (Fig. 5.8a), result in a normalized RMS value of approximately 0.35, seen when $F^* = 0.58$ in Fig. 5.7, whereas the plateau, occurring when the valve is completely open (Fig. 5.8b), results in a normalized RMS value of approximately 0.4, seen when $F^* = 0.7$ in Fig. 5.7. This plateau serves to show that the unsteady flow effects are integral to understanding the flow characteristics in spring-loaded valves, unlike studies of vocal folds, which exhibit a similar flow-sound-structure interaction mechanism. However, for vocal folds, studies have found that the viscous effects of the flow are more dominant (Deverge et al., 2003).

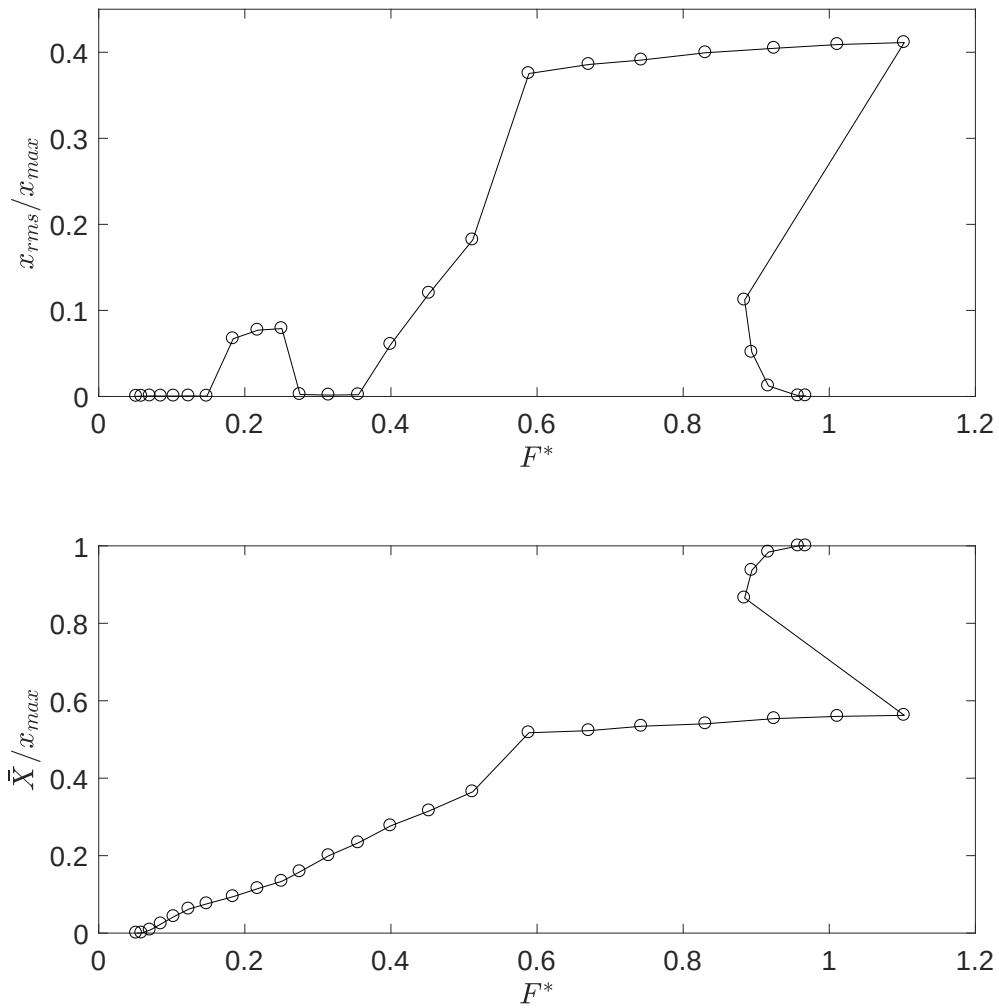

Figure 5.7: Top: Normalized RMS oscillation *vs.* steady fluid force ratio. Bottom: Mean displacement component *vs.* steady fluid force ratio for reference case.

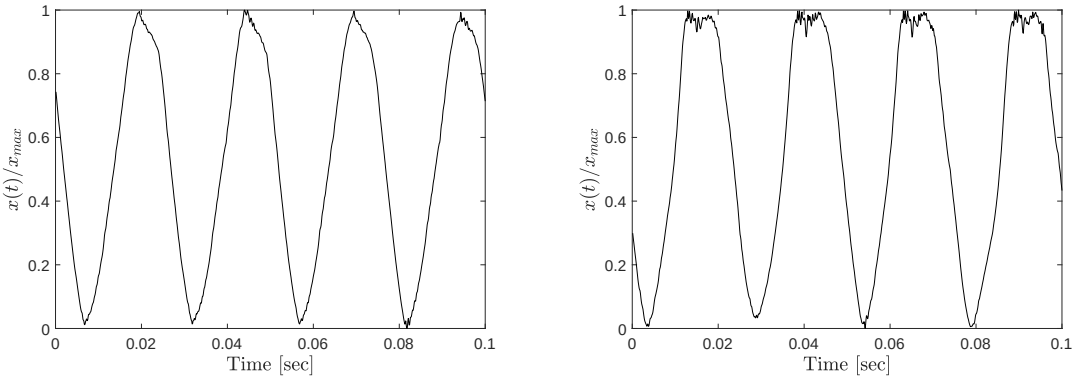

(a) $F^* = 0.58$ (b) $F^* = 1.01$

Figure 5.8: valve plate displacement samples during impact.

Anechoic Termination

The effect of the anechoic termination is shown in Fig. 5.9. The RMS amplitude of oscillation is presented against the fluid force ratio F^*, with the results from the reference case provided for comparison. For the anechoic termination, the onset of

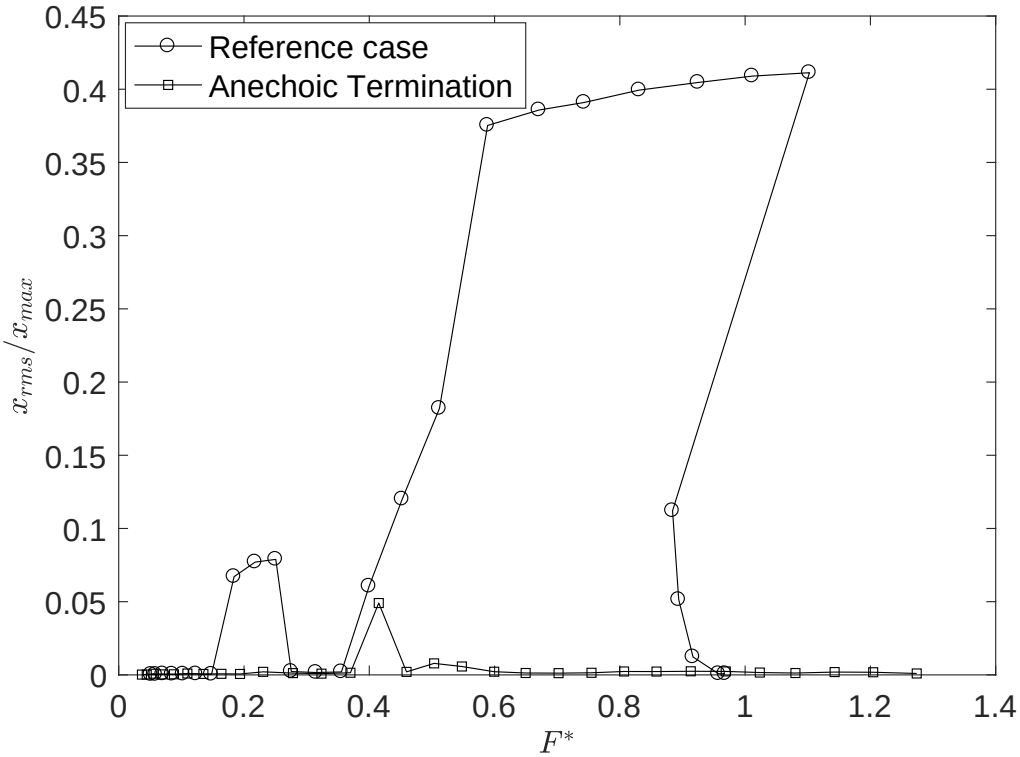

Figure 5.9: Normalized valve displacement RMS fluctuation *vs.* fluid force ratio for anechoic termination.

the instability occurs at the same fluid force ratio $F^* \approx 0.38$ as the reference case. However, oscillation normalized RMS amplitudes do not exceed 0.05, and decay to less than 0.01 once F^* exceeds 0.45. This short and low amplitude oscillation window demonstrates that the instability is largely suppressed by eliminating the acoustic reflection. Inspection of the valve displacement time signals recorded indicates that the residual oscillations still occur at the frequencies previously observed.

The use of this acoustic device demonstrates that the acoustic feedback is essential to the instability phenomenon. However, the practical considerations involved in manufacturing this device require usage of acoustic insulation in contact with the fluid in the piping system. This may constitute a serious limitation to the implementation of this device in industrial piping systems. Namely, gas pipelines could carry particulate matter contaminants which may accumulate in the porous insulation and decrease its effectiveness over time. In addition, temperature and pressure conditions in these systems may seriously damage the insulation. However, insight gained by testing this device is valuable inasmuch as it validates the hypothesis that by attenuating the acoustic pressure of the reflected wave, it is possible to prevent the establishment of destructive oscillations.

Orifice Plate

The effectiveness of the orifice plate placed at various locations can be seen in Fig. 5.10. As expected, the optimal case occurs at the acoustic pressure node, as demonstrated by the results for the orifice placed 2.25 m downstream. Placing the orifice away from this optimal point (*e.g.* closer to the valve exit) has the effect of increasing the severity of the vibration, and widening the range of unstable pressure drops. When the orifice is placed at the valve's exit, the valve is fully unstable, and the only difference with the reference case is a rightward shift due to the increased pressure losses caused by the orifice. While the plots shown in Fig. 5.10 provide a useful description of the overall instability behaviour of the valve over its entire range of opening, it may be insightful to analyze valve displacement time signals at a fixed fluid force ratio F^* (*i.e.* fixed pressure difference), which are provided in Fig. 5.11. It can be seen that for the time signal corresponding to an orifice placement at $z/L_e = 0$, the waveform consists in

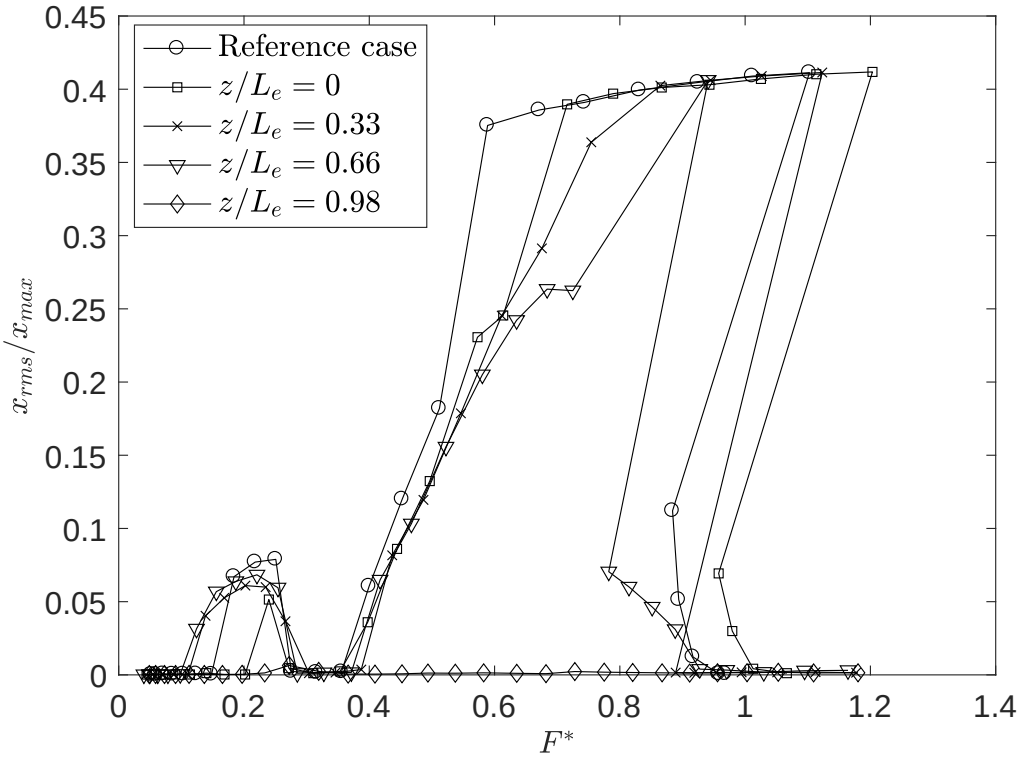

Figure 5.10: Normalized valve displacement RMS *vs.* fluid force ratio for orifice plate.

sharp edges due to the repeated impacts on seat and limiter, while the displacement waveform is practically sinusoidal when the orifice is placed at $z/L_e = 0.33$ and 0.66, when contact is absent. When the orifice plate is placed at $z/L_e = 0.98$, oscillations are virtually absent. One can observe the amplitude decay as a result of the orifice placement away from the acoustic particle velocity antinode. For the case with the orifice placed at $z/L_e = 0$, the frequency of oscillation is 39 Hz, whereas it is 36 Hz for $z/L_e = 0.33, 0.68$. These frequencies are comparable with those seen in previous work (El Bouzidi et al. (2018)).

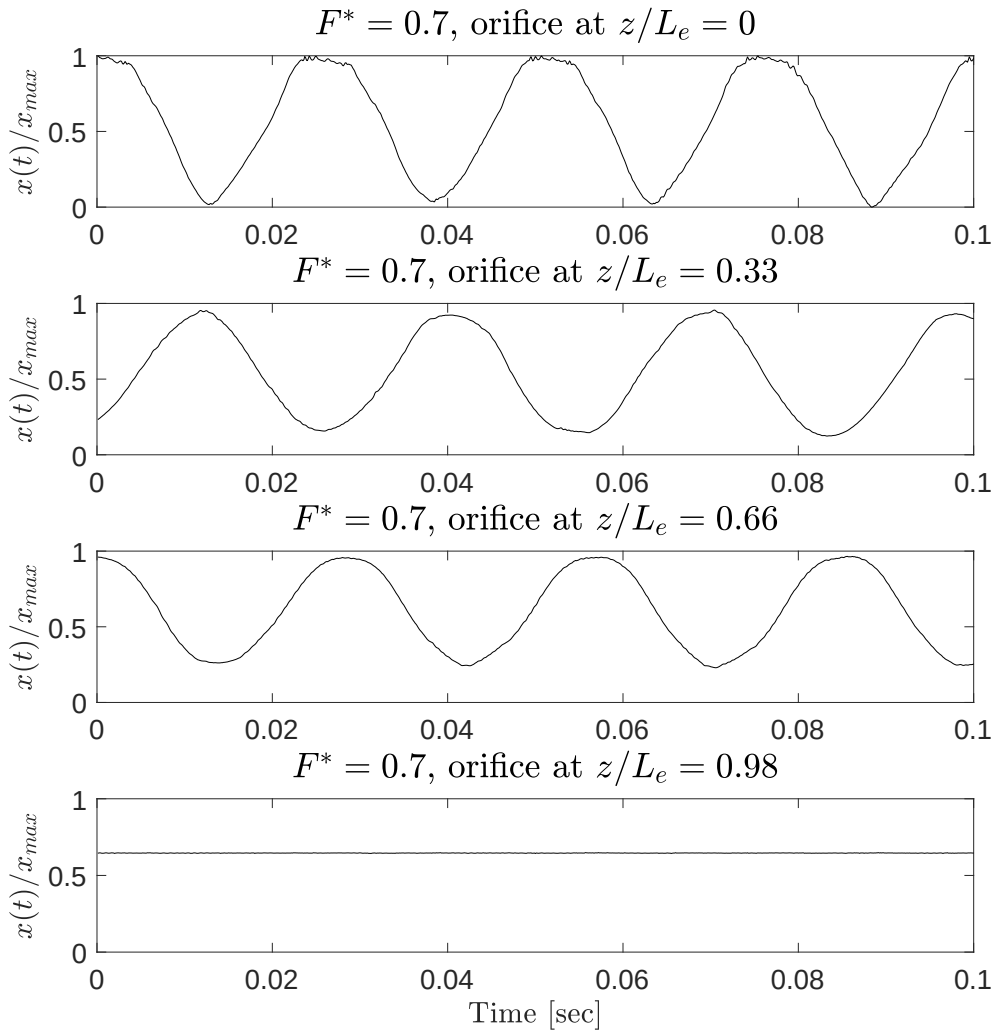

Figure 5.11: Time domain signals for the valve plate displacement, with the orifice placed at various locations and $F^* = 0.7$.

Concentric Cavity Resonator

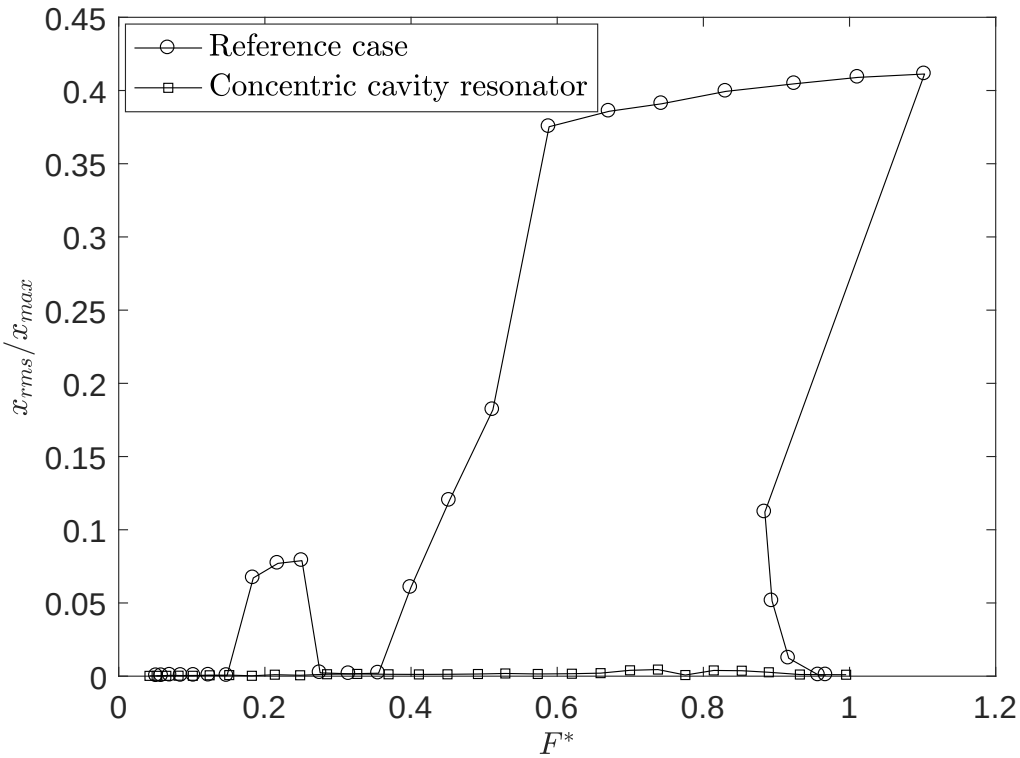

Figure 5.12: Normalized valve displacement RMS *vs.* fluid force ratio for concentric cavity resonator.

The final device to be assessed as part of this investigation is the concentric cavity resonator. Figure 5.12 shows that this device is able to suppress the oscillations completely, with the added benefit of being hydraulically invisible. Thus, it can be connected in a pipeline without concerns of loss of performance.

While Fig. 5.12 shows that unstable vibrations are suppressed, it can be seen that some residual oscillations remain, which is illustrated in the time domain signal sample of the valve plate displacement plotted in Fig. 5.13. The measured frequency of oscillation is 39 Hz. It can be seen that to the amplitude of these fluctuations is 1% of the total valve opening, which is a vast improvement compared to the seat-to-limiter

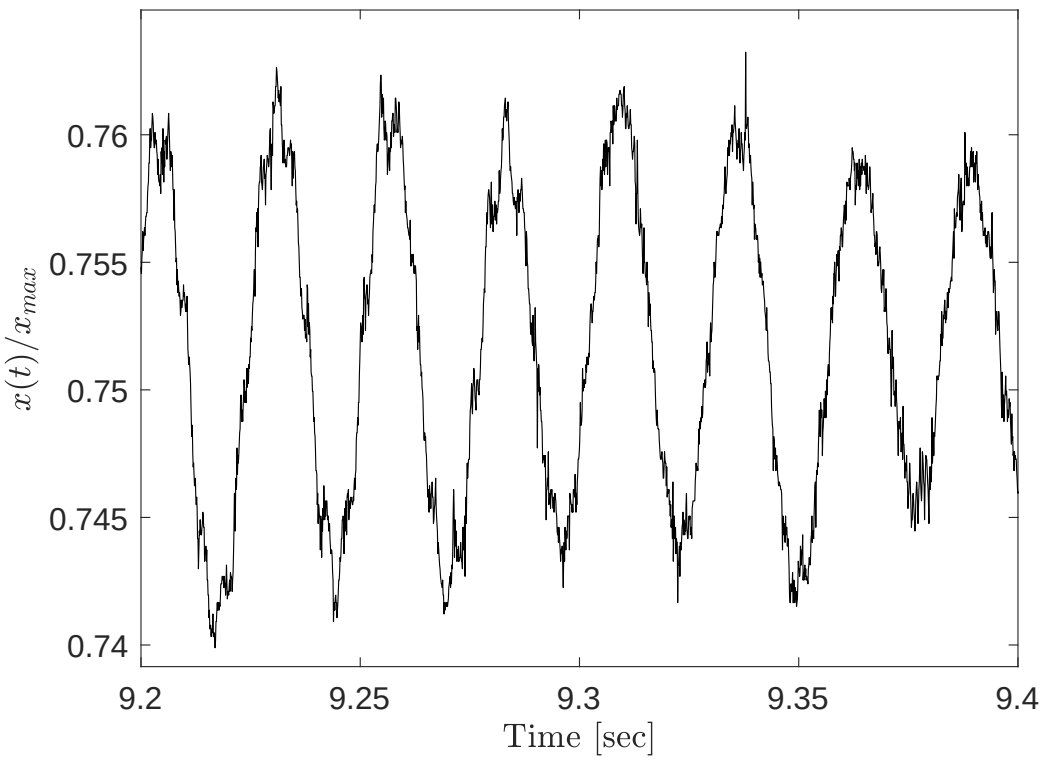

Figure 5.13: Normalized valve displacement *vs.* time for a fluid force ratio $F^* = 0.74$ with a concentric cavity resonator.

oscillations seen in Fig. 5.8. The presence of these oscillations highlights the importance of proper tuning of the concentric cavity resonator. If the design frequency differs too much from the instability frequency, or if the damping capability of the device is insufficient (here provided by steel wool inserted in the resonator holes), the device may not attenuate the oscillations sufficiently. If implemented in industrial applications, the device may be designed with the ability to reduce the outer cavity volume, perhaps through movable end caps, allowing for *in situ* tuning of the resonator to ensure that maximum attenuation is achieved.

5.5 Conclusion

This paper provides an experimental assessment of the effectiveness of acoustic devices to suppress the structural vibrations of a spring-loaded valve. The usage of acoustic methods to attenuate structural vibrations of spring-loaded valves is a novel approach to mitigating the destructive effects of a self-excited instability resulting from coupling between the flow field, the valve structure, and the acoustic field. The valve was installed in a configuration that previously demonstrated severe vibrations. Three devices were built and manufactured to attenuate the acoustic wave in the downstream pipe based on the theoretical understanding of the interaction mechanism.

The first device assessed was an anechoic termination, which demonstrated that suppressing the acoustic feedback mechanism would in turn eliminate the valve instability. However, beyond providing physical insight, this solution may not be practical in a plant environment, as it relies on acoustic insulation, which may accumulate particulates and impurities over time. The second device was an orifice plate. It was most effective in suppressing the instability when placed at the acoustic velocity anti-node (*i.e.* acoustic pressure node), but is intrinsically a source of pressure losses, which may not be acceptable for a given pipeline. Finally, the third device was a concentric cavity resonator. It was designed to attenuate acoustic waves around a known instability frequency. Its installation significantly reduced the vibrations of the spring-loaded valve, making it a desirable solution, as it is virtually hydraulically invisible.

Bibliography

Baldwin, R., & Simmons, H. R. (1986). Flow-induced vibration in safety relief valves. *Journal of Pressure Vessel Technology*, *108*, 267–272.

Deverge, M., Pelorson, X., Vilain, C., Lagrée, P.-Y., Chentouf, F., Willems, J., & Hirschberg, A. (2003). Influence of collision on the flow through in-vitro rigid models of the vocal folds. *The Journal of the Acoustical Society of America*, *114*, 3354–3362.

El Bouzidi, S., Hassan, M., & Ziada, S. (2017). Characterization of flow-sound-structure coupling in spring-loaded valves. In *Proceedings of the 2017 ASME Pressure Vessels and Piping Conference, Waikoloa Village, Hawaii, USA, July 2017* PVP2017-65767. Waikoloa, Hawaii, USA.

El Bouzidi, S., Hassan, M., & Ziada, S. (2018). Experimental characterisation of the self-excited vibrations of spring-loaded valves. *Journal of Fluids and Structures*, *76*, 558–572.

Erdődi, I., & Hős, C. (2017). Prediction of quarter-wave instability in direct spring operated pressure relief valves with upstream piping by means of CFD and reduced order modelling. *Journal of Fluids and Structures*, *73*, 37–52.

Habing, R. A., & Peters, M. C. A. M. (2006). An experimental method for validating compressor valve vibration theory. *Journal of Fluids and Structures*, *22*, 683–697.

Karthik, B., Chakravarthy, S., & Sujith, R. (2008). Mechanism of pipe-tone excitation by flow through an orifice in a duct. *International Journal of Aeroacoustics*, *7*, 321–347.

Killmann, I. (1972). Aerodynamic forces acting on valve discs. In *International Compressor Engineering Conference*.

Kinsler, L. E., Frey, A. R., Coppens, A. B., & Sanders, J. V. (1999). *Fundamentals of acoustics* volume 1 of *ISBN 0-471-84789-5*. (4th ed.). Wiley-VCH.

Kolkman, P. A. (1976). *Flow-induced gate vibrations*. Technische Hogeschool Delft.

Lacombe, R., Moussou, P., & Aurégan, Y. (2011). Whistling of an orifice in a reverberating duct at low mach number. *The Journal of the Acoustical Society of America*, *130*, 2662–2672.

Madani, V. (2002). *Noise Sources Characterization of Automotive HVAC Systems*. Master's thesis, McMaster University.

Moussou, P., Gibert, R. J., Brasseur, G., Teygeman, C., Ferrari, J., & Rit, J.-F. (2010). Instability of pressure relief valves in water pipes. *Journal of Pressure Vessel Technology*, *132*, 041308.

Munjal, M. L. (2014). *Acoustics of ducts and mufflers*. John Wiley & Sons.

Testud, P., Aurégan, Y., Moussou, P., & Hirschberg, A. (2009). The whistling potentiality of an orifice in a confined flow using an energetic criterion. *Journal of Sound and Vibration*, *325*, 769–780.

Tsui, C., Oliver, C., & Cohen, R. (1972). Discharge phenomena of a two-dimensional poppet-type valve. In *Internal Compressor Engineering Conference*. Purdue, Indiana: Purdue University.

Ziada, S., Shine, S., & Bühllmann, E. (1986). Self-excited vibrations of reciprocating compressor plate valves. In *International Compressor Engineering Conference*.

Ziada, S., Shine, S., & Buhlmann, E. (1987). Tests on the flutter of a multi-ring plate valve. In *Proceedings of the International Conference on Flow Induced Vibrations* (pp. 393–402). Bowness-on-Windermere, England: BHRA.

Nomenclature

A_v	Valve plate area.
c	Viscous damping of the valve structure.
c_0	Sound propagation speed in the medium.
d	Pipe diameter.
F^*	ratio of the fluid force to spring force at maximum opening.
k	Valve spring stiffness.
k_0	Plane wave number.
l_{eq}	Equivalent resonator neck length.
L	Pipe length.
L_a, L_b	Distance from hole pattern to cavity left and right edges.
L_e	Effective acoustic length of the pipe.
m	Valve mass.
n_h	Number of holes.
$\|p^-/p^+\|$	Pressure reflection coefficient.
ΔP	Static pressure difference across the system.
S_c	Transverse concentric cavity resonator cross- sectional area.

Nomenclature (continued)

S_h	Concentric cavity resonator hole area.
U	Pipe inlet velocity.
$\bar{u}(0,t)$	Acoustic particle velocity at the valve.
x	valve plate displacement.
x_{max}	Maximum valve opening.
x_{rms}	RMS value of the valve plate oscillation.
$\bar{X}$	Mean valve opening.
z	Axial location along the pipe.
$\boldsymbol{Z}_{m0}$	Inlet mechanical impedance of the pipe.
$\boldsymbol{Z}_{mL}$	Mechanical impedance at the flanged outlet.
$\boldsymbol{Z}_{mv}$	Mechanical impedance of the valve.
ρ_0	Density of the propagation medium in the pipe.
ω	Filter target angular frequency.

Chapter 6

Summary and Conclusions

6.1 Thesis Summary

The flow-sound-structure interaction mechanism in spring-loaded valves is investigated. Specifically, a model valve, designed based on dimensional similarity to a reciprocating gas compressor valve, is placed at the inlet of a Roots blower operating in suction. An experimental study is conducted to determine the effects of valve geometry, flow properties, and acoustic field on the onset and severity of the self-excited instability mechanism. The experimental results provided a basis for the development of a simplified theoretical model to describe the complex interaction mechanism between the fluid, the structure, and the acoustic field. The model relies on a single-degree-of-freedom description of the structure with non-linear impact conditions, an unsteady Bernoulli description of the flow, and a plane wave propagation model of the acoustic field.

The model valve was found to undergo self-excited oscillations only when acoustic interaction was a dominant mechanism. That is, instability occurred only if the

upstream or downstream piping was sufficiently long, such that the fundamental frequency of the piping was close enough to the valve's structural natural frequency. The absence of any piping upstream or downstream of the valve test section resulted in a stable valve, no matter the blower speed, spring stiffness, or any other geometrical parameters. Phase plots of the valve plate motion ($\dot{x}$ *vs.* x) showed interesting non-linear characteristics of the system, such as limit cycle behaviour. Furthermore, the frequency of oscillation was not that of the valve structure. Rather, the valve vibrated primarily at the frequency of the combined valve-pipe system, which can be estimated using the driver-pipe analysis method of Kinsler et al. (1999). Various valve parameters, such as valve plate diameter, initial spring force, maximum valve lift, and spring stiffness were tested in order to establish operational regimes under which instability persists. The spring stiffness value had a significant effect on the amplitude of oscillation, whereby an increase in spring stiffness had a destabilizing effect on the valve.

The theoretical model was able to reliably reproduce the key characteristics of the instability. In addition, its numerical formulation allowed for a time domain resolution of the valve plate and flow dynamics. Furthermore, the pseudo-force technique, utilized to describe the contact dynamics during impact of the valve plate on the seat and limiter, presented several advantages, such as second-order continuity for the valve displacement, in addition to the ability to compute a time history of the contact forces. These features are instrumental for predicting valve fatigue and wear. Simulations were conducted while varying parameters such as static pressure drop, downstream pipe length, and spring stiffness. In addition, cases were also considered without acoustic feedback, demonstrating that the presence of acoustic interaction is essential to the onset of the instability.

Practical countermeasures were devised and assessed in order to provide designers

and operators with methods to mitigate the severe oscillations that may occur. An anechoic termination was tested to gain insight on the effects of acoustic feedback, while an orifice plate and a Helmholtz-type concentric resonator were tested to assess potential solutions that could be implemented in the industry. The acoustic devices designed were seen to effectively suppress the self-excited oscillations experienced by the spring-loaded valve. The anechoic termination showed that through suppression of reflected acoustic waves, it is possible to mitigate undesirable vibrations in the valve. Furthermore, the orifice plate completely eliminated the instability if placed at the acoustic particle velocity antinode of the downstream pipeline. When placed away from this optimal point, this device partially attenuated the oscillations, with diminishing influence correlating with farther placement from the antinode. Finally, the additional success of the concentric cavity resonator as a countermeasure provides an alternative method that can be implemented in industrial applications.

6.2 Conclusions

This thesis provides the first comprehensive investigation into the self-excited vibrations of spring-loaded valves due to a flow-sound-structure interaction mechanism. This undertaking consisted in an experimental investigation to characterize the physics of the phenomenon, theoretical and computational modelling to provide predictive capabilities to designers, and the development of acoustic devices to mitigate self-excited instability for valves already in operation. The major conclusions of this thesis are:

1. The acoustic feedback is a necessary condition for the establishment of this self-excited instability. This was demonstrated both experimentally and numerically.

2. The frequency of oscillation is dependent on the properties of the coupled structural-acoustic system.

3. An increase in stiffness resulted in more severe vibrations.

4. A simplified reduced-order model was able to describe the coupled non-linear dynamic behaviour of a spring-loaded valve.

5. The instability mechanism is independent of the complex flow geometry in valves, as a 1-D unsteady Bernoulli model with viscous losses is able to characterize the flow.

6. Contact dynamics of the valve can be described using a pseudo-force method, rather than other more computationally intensive methods.

7. The anechoic termination was successful in suppressing the instability, and demonstrated that suppressing the acoustic feedback impedes the establishment of the instability. However, its practicality is mainly academic due to the limitations of using acoustic foam.

8. The orifice plate was successful in eliminating the oscillation frequency, but its placement at the acoustic pressure node was critical. On the other hand, it can cause significant hydraulic losses. This device can be used in applications where these losses are acceptable to the operator.

9. The concentric cavity resonator dampened the oscillations to very small amplitudes, but a knowledge of the oscillation frequency was necessary. However, a significant advantage is that this device is hydraulically invisible (no measured losses).

6.3 Original Contributions

6.3.1 Characterization of the coupled self-excitation mechanism in valves

- This study represents the first thorough experimental investigation providing an understanding of the valve's flow-sound-structure interaction mechanism.
- The necessity of acoustic feedback, for the instability mechanism to prevail, is established.
- The sensitivity of valve instability to various parameters is established. The key parameters are shown to be the static pressure drop, the spring stiffness value, and the pipe length.

6.3.2 Development of a nonlinear model of the flow-sound-structure interaction

A comprehensive flow-sound-structure interaction model with valve impact has been developed. The main characteristics of the model are:

- The model relies on explicit coupling between the acoustic field, the hydrodynamics, and the valve plate motion. Impact is handled with an iterative contact force computation method.
- Individual features have been validated using experiments, Finite Element Analysis, and analytical solutions.
- The model demonstrates that acoustic feedback is necessary for instability to occur (as seen in experiments).

- The frequencies predicted reasonably match experimental measurements.

6.3.3 Design and testing of effective countermeasures

- Practical countermeasures were designed, pursuing a novel approach to mitigate the valve vibrations, relying on suppressing acoustic feedback, rather than altering the valve or its operational characteristics.
- The concentric cavity resonator can be used in applications where there aren't any spatial limitations, and if pressure losses are not acceptable. In addition, knowledge of the instability frequency is required.
- The orifice plate should be used in applications where pressure losses are not critical and where the location of the acoustic particle velocity antinode is known.

6.4 Recommendations for Future Work

Although the topic of vibrations of spring-loaded valves has been an active area of research for more than fifty years, a great deal remains to be uncovered, specifically for the influence of acoustic feedback. The following are suggestions to expand and further work upon the three categories of original contributions listed above:

1. Further experimental work could be conducted to provide additional insight regarding valve instability. Due to limitations with the experimental facility, valve behaviour was not considered for pipes longer than 2.7 m. The behaviour of the valve for longer pipe lengths could be of interest. Furthermore, to account for the complex piping networks present in plants, the effect of area changes, bends, and elbows, could also be investigated.

2. The modelling approach can be extended to more complex geometries. Specifically, compressor manifolds can often consist of complex bends and cross-sectional area changes, which may not be adequately modelled using the 1-D finite difference wave propagation method implemented in this thesis. The wave equation may instead by resolved on a 2-D or 3-D grid. In addition, the contact forces predicted by the model could be used to develop simulation procedures to predict crack propagation and fatigue wear in valves, based on analysis methods developed for steam generator life assessment (Vincent et al., 2009).

3. The acoustic countermeasures could be further developed to improve suitability in an industrial environment. Namely, the concentric cavity resonator design could incorporate the ability to move the end caps, to allow for adjusting the cavity volume. Moreover, if the end caps are designed to be driven by a motor, active control techniques could be implemented, based on real-time measurements of the valve oscillation frequency.

Bibliography

Allison, T. C. and Brun, K. (2016). Testing and modeling of an acoustic instability in pilot-operated pressure relief valves. *Journal of Engineering for Gas Turbines and Power*, 138(5):052401.

Atig, M., Dalmont, J.-P., and Gilbert, J. (2004). Saturation mechanism in clarinet-like instruments, the effect of the localised non-linear losses. *Applied Acoustics*, 65(12):1133–1154.

Baldwin, R. and Simmons, H. R. (1986). Flow-induced vibration in safety relief valves. *Journal of pressure vessel technology*, 108(3):267–272.

Bazsó, C. and Hős, C. (2013). An experimental study on the stability of a direct spring loaded poppet relief valve. *Journal of fluids and structures*, 42:456–465.

Blevins, R. D. (1984). *Applied fluid dynamics handbook*. Van Nostrand Reinhold Co., New York.

Darby, R. (2013). The dynamic response of pressure relief valves in vapor or gas service, part i: Mathematical model. *Journal of loss prevention in the process industries*, 26(6):1262–1268.

Darby, R. and Aldeeb, A. (2014). The dynamic response of pressure relief valves in

vapor or gas service. part iii: Model validation. *Journal of Loss Prevention in the Process Industries*, 31:133–141.

Deverge, M., Pelorson, X., Vilain, C., Lagrée, P.-Y., Chentouf, F., Willems, J., and Hirschberg, A. (2003). Influence of collision on the flow through in-vitro rigid models of the vocal folds. *The Journal of the Acoustical Society of America*, 114(6):3354–3362.

D'Netto, W. and Weaver, D. S. (1987). Divergence and limit cycle oscillations in valves operating at small openings. *Journal of Fluids and Structures*, 1(1):3–18.

El Bouzidi, S., Hassan, M., and Ziada, S. (2017). Characterization of flow-sound-structure coupling in spring-loaded valves. In *Proceedings of the 2017 ASME Pressure Vessels and Piping Conference, Waikoloa Village, Hawaii, USA, July 2017*, number PVP2017-65767, Waikoloa, Hawaii, USA.

El Bouzidi, S., Hassan, M., and Ziada, S. (2018). Experimental characterisation of the self-excited vibrations of spring-loaded valves. *Journal of Fluids and Structures*, 76:558–572.

Erdődi, I. and Hős, C. (2017). Prediction of quarter-wave instability in direct spring operated pressure relief valves with upstream piping by means of cfd and reduced order modelling. *Journal of Fluids and Structures*, 73:37–52.

Habing, R. A. and Peters, M. C. A. M. (2006). An experimental method for validating compressor valve vibration theory. *Journal of Fluids and Structures*, 22(5):683–697.

Hassan, M., Weaver, D., and Dokainish, M. (2002). A simulation of the turbulence

response of heat exchanger tubes in lattice-bar supports. *Journal of Fluids and Structures*, 16(8):1145–1176.

Hayashi, S. (1995). Instability of poppet valve circuit. *JSME international journal. Ser. C, Dynamics, control, robotics, design and manufacturing*, 38(3):357–366.

Hayashi, S., Hayase, T., and Kurahashi, T. (1997). Chaos in a hydraulic control valve. *Journal of fluids and structures*, 11(6):693–716.

Hirschberg, A., Van de Laar, R., Marrou-Maurieres, J., Wijnands, A., Dane, H., Kruijswijk, S., and Houtsma, A. (1990). A quasi-stationary model of air flow in the reed channel of single-reed woodwind instruments. *Acta Acustica united with Acustica*, 70(2):146–154.

Hős, C., Champneys, A., Paul, K., and McNeely, M. (2014). Dynamic behavior of direct spring loaded pressure relief valves in gas service: Model development, measurements and instability mechanisms. *Journal of loss prevention in the process industries*, 31:70–81.

Hős, C., Champneys, A., Paul, K., and McNeely, M. (2015). Dynamic behaviour of direct spring loaded pressure relief valves in gas service: Ii reduced order modelling. *Journal of Loss Prevention in the Process Industries*, 36:1–12.

Hunt, K. and Crossley, F. (1975). Coefficient of restitution interpreted as damping in vibroimpact. *Journal of applied mechanics*, 42(2):440–445.

Ishii, N., Fukuoka, H., Matsunaga, H., Fukushima, M., and Nakazumi, K. (1993). Dynamic stability criterion for reed valves in refrigerant compressors. *JSME international journal. Ser. C, Dynamics, control, robotics, design and manufacturing*, 36(1):69–76.

Johansson, L. (1997). Beam motion with unilateral contact constraints and wear contact sites. *Journal of Pressure Vessel Technology*, 119:105–110.

Karthik, B., Chakravarthy, S., and Sujith, R. (2008). Mechanism of pipe-tone excitation by flow through an orifice in a duct. *International Journal of Aeroacoustics*, 7(3-4):321–347.

Kasai, K. (1968). On the stability of a poppet valve with an elastic support: 1st report, considering the effect of the inlet piping system. *Bulletin of JSME*, 11(48):1068–1083.

Killmann, I. (1972). Aerodynamic forces acting on valve discs. In *International Compressor Engineering Conference*.

Kinsler, L. E., Frey, A. R., Coppens, A. B., and Sanders, J. V. (1999). *Fundamentals of acoustics*, volume 1 of *ISBN 0-471-84789-5*. Wiley-VCH, 4th edition edition.

Kolkman, P. A. (1976). *Flow-induced gate vibrations*. Technische Hogeschool Delft.

Lacombe, R., Moussou, P., and Aurégan, Y. (2011). Whistling of an orifice in a reverberating duct at low mach number. *The Journal of the Acoustical Society of America*, 130(5):2662–2672.

Madani, V. (2002). Noise sources characterization of automotive hvac systems. Master's thesis, McMaster University.

Margolis, D. and Hennings, C. (1997). Stability of hydraulic motion control systems. *Journal of dynamic systems, measurement, and control*, 119(4):605–613.

Misra, A., Behdinan, K., and Cleghorn, W. (2002). Self-excited vibration of a control valve due to fluid–structure interaction. *Journal of fluids and structures*, 16(5):649–665.

Moussou, P., Gibert, R. J., Brasseur, G., Teygeman, C., Ferrari, J., and Rit, J.-F. (2010). Instability of pressure relief valves in water pipes. *Journal of Pressure Vessel Technology*, 132(4):041308.

Munjal, M. L. (2014). *Acoustics of ducts and mufflers*. John Wiley & Sons.

NASA (2013). Nasa works towards dec. 19 cygnus launch; possible repair space walks. http://www.nasa.gov/content/nasa-works-towards-dec-19-cygnus-launch-possible-repair-space-walks. Last accessed on September 2, 2015.

Naudascher, E. (1963). On the role of eddies in flow induced vibrations. In *Proceedings of 10th Congress, IAHR, London, UK*, volume 3, pages 61–72.

Nayfeh, A. and Bouguerra, H. (1990). Non-linear response of a fluid valve. *International Journal of Non-Linear Mechanics*, 25(4):433–449.

Oengören, A. (1987). Experimental investigation of valve plate flutter on a compressor under actual working conditions. Technical Report 3503, Sulzer Laboratorium für Schwingungen und Akustik.

Rogovin, M. (1979). Three mile island: A report to the commissioners and to the public. Technical report, Nuclear Regulatory Commission, Washington, DC (USA).

Shine, S. (1987). Experimental investigation on self-excited vibrations of reciprocating compressor multi-ring plate valves. Technical Report 3450, Sulzer Laboratorium für Schwingungen und Akustik.

Testud, P., Aurégan, Y., Moussou, P., and Hirschberg, A. (2009). The whistling potentiality of an orifice in a confined flow using an energetic criterion. *Journal of Sound and Vibration*, 325(4):769–780.

TransCanada Corporation (2005). *Blowdown Notification Fact Sheet*. TransCanada Corporation.

Tsui, C., Oliver, C., and Cohen, R. (1972). Discharge phenomena of a two-dimensional poppet-type valve. In *Internal Compressor Engineering Conference*, Purdue, Indiana. Purdue University.

US-NRC (2006). Information notice 2006-15: Vibration-induced degradation and failure of safety-related valves. Technical report, U.S. Nuclear Regulatory Commission.

Vincent, B. T., Hassan, M. A., and Rogers, R. J. (2009). A probabilistic assessment technique applied to a cracked heat exchanger tube subjected to flow-induced vibration. *Journal of pressure vessel technology*, 131(3).

Weaver, D. S. and Ziada, S. (1980). A theoretical model for self-excited vibrations in hydraulic gates, valves and seals. *Journal of Pressure Vessel Technology*, 102(2):146–151.

Wilson, T. A. and Beavers, G. S. (1974). Operating modes of the clarinet. *The Journal of the Acoustical Society of America*, 56(2):653–658.

Woollatt, D. (1972). Some practical applications of modern compressor valve technology. In *International Compressor Engineering Conference*.

Ziada, S., Shine, S., and Bühllmann, E. (1986). Self-excited vibrations of reciprocating compressor plate valves. In *International Compressor Engineering Conference*.

Ziada, S., Shine, S., and Buhlmann, E. (1987). Tests on the flutter of a multi-ring plate valve. In *Proceedings of the International Conference on Flow Induced Vibrations*, pages 393–402, Bowness-on-Windermere, England. BHRA.

Appendix A

Acquisition and Instrument Calibration

A.1 Signal Acquisition and Processing

The acquisition of instrument signals for this study was conducted using a National Instruments DAQ PCI-6221 through a LabVIEW Virtual Instrument (VI) interface. Time signals were collected at a sampling rate of 10 kHz for 30 seconds. Further signal processing was conducted using a Butterworth bandpass filter with a low-pass frequency of 600 Hz and a high-pass frequency of 1 Hz.

A.2 Calibration Procedure for the Magnetic Proximity Sensor

The proximity transducer outputs a voltage that is proportional to its distance from a flat ferromagnetic surface. For such an application, the manufacturer provides reliable

calibration coefficients to convert the output signal into the distance from the proble. However, in the current application, the sensor is placed against an inclined circular rod. Consequently, a calibration of the sensor properties is required. The calibration

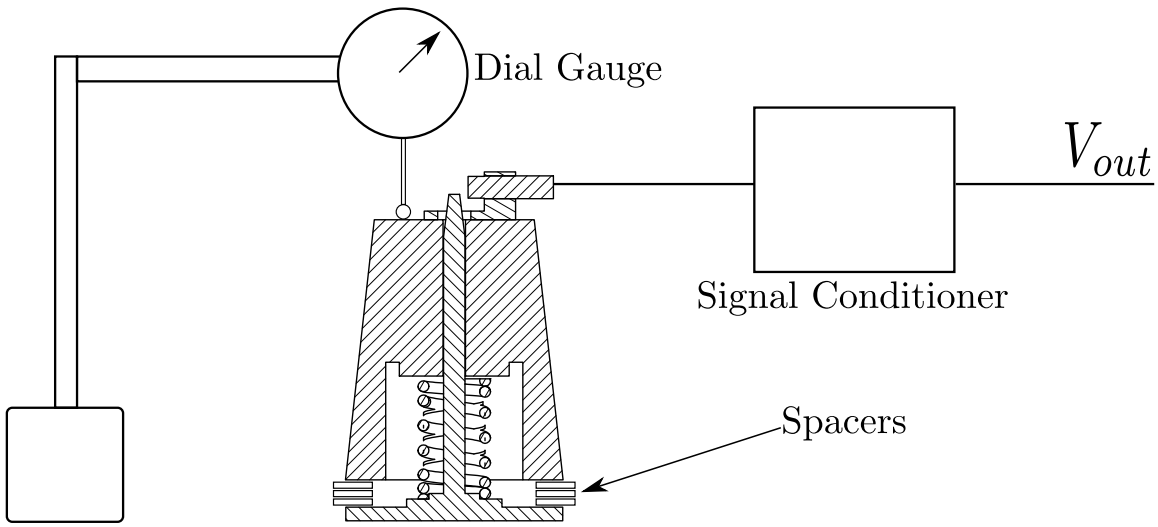

Figure A.1: Bently Nevada 3300XL calibration procedure diagram

procedure is shown in Figure A.1. A dial gauge is vertically levelled against the flat surface on the valve seat. Spacers are added to displace the valve plate, and the valve displacement value measured with the dial gauge is recorded with the corresponding transducer voltage. The correlation is shown in Figure A.2. It can be seen that the transducer behaviour is nonlinear. A third order polynomial is used to correlate the valve displacement to the output voltage of the transducer.

Furthermore, it may be of interest to ensure that the static calibration constant of the probe is still valid for dynamic measurements. For this purpose, the manufacturer provides frequency response data for the proximity sensor, in various operational conditions. It can be seen for the current case of no field wiring, there is hardly any amplitude (Fig. A.3a) or phase (Fig. A.3b) loss below 200 Hz. This was the frequency range of interest during this investigation.

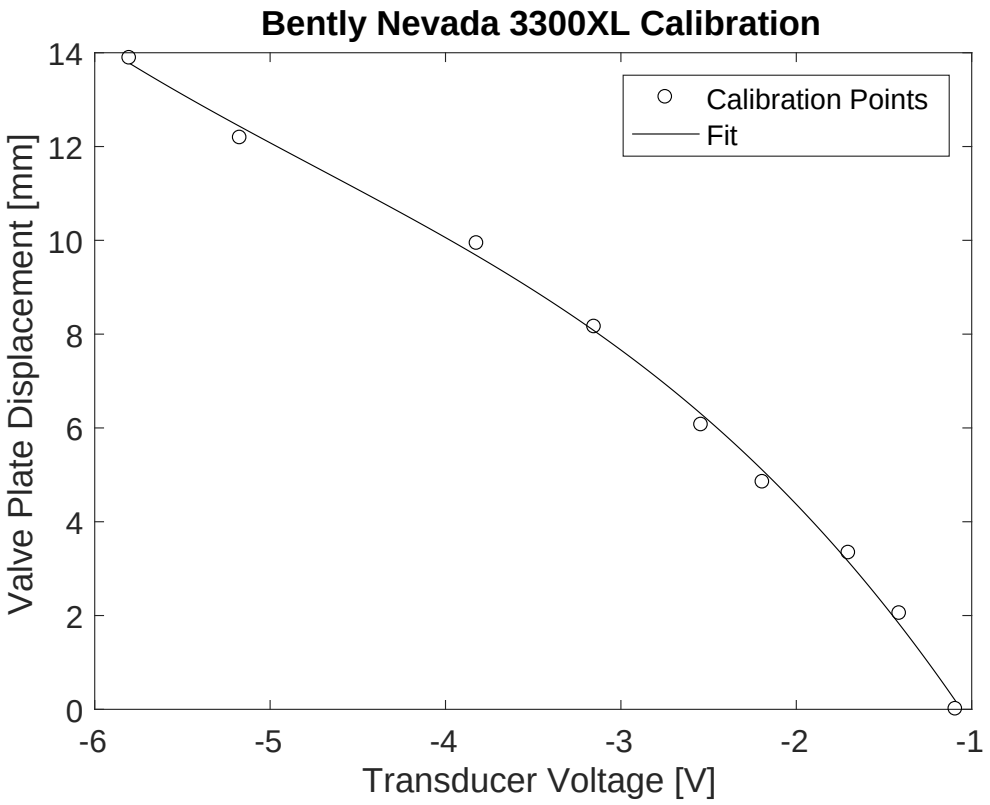

Figure A.2: Bently Nevada 3300XL calibration curve

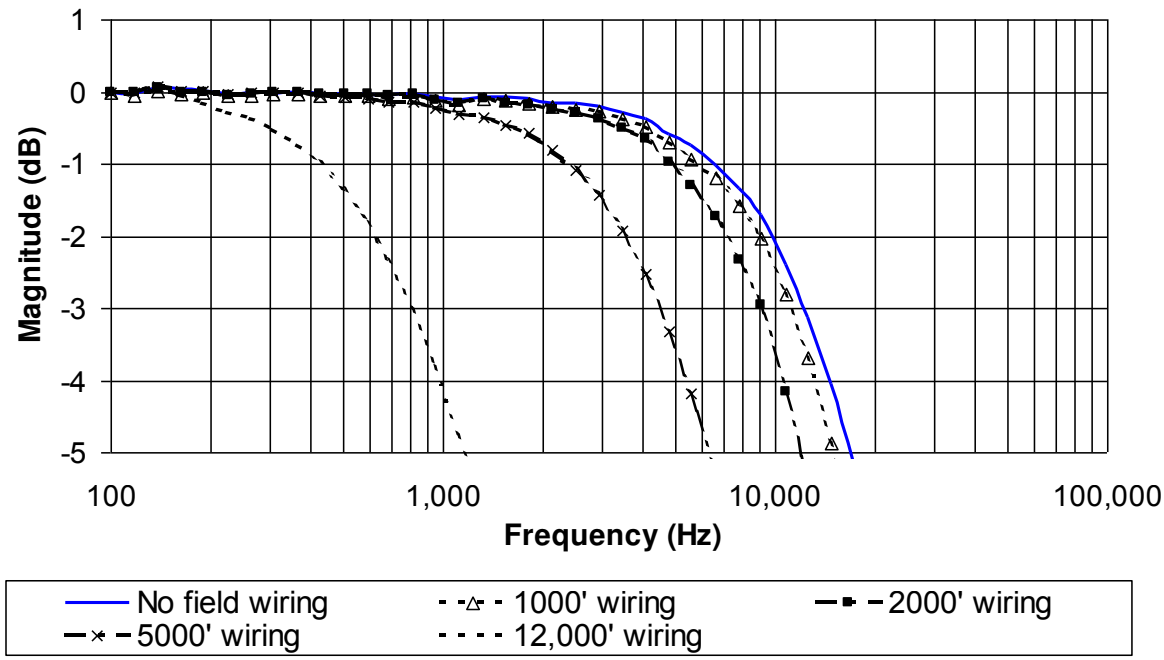

(a) Amplitude Response

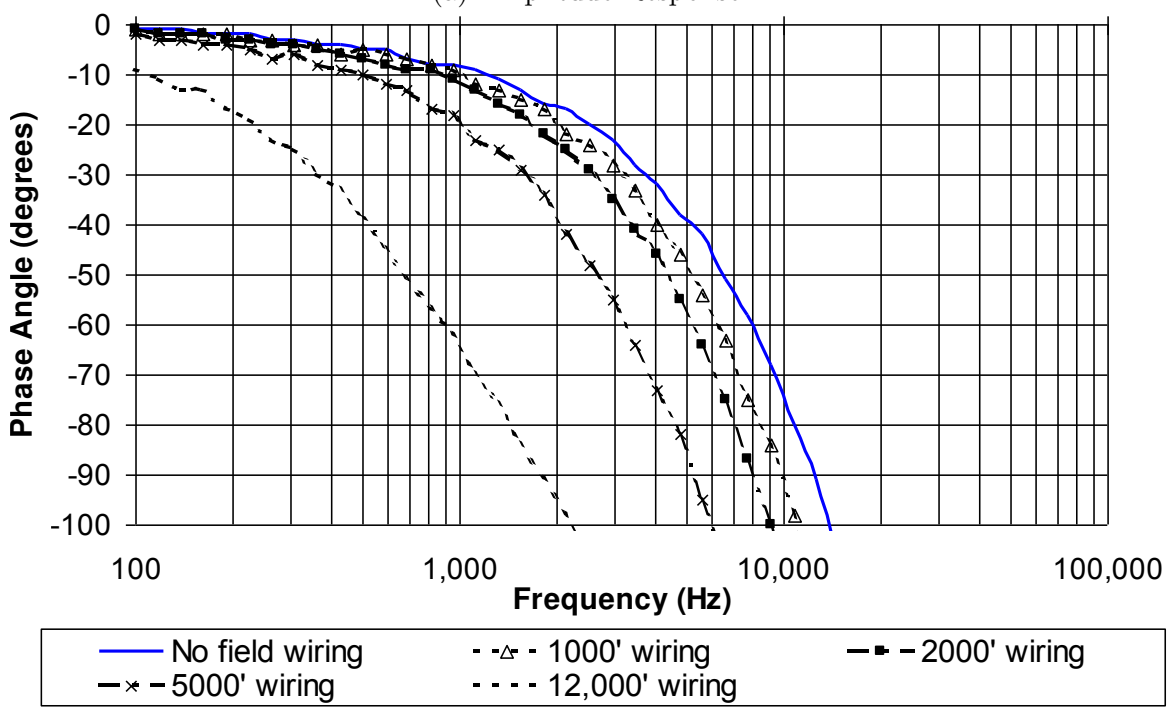

(b) Phase Response

Figure A.3: Frequency response function of the Bently Nevada 3300XL magnetic proximity sensor. *Source:* GE Measurements.

A.3 Calibration Procedure for the Differential Static Pressure Transducer

The differential diaphragm static pressure transducer requires calibration. The procedure is presented in Figure A.4. A Ralston hand pump is used connected to a

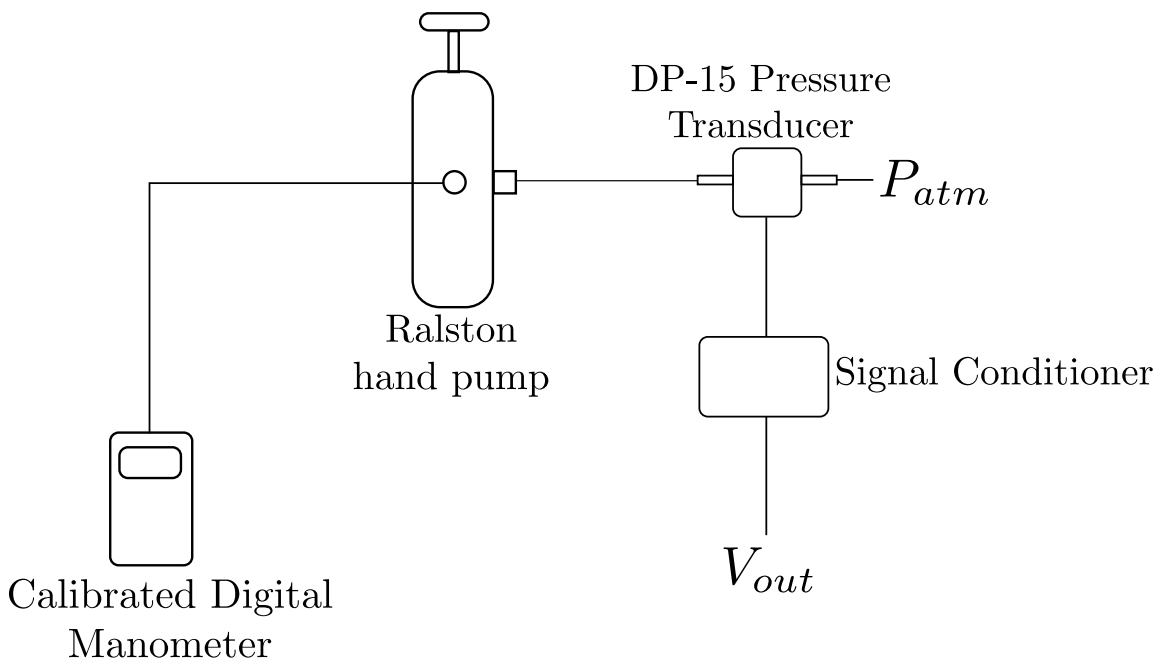

Figure A.4: Validyne DP-15 calibration procedure diagram

calibrated high precision manometer (accurate to 10 Pa), as well as the uncalibrated DP-15 transducer. The hand pump is used to gradually increase the pressure while measurements of the applied pressure and corresponding voltage output V_{out} by the pressure transducer are monitored. A calibration curve can hence be drawn, and is shown in Figure A.5. The latter shows that the pressure transducer is linear over the range of pressures considered, and a calibration constant of -3.439 can be extracted.

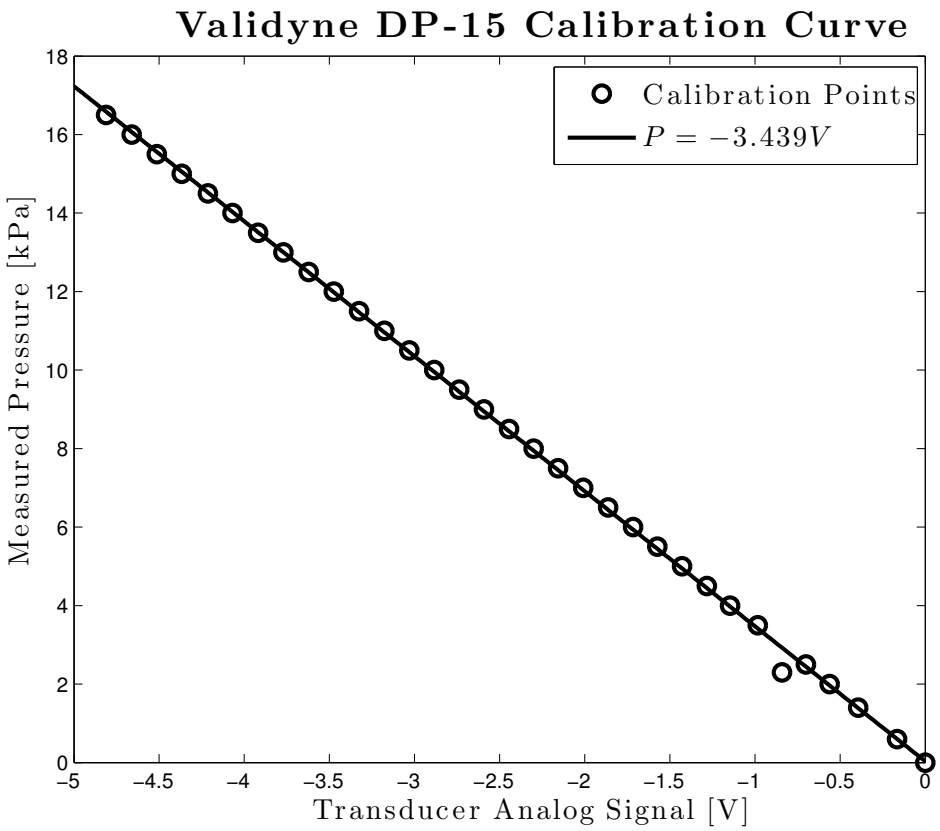

Figure A.5: Validyne DP-15 calibration curve